

**Jorma Koponen, Erkki Alasaarela, Kari Lehtinen, Juha Sarkkula,  
Pawel Simbierowicz, Heimo Vepsä and Markku Virtanen**

## **Modelling the dynamics of a large sea area**

Yhteenveto: Laajan merialueen dynamiikan mallintaminen



# 7

**Jorma Koponen, Erkki Alasaarela, Kari Lehtinen, Juha Sarkkula,  
Pawel Simbierowicz, Heimo Vepsä and Markku Virtanen**

## **Modelling the dynamics of a large sea area**

Yhteenveto: Laajan merialueen dynamiikan mallintaminen

The authors are responsible for the contents of the publication.  
It may not be referred to as the official view or policy  
of the National Board of Waters and the Environment.

ISBN 951-47-4284-2  
ISSN 0783-9472

Helsinki 1992. Valtion painatuskeskus

## CONTENTS

1	Introduction	5
2	Research area	7
3	Current measurements in the Bothnian Bay	8
3.1	Measurement strategy	8
3.2	Observations	8
3.3	Results	8
3.3.1	Flow and wind distributions	9
3.3.2	Dependence of flow on wind and water level variation	9
3.3.3	Flow vectors corresponding to different wind directions	11
4	Data acquisition	12
4.1	Digitization of the depths	12
4.2	Meteorological data	13
4.3	Water quality data	13
5	Mathematical models in Finland and abroad	16
5.1	Inquiry of the model use and other sources of information	16
5.1.1	Available sources of information	16
5.1.2	Emphasis of the different sources	16
5.2	Distribution of the inquiry answers	17
5.2.1	Institutions and models reported	17
5.2.2	Computational aspects of the models reported	17
5.2.3	Physical scales of the models reported	17
5.2.4	Availability and co-operation aspects	17
5.3	Centres of model work	18
5.3.1	Experience and staffs reported	18
5.3.2	Information gaps noticed	18
5.3.3	Recent trends in the model work	18
5.4	Model efforts in Finland	19
5.4.1	Backgrounds of the models	19
5.4.2	Development of model types	20
5.4.3	Use of the models	20
5.5	Conclusions of the model use	20
6	Development of the models and programs	21
6.1	Development of the 3D current model	22
6.1.1	Background	22
6.1.2	Local resolution improvement	25
6.1.3	Direct calculation of the layer velocities	26
6.1.4	Vectorization of the code	28
6.2	Development of the multigrid current model	29
6.2.1	Outline of the multigrid method	29
6.2.2	Inverse multigrid approach	29
6.2.3	The multigrid solver	29
6.2.4	Kernel correction method	30
6.3	Development of the 3D temperature and salinity model	31
6.3.1	Temperature model	31
6.3.2	Source and sink term	31
6.3.3	Boundary values	32
6.3.4	Realization of the temperature model	33
6.3.5	Implementation features	34
6.3.6	Sampling of the statistical characteristics of the simulation	34

6.4	Development of the oil and drifting model	35
6.5	Development of the grid generation system	36
7	Application of the models to the Bothnian Bay	37
7.1	Hydrodynamics	37
7.1.1	3D flow model compared with observations	37
7.1.2	3D flow model compared with other models	43
7.1.3	3D flow model compared with observed wind induced time series	43
7.1.4	Observed and calculated wintertime flow characteristics	49
7.1.5	High resolution flow fields	51
7.2	Comparison of measured and calculated incoming short wave radiation	53
7.3	Comparison of 3D and 1D temperature models	54
7.4	Salinity and temperature	56
7.5	Water quality simulation in the northern Bothnian Bay	65
7.6	Simulation of the oilspill transport after the Eira accident	68
7.7	Simulation of the drifting objects	71
7.8	Sensitivity tests for improved water quality monitoring	72
7.8.1	General requirements for effective sampling program	72
7.8.2	Analysis of the variations of water quality	73
8	Proceeding of the development work	77
8.1	Model for chemical and oil spill accidents	77
8.2	Water quality model	78
8.3	International co-operation	79
8.3.1	Co-operation tasks realized and projects in the near future	79
8.3.2	Coordination needs and alternatives	79
9	Conclusions	80
9.1	Modelling	80
9.2	Water quality monitoring	80
9.3	Development needs	82
9.4	Proceeding of the Bothnian Bay project	83
10	Summary	83
10.1	General	83
10.2	Research area	83
10.3	Research background	83
10.4	Data acquisition	84
10.5	Development of the models	84
10.6	Model use	85
10.7	Proceeding of the work	85
	Acknowledgements	86
	Yhteenveto	86
	References	89

## MODELLING THE DYNAMICS OF A LARGE SEA AREA

**Jorma Koponen<sup>1,3,6</sup>, Erkki Alasaarela<sup>1,4</sup>, Kari Lehtinen<sup>5</sup>,  
Juha Sarkkula<sup>2</sup>, Pawel Simbierowicz<sup>3</sup>, Heimo Vepsä<sup>4</sup> &  
Markku Virtanen<sup>3,6</sup>**

KOPONEN, J., ALASAARELA, E., LEHTINEN, K., SARKKULA, J., SIMBIEROWICZ, P., VEPSÄ, H. & VIRTANEN, M. 1991. Modelling the dynamics of a large sea area. Publications of the Water and Environment Research Institute, National Board Waters and the Environment, Finland, No. 7.

---

The dynamics of the Bothnian Bay was studied mainly by means of numerical models. The model results were supported by flow velocity measurements and by water quality components sampled for more than twenty years in the research area. Prior to the study an extensive review was made on the model useage abroad. The main tools of the project, 3-dimensional (3D) current and water quality models were developed in many aspects. An efficient 2D multigrid model for flow fields and an automatic grid generation program were developed for applications where good horizontal resolution is needed over large sea areas. The success in computing the surface currents was tested in several cases (oil accident, drifting of objects). As a local application of the models, the effects of different loading alternatives on the water quality off the town of Kemi was calculated. Based on model results and measurements a proposal was made to develop the water quality monitoring program.

---

Index words: Bothnian Bay, hydrodynamics, models, water quality.

---

### 1 INTRODUCTION

The monitoring of Finnish coastal waters was started in the mid 1960's. In these studies extensive but incoherent data has been gathered. The regional studies are reported separately by the institutions and the consultants responsible for the monitoring work. There is a need for a comprehensive interpretation of this extensive field data.

Most of the monitoring data is collected from the coastal waters where physical transport of waste and river waters and dispersion properties of the currents are quite complex. The water quality depends on the complex interactions of marine

system, mixing between layers and between subregions and between coastal waters and the open sea mass. Detailed model approach is necessary in interpreting the heterogenous monitoring data and in studying the factors influencing the water quality.

The present study aims at a consistent interpretation of this wide variety of local and special results, their causes and dynamics. Simultaneously the local, regional, temporal and seasonal variations of the flow patterns, salinity and temperature distributions, as well as the transport and dilution of waste waters and river waters are modelled. As the main tool for attaining these

1) University of Oulu/Academy of Finland

2) National Board of Waters and the Environment

3) Technical Research Centre of Finland, Reactor Laboratory

4) Water and Environment District of Oulu

5) Water and Environment District of Central Finland

6) Environmental Impact Assessment Centre of Finland

objectives the numerical flow field-, transport- and water quality models are used. They will be developed and tested to meet the special requirements of the Bothnian Bay. The work is aimed at

- an improved basis for comprehensive interpretation of the heterogeneous field data and monitoring programs,
- an improved basis for water quality management and planning and — an improved basis for water quality management and planning and

— an improved readiness for future applications and more adequate response to sea catastrophes.

The work is based on the water quality data gathered for more than 20 years at up to 200 stations in the Bothnian Bay, on special studies including flow velocity measurements, ecological research of the area and previous model applications of about 70 coastal areas and lakes mainly in Finland since 1974.

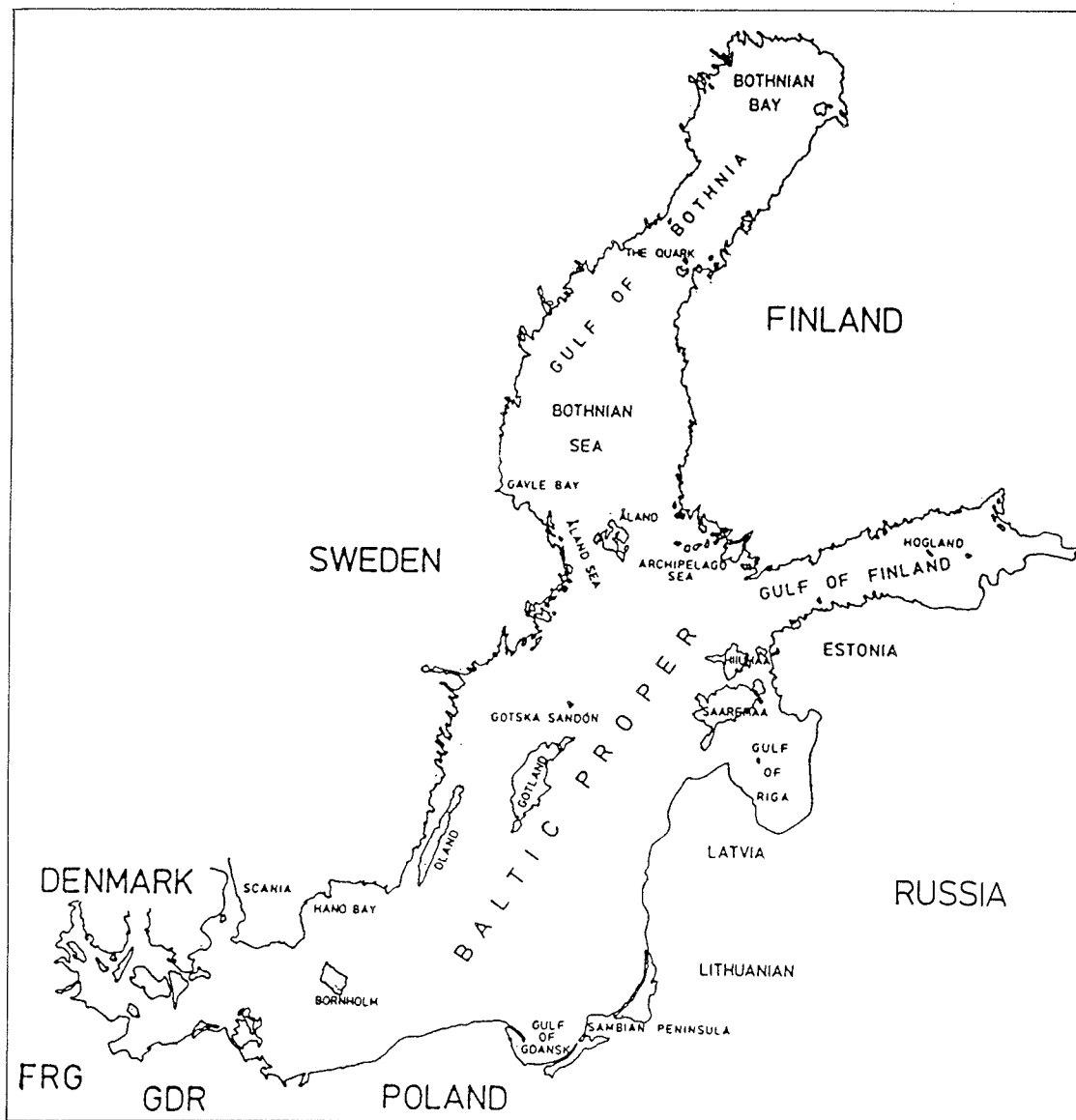


Fig. 1. The location of the Bothnian Bay.



## 2 RESEARCH AREA

The study area is the Bothnian Bay, the northernmost part of the Gulf of Bothnia between Finland and Sweden (Fig. 1). Its surface area amounts to 36 800 km<sup>2</sup>, volume 1 490 km<sup>3</sup>, mean depth 40.5 m and maximum depth 140 m (Mälkki and Tamsalu 1985).

The Bothnian Bay forms a hydrographically isolated part of the Baltic Sea and therefore has

distinctive properties. About 30 rivers of various sizes discharge their water into the Bothnian Bay from the Scandinavian mountains and from the forest areas on both sides of the Bay. The low salinity of Bothnian Bay (2–4 ‰, Fig. 2) is due to the abundance of river waters (100 km<sup>3</sup>a<sup>-1</sup>) and a minor inflow of sea water through the Quark (300–400 km<sup>3</sup>a<sup>-1</sup>).

The residence time of the Bothnian Bay is about three years. Due to these properties the conditions

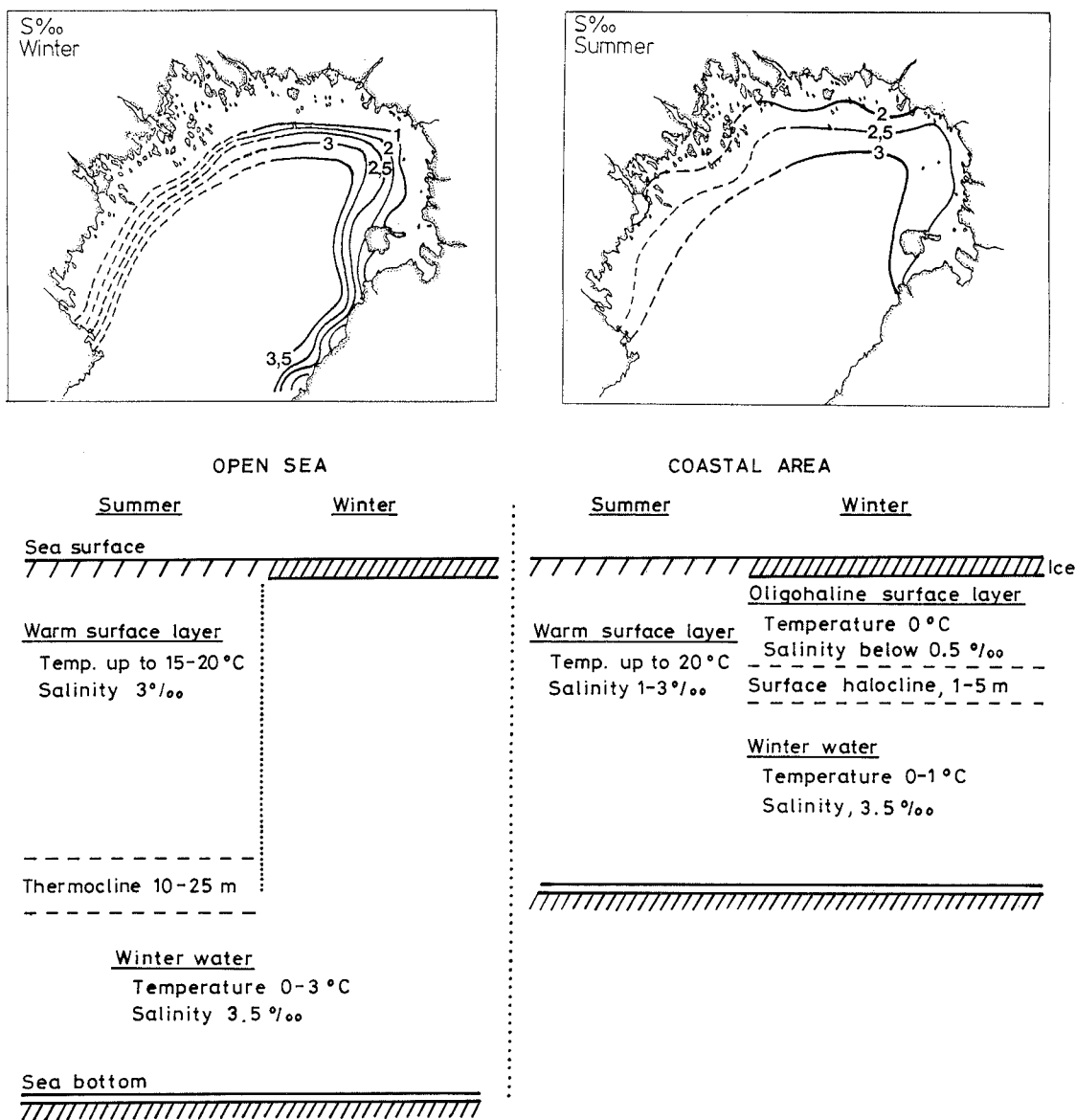


Fig. 2. The surface salinity of the Bothnian Bay (upper) and a schematic representation of the vertical structure of the water masses.

in the Bothnian Bay are more limnic than marine.

The different water layers, haloclines and thermocline in the Bothnian Bay are illustrated in Figure 2. The physical factors show marked seasonal variations especially in the coastal waters of the Bothnian Bay. The ice-bound period lasts from December till mid-May. In winter, the vertical differences are small in the centre of the Bothnian Bay but in coastal area river waters spread out in a 2–3 meter thick layer just below the ice. In the northern part of the Bothnian Bay this river water layer can spread as far as 30–40 km from the river outlet. In summer, the deeper parts are thermally stratified and the river waters disperse above the thermocline throughout the northern part of the Bothnian Bay. In summer, no permanent stratification exists in the shallow coastal areas of the northeastern Bothnian Bay. The tides in the area are negligible.

### 3 CURRENT MEASUREMENTS IN THE BOTHNIAN BAY

#### 3.1 Measurement strategy

A series of current measurements was carried out in the coastal zone of the Bothnian Bay, to observe the behaviour of the wind driven surface currents, to detect large eddies formed in this zone and transport phenomena related to the wind and in this way to achieve data for model verification. The available amount of measuring equipment in proportion to the area to be modelled was not big, so the observation points had to be chosen in a way that the results describe the transport of as large water masses as possible. The choice of the points was aided by earlier investigations (Huttula and Sarkkula 1980, 1981) and preliminary runs with the 3-dimensional Bothnian Bay model.

#### 3.2 Observations

When selecting the observation points in order to find the most important and informative ones, two areas were selected to be focused on. The area on the southern side of the town of Kemi is important because of the loading entering from the river Kemijoki, from the pulp and paper mills and municipalities. Earlier measurements indicated that in this area there exist strong currents perpen-

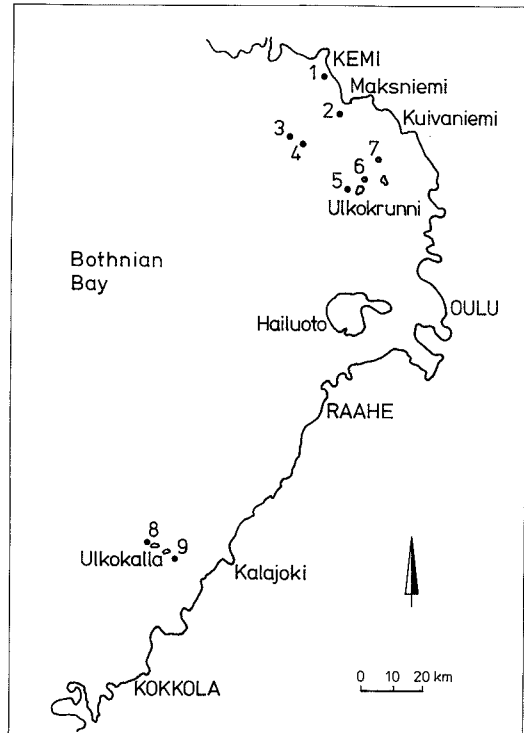


Fig. 3. Current measurement points in the Bothnian Bay.

dicular to the shore line i.e. in SW-NE direction, thus affecting strongly the waste water distribution in the area.

The coastal reach between the towns Kokkola and Raahe was also of special interest. The measurement points were chosen near Ulkokalla and Maakalla islands. The focus was in finding the dependence between the wind and the flow along the coast.

Naturally, when choosing the observation points and depths restrictions determined by boat traffic, wave action etc. had to be taken into consideration.

The measurements were made with Aanderaa recording current meters during autumns 1987 and 1988 with 10 minutes sampling. The recorded parameters were water temperature and conductivity and flow direction and velocity.

The observation points and periods are given in Table 1 (points are indicated in Figure 3).

The measurements at points 8 and 9 in autumn 1988 were delayed from the ones at points 3, 4, 5 and 7 as strong winds prevented instrument deployment. Furthermore, the observation period was accidentally broken at point 9 during a storm.

The measurements were made during autumn period, when there was practically no temperature stratification in the observed surface layer (0—10 m).

### 3.3 Results

#### 3.3.1 Flow and wind distributions

The observed flow and wind vectors were divided into two components, perpendicular to each other. The two wind components are from the north and from the east. The average flow and wind components as well as the standard deviations and extremes of the daily values of flow, wind and water level change are presented in Tables 2 and 3.

During all measurement periods the wind was blowing, in average, from south or south-west according to the long-term distribution.

During 1987 measurements mean circulation was anti clock-wise. Water was flowing to the north in Ulkokrunni area and to the south-west in Maksniemi area. The average flow was nearly the same near the surface and at 10 m depth in both points.

In 1988 a mean circulation similar to 1987 measurements was detected in Ulkokrunni-Maksniemi area (points 3, 4, 5 and 7). The flow velocities to south and south-west outside Maksniemi were much higher (highest values 20—25  $\text{cm s}^{-1}$  in points 3 and 4) than velocities towards the coast (highest values 5—10  $\text{cm s}^{-1}$ ). The same was true for north-south velocity component on the western side of Ulkokrunni (point 5). Actually, a clear clock-wise circulation in Maksniemi Ulkokrunni area was not detected during the measure-

ments. A clock-wise mean circulation was found in front of the town of Kemi (point 1) and a mean flow along the coast to the north-east in Ulkokalla area in the southern part of Bothnian Bay (points 8 and 9).

Flow direction was much more evenly distributed outside the town of Kemi (point 1), between Ulkokrunni and the coast and in Ulkokalla area than in Maksniemi and Ulkokrunni area (points 3, 4 and 5).

The circulation patterns corresponding to different wind directions will be discussed in the following chapters.

#### 3.3.2 Dependence of flow on wind and water level variation

Regression analysis was used in studying the dependence of flow on wind and water level variation. Daily average values were used in order to filter out short term flow variation. The set of variables explaining flow variation consisted of the wind observations simultaneously with flow observation and with a time lag of -3, -6, -9 and -12 hours and the change of the sea water level. The daily water level change was calculated as the difference between midnight observations. The best correlations were found with the variable combinations indicated in Tabel 4.

Wind observations for points 8 and 9 are taken from Ulkokalla station.

The total variation of flow components is well explained by the regression equations in most of the observation points. More than 80 of the variation of the main flow component is explained in points 1, 3, 7, 8 and 9. Only in points 5 and 7 the explanation degree ( $r^2$ ) is less than 50 %.

Table 1. Current measurement periods in 1987 and 1988.

Point	Description	Depth (m)		Obs. period
		Obs.	Total	
2	Maksniemi S	3.5	16.8	24.9. — 6.11.1987
2	Maksniemi S	9.5	16.8	24.9. — 6.11.1987
6	Ulkokrunni N	3.7	17.8	24.9. — 6.11.1987
6	Ulkokrunni N	10.0	17.8	24.9. — 6.11.1987
1	Kemi harbour	1.0	2.0	13.9. — 15.10.1988
3	Maksniemi WSW	4.5	11.0	12.9. — 18.10.1988
4	Maksniemi SW	4.5	12.0	12.9. — 18.10.1988
5	Ulkokrunni W	7.0	17.0	13.9. — 19.10.1988
7	Maakrunni N	4.0	8.0	13.9. — 19.10.1988
8	Ulkokalla	6.5	18.0	6.10. — 22.10.1988
9	Maakalla	6.0	14.0	6.10. — 19.11.1988

Table 2. Statistics of current measurements in 1987. Mean value ( $\bar{x}$ ) of flow components  $v_a$  and  $v_b$  ( $\text{cm s}^{-1}$ ), standard deviation ( $s$ ), minimums and maximums of daily means in measuring points (2) and (6) during period 24.9.—6.11.1987.

	Meas. depth	Flow direction	$\bar{x}$	$s$	min	max
$v_a$ (2)	3.5	0	-3.0	2.4	-7.1	2.0
$v_b$ (2)	3.5	90	-4.9	9.3	-26.8	5.3
$v_a$ (2)	9.5	0	-5.3	6.9	-16.8	11.2
$v_b$ (2)	9.5	90	-6.1	10.6	-25.0	13.7
$v_a$ (6)	3.7	0	3.8	3.7	-6.7	10.2
$v_b$ (6)	3.7	90	-0.7	2.7	-7.7	3.5
$v_a$ (6)	10.0	0	5.3	9.4	-12.8	17.1
$v_b$ (6)	10.0	90	-0.7	5.3	-14.7	9.3
TN			-6.2	6.4	-16.2	7.4
TE			-1.2	4.7	-10.1	7.4
W				31.0	-76.0	66.0

Table 3. Statistics of current measurements in 1988. Mean value ( $\bar{x}$ ) of flow components  $v_a$  and  $v_b$  ( $\text{cm s}^{-1}$ ), wind components TN and TE ( $\text{m s}^{-1}$ ) and daily water level change  $W$  ( $\text{cm d}^{-1}$ ), standard deviation ( $s$ ), minimums and maximums of daily means in measuring points (1), (3), (4), (5), (7) and Ajos wind during period 14.9.—14.10.1988 and in points (8), (9) and Ulkokalla (wind) during period 6.10.22.10.1988.

	Flow direction	$\bar{x}$	$s$	min	max
$v_a$ (1)	320	-4.0	7.6	-21.4	12.5
$v_b$ (1)	50	-1.4	2.4	-5.4	3.5
$v_a$ (3)	0	-3.0	2.6	-9.8	1.9
$v_b$ (3)	90	-9.0	7.1	-21.7	5.5
$v_a$ (4)	0	-0.2	3.3	-6.6	8.4
$v_b$ (4)	90	-5.2	5.6	-18.4	7.0
$v_a$ (5)	0	6.3	2.9	0.0	12.6
$v_b$ (5)	90	0.0	1.2	-2.1	2.7
$v_a$ (7)	0	2.8	8.7	-16.4	14.8
$v_b$ (7)	90	0.9	4.3	-4.9	9.5
TN (Ajos)		-4.2	5.9	-13.5	10.1
TE (Ajos)		-3.4	4.7	-14.4	4.5
W (Kemi)			22.9	-58.0	60.0
$v_a$ (8)	40	8.3	9.0	-8.4	21.1*
$v_b$ (8)	130	-1.5	2.5	-5.8	3.2
$v_a$ (9)	40	2.8	13.4	-33.5	27.4
$v_b$ (9)	130	-1.0	4.2	-10.5	6.2
TN (Ulkokalla)		-2.0	7.5	-15.8	14.9
TE (Ulkokalla)		-3.4	3.9	-11.2	8.6
W (Kokkola)			30.3	59.0	75.0

\* period 6.—22.10.1988

Table 4. Regression equations for flow components  $v_a$  and  $v_b$  ( $\text{cm s}^{-1}$ ) in Autumn 1987. Directions of components  $v_a$  and  $v_b$  is given in Table 2. TN and TE are the wind components ( $\text{m s}^{-1}$ ) from the north and east respectively and the number after the wind component indicates the time lag in hours between flow and wind observation.  $W$  is the water level change ( $\text{cm d}^{-1}$ ).

Point	Wind north	Wind east	Water level	Constant	$r^2$ n=24
2	$v_a = 0.19 \text{ TN}_6 + 0.12 \text{ TE}_6$			-1.69	0.33
2	$v_b = 0.61 \text{ TN}_6 - 1.45 \text{ TE}_6$			-2.90	0.68
2	$v_a = 0.99 \text{ TN}_9$			+1.15	0.79
2	$v_b = 0.91 \text{ TN}_9 - 1.30 \text{ TE}_0$		-0.06 $W$	-1.87	0.63
6	$v_a = -0.27 \text{ TN}_6$			+2.11	0.22
6	$v_b = -0.22 \text{ TN}_6 - 0.16 \text{ TE}_0$		+0.02 $W$	-2.29	0.36
6	$v_a = -0.79 \text{ TN}_6 - 0.63 \text{ TE}_6$		+0.07 $W$	-0.40	0.40
6	$v_b = -0.20 \text{ TN}_6 + 0.38 \text{ TE}_6$			-1.50	0.17

3.3.3 Flow vectors corresponding to different wind directions

The flow velocities linked with different wind events, calculated from the regression equations based on 1987 and 1988 measurements, are shown in Figures 4 to 6. The figures are completed with some results (flow directions in surface layer) from autumn 1979 and 1980 measurements (Huttula and Sarkkula 1980, 1981), in order to get a more comprehensive picture of the flow patterns. Furthermore, results from a measurement series in the coastal zone off Kuivaniemi are added to the Figures 4 to 6. The results in question are from a measurement point on the sea-side of the inner islands and represent the flow along the coast. The measurement depth was 4 metres. Based on 30 days measurement, velocity component along the coast ( $\text{cm s}^{-1}$ ) depends on the wind components from north and south ( $\text{m s}^{-1}$ ), the regression equation ( $r^2 = 0.67$ )

$$v_a = -0.46TN - 0.90TE - 0.6 \quad (1)$$

$v_a$  is the current component to direction  $350^\circ$

TN, TE are north and east components of the wind.

The results show that an anti clock-wise circulation is created in Ulkokrunni-Kemi area during E, SE and S winds, so that a strong current out to the sea from cape Maksniemi is developed. Near shore current at Kuivaniemi is not directly connected with the large circulation and has usually a flow direction opposite to the main flow.

During SW, W and NW winds the circulation is anti clock wise in Ulkokrunni-Maksniemi area but there appears a SE going flow in front of Kemi town and through a zone between Ulkokrunni and Kuivaniemi.

The results give no clear horizontal circulation pattern during N and NE winds.

In Ulkokalla-Kalajoki area a north going flow is created during SE, S and SW winds while the opposite picture is seen during NW, N and NE winds.

Comparison of regression model to calculations with a 3-D flow model will be presented later in chapter 7 "Application of the models to the Bothnian Bay.

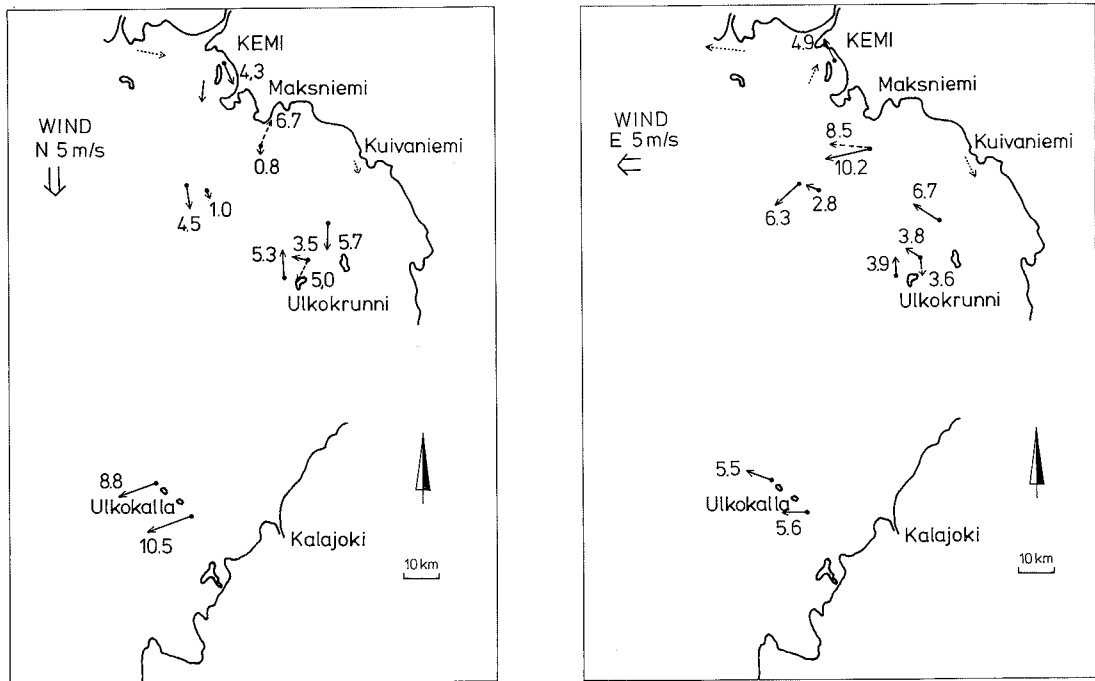


Fig. 4. Flow velocities ( $\text{cm s}^{-1}$ ) and directions in the coastal reach of Bothnian Bay during northern (left) and eastern (right) wind. Dotted arrows indicate the lower measurement depth.

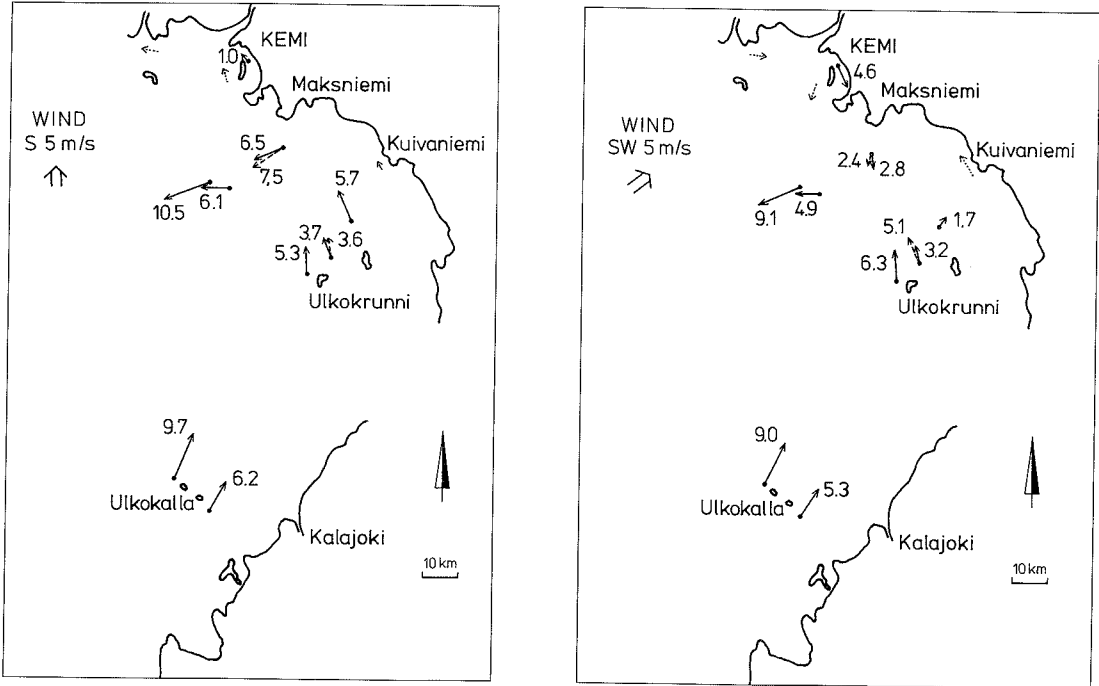


Fig. 5. Flow velocities ( $\text{cm s}^{-1}$ ) and directions in the coastal reach of Bothnian Bay during southern (left) and south-western (right) wind. Dotted arrows indicate the lower measurement depth.

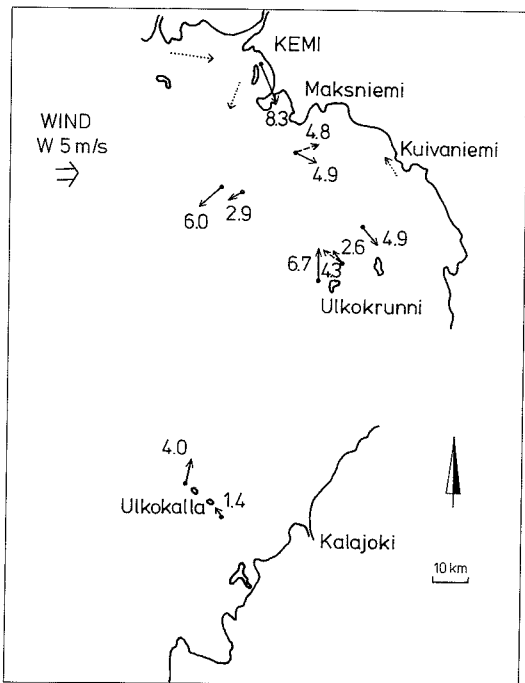


Fig. 6. Flow velocities ( $\text{cm s}^{-1}$ ) and directions in the coastal reach of Bothnian Bay during western wind. Dotted arrows indicate the lower measurement depth.

## 4 DATA ACQUISITION

### 4.1 Digitization of the depths

The mathematical models used in the Bothnian Bay research project required for the most part realistic information about the depths and coast line. In the past the calculation geometry has been estimated manually. In the project one task was to test the effect of different grid configurations. The idea was to digitize the depths and generate any needed grid by a grid generation program. The digitization program used was devised from scratch because the commercial digitization program available was not very fast or flexible.

The digitization of the Bothnian Bay maps resulted in a data base of over 100 000 points. The digitization work required months. The correction of the digitized information was also time-consuming. The main problem was that the depths and depth contours digitized from different maps or at different times didn't many times fit together very well. The correction of the data was very laborious because of the lack of right tools. It would require an interactive program where the data could be scaled, rotated and transferred at will.

In the future such digitization projects wont be necessary because the maps will be available in digital form. Also the GIS:s (Geographical Information Systems) will become more popular and they will facilitate the information retrieval. GIS:s combine CAD-techniques with geographical data bases.

## 4.2 Meteorological data

Different kind of meteorological data is needed for water temperature and current calculations: air temperature, cloudiness, humidity, air pressure, incoming short wave radiation, wind direction and speed. If radiation data is not available it is possible to calculate it using cloudiness data. Data was collected for periods 1.1.1975—31.7.1985 (Holmögadd) and 1.1.1975—31.12.1987 (Hailuoto). The interval between the measurements is 3 hours.

The wind data has very important influence for the success of transport simulations. When the model area is about 300 km long the wind field is far from uniform. That is why a comparison of wind data from five different weather stations along the Finnish coast of the Bothnian Bay was made.

The selected weather stations and trajectories created by superposing daily wind vectors for the period 1.—30.9.1986 are shown in Figure 7. The stations of Valassaaret, Mäskär and Hailuoto were located in the island and the stations of Oulu and Kemi were located in an airport. It can be seen that wind direction and speed can occasionally vary quite much between northeast and southeast stations.

Comparison between the stations of Hailuoto and Oulu airport showed that wind speed measured far from the coast may be much higher than wind speed measured on the coast. The same phenomena has been found between the stations of Valassaaret and Mäskär. Regression analysis for the north and east wind component of the Holmöarna and Hailuoto stations were carried out. Wind period was 1.1.1976—31.12.1976.

The regression equations for the wind components in Hailuoto are

$$W_N = 0.44W_{N,Holm} + 0.22$$

$$W_E = 0.41W_{E,Holm} - 0.12$$

$W_N, W_E$  north and east component of wind in Hailuoto

$W_{N,Holm}, W_{E,Holm}$  north and east component of wind in Holmöarna.

The correlation coefficient squared for the north component equation was 0.53 and for the east component 0.35 (n=1933).

This means that the average wind directions for long period are quite near to each other in the southern and northern part of the Bothnian Bay. In this case the wind speed was in the south nearly twice as high as in the north.

## 4.3 Water quality data

The open sea monitoring is carried out by the Finnish Institute of Marine Research (FIMR) and Fiskeristyrelsen (the Swedish National Board of Fisheries) for providing material for bilateral monitoring between Finland and Sweden. The programs of these institutes join up with the coastal water monitoring program of the National Board of Waters and the Environment (NBWE). This Baltic Monitoring Programme (BMP) comprises of 13 sampling stations with a sampling frequency of four times a year (since 1979). Intensive monitoring has been made by the SMHI (3 st., 1—4 times a, since 1970) and by the FIMR (5 st., about 20 times per open water period, since 1970). The observation points of water quality monitoring are shown in Fig. 8.

The regular monitoring of coastal waters was started in the mid 1960's. Samples are collected by the NBWE in 35 monitoring stations four times a year. Intensive monitoring is performed at four stations in the reseach area (15—20 times a, since 1986).

The monitoring of the effects of pollution on waters receiving wastes is based on the Water Act. The sampling frequency in 150 sampling points varies from 2—7 times per year. The recipient control programs are mostly carried out by private laboratories, which are authorized and supervised by the NBWE.

In Swedish coastal waters there is no actual recipient control program. In some resipients with municipal or industrial loading water samples are collected near the loading points about two times per year.

The discharges of different substances into the Bothnian Bay are monitored by the NBWE and the SMHI every month. Since 1985 the sampling in Finland has been arranged according to the variation in water flow of each river.

Fiskeristyrelsen and the SMHI report the monitoring results every year, the FIMR and the NBWE at some years intervals. Studies in each resipient area are reported separately every year.

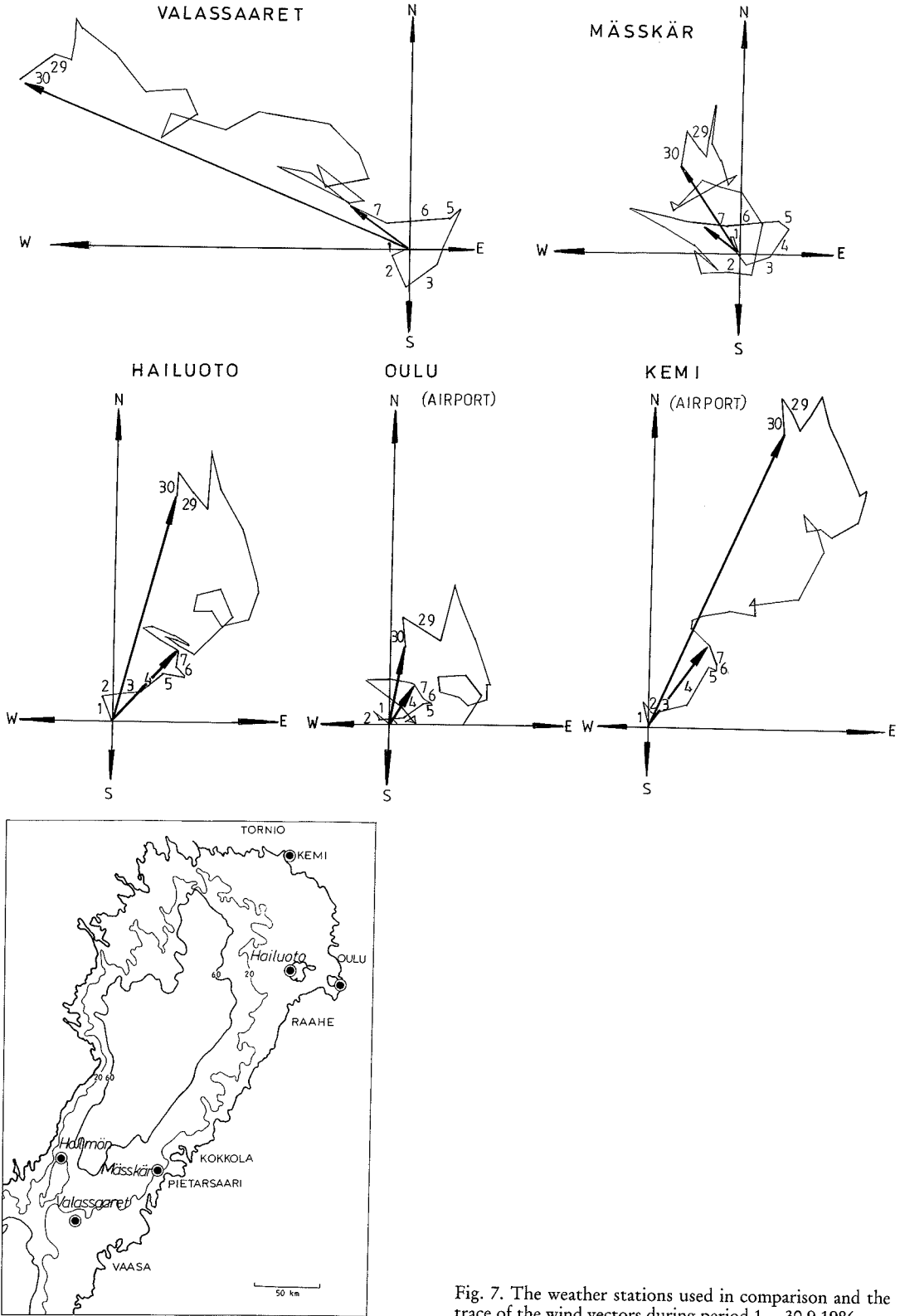


Fig. 7. The weather stations used in comparison and the trace of the wind vectors during period 1.—30.9.1986.



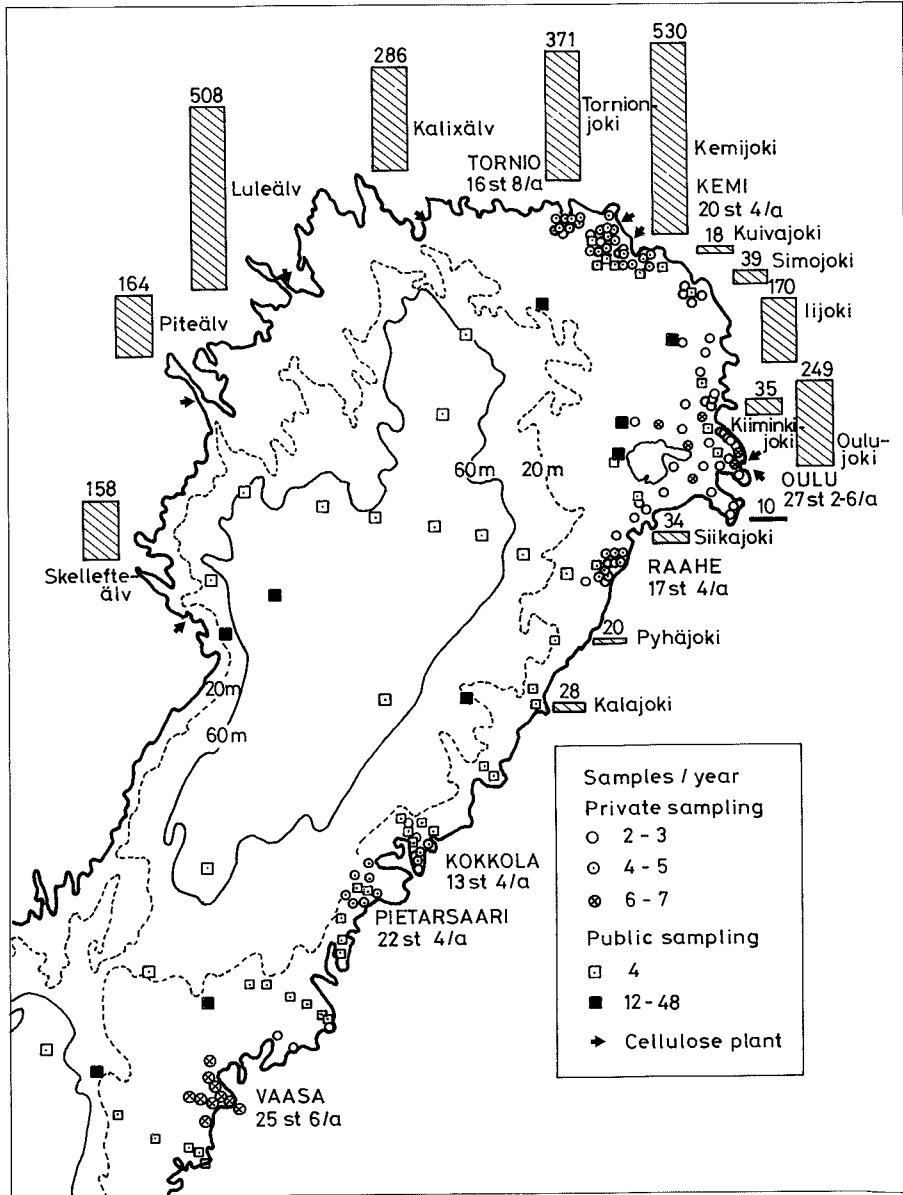


Fig. 8. The mean discharges from the biggest rivers flowing into the Bothnian Bay, cellulose plants and sampling stations of water quality in the Bothnian Bay.

## 5 MATHEMATICAL MODELS IN FINLAND AND ABROAD

### 5.1 Inquiry of the model use and other sources of information

#### 5.1.1 Available sources of information

Along the course of the model work some basic information about the existing numerical models has accumulated all the time. To large extent this information is based on the litterature used and viewed and on personal contacts tied trough correspondence, discussion and meetings together with the experiences gained in calculations and in their comparisons with measurements. For a more systematic view at the state-of-the-art model use, an inquiry was introduced.

Prior to the inquiry, in March 1986, a litterature review was carried out as a computer search from the Aqualine database. With a combination of keywords Hydr-/Flow-/Transport, Water quality, 3D/Three-/Multi-/Stratif- and Mod- the search resulted in about 260 more or less relevant references. 145 of them were dealing with hydraulic, flow and transport modelling and 122 with water quality models. These included altogether 23 three-dimensional model approaches. In addition to lake, sea, ocean, estuary and coastal models the refences included e.g. models of hydrological runoff, sub-surface flow and waste water treatment basins and about 15 calculations of statistical correlations called models. A considerable part of the relevant referenses were already known on the basis of institutional contacts and the continuous view at the current journals. However, several new addresses were picked up from the litterature search for mailing the inquiry.

The questionnaires of the inquiry were mailed to more than 100 institutes mainly in Western Europe in September 1987. Most part of the answers were received till December the same year. The inquiry was accompanied and supplemented by an exploration trip to several research institutes in Denmark, Germany, United Kindom and the Netherlands in autumn 1987.

The results of the inquiry and expedition contacts were analyzed in the beginning of the year 1988. Simultaneously, however, new possibilities appeared to extend the survey to Eastern Europe as well. In hope of this extension — together with a hope for better coverage of the other continents, too — the publication of the survey was postponed — for a few months as it was thought then, with fatal delay as it can be seen now. Viz., during the next few years the publication plans were repeatedly confused by the urgent demands of several

emerged activities, e.g. employment and location changes of staff, financing arrangements, reorganization alternatives, acute demand of other applications, mailing delays and tasks within the considerably increased European co-operation, e.g. preparations for the EUREKA and EC research programs.

#### 5.1.2 Emphasis of the different sources

The computer search of the titles and keywords of journal articles is considerably confused by the unstable, incoherent, multiple-meaning terminology, by the different meaning of words to different authors in different contexts. In the inquiry this problem has been significantly reduced by the fixed context of the questionnaire. In personal discussions the immediate feedback of dialog has practically eliminated this problem.

The journal articles are often concentrated on the new, recently implied details of research development. Wide background descriptions are usually eliminated by the required brevity of the papers. Detailed descriptions of the calculation problems can be usually given in internal reports only. In addition, most of the commercial applications are not sent for publication — the conventional applications as being not interesting and the most advanced applications as confidential. Information about these most advanced and routine applications can be touched by the inquiry. During the visits and in personal discussions these are considered but usually less systematically. In official visits the attention is easily directed from real achievements to plans for future development.

The different sources of information thus seem to supplement and support each other in many ways. From the very beginning it was clear that a survey centrally based on an inquiry can not cover all the work done within modelling. The mailing list was certainly incomplete and biased, it was even intentionally concentrated on the countries of the Western and Central Europe. In this respect, the limited number of important research institutes lacking from the inquiry and that of less important or irrelevant ones included seem to support the validity of the survey.

The results of the inquiry are mainly from autumn 1987. They could be partly checked and their relevance evaluated with the information received from other sources. In order to avoid still extra delay, however, this is not done but the answers of questionnaire are reported in the form they were given without attempting to update them.

## 5.2 Distribution of the inquiry answers

### 5.2.1 Institutions and models reported

Altogether the questionnaire was mailed to almost 200 institutes between September 1987 and September 1989. In response, descriptions of 105 models were received from 56 institutes in 17 countries. In addition, almost 40 questionnaires were returned unfilled for the sake of changes in addresses, staff or activities. The total number of applications reported amounted to about 800 case studies, when the lacking answers were replaced by minimum order of magnitude estimates from other sources. More than 500 person work years (pwys) were used for the development and application of the models. According to the answers almost 250 persons have been involved with surface water modelling at the time of the inquiry.

65 of the models were used in describing the water currents, 54 in transport and mixing, 42 in stratification and its development and 33 for water quality indicators. All categories were present in 8 models, three of them in 23 and two in 21 models. The most frequently reported combinations were a pure hydrodynamic model with 26 cases and a combined hydrodynamics, transport and stratification model with 13 cases.

### 5.2.2 Computational aspects of the models reported

Three-dimensional (3D) computation was possible with 34 models, 2D with 45, 1D with 20 and no space resolution (0D) in 3 models. Alternatives for the number of space dimensions were mentioned for 16 models.

As the numerical solution techniques the finite differences were used in 72 models, finite elements in 5, both of them in 2 and other techniques (analytical solution, pseudospectral methods, numerical integration schemes of ordinary differential equations (ODEs), method of lines with Monte Carlo dispersion etc.) in 7 models. The solution methods of 19 models were not specified.

Time-dependent solution was emphasized in 88 models, steady-state in 8 and both of them in 6 models.

The time evolution — when it was mentioned — was described with explicit algorithms in 42 models, with implicit methods in 33 models including 13 models with ADI (alternating direction implicit) solutions and 3 with semi implicit algorithms. Both explicit and implicit methods were utilized in 8 models and other techniques

(frequency domain, analytical solutions, numerical integration of ODEs etc.) in 9 models.

52 of the models were based on the institutes own ideas, own computer code was additionally written for 26 models. 21 models were acquired from outside the institute in question. 6 of them were used without any modifications and 15 with minor modifications in the computer code.

### 5.2.3 Physical scales of the models reported

Horizontal extensions of the typical application areas were classified to spotty (less than 5 km by 5 km), local (up to 50 km by 50 km), regional (up to 500 km by 500 km) and global (more than 500 km by 500 km) scales. According to this classification, 12 models were typically applied to spotty scales, 44 to local scales, 27 to regional and 7 models to global scales. Any (or problem dependent etc.) scale was expressed typical to the applications of 14 models.

Typical depth of the application areas was mentioned to be very shallow (less than 6 m) in 26 models, shallow (6 to 20 metres) in 52 models, medium (21 to 65 metres) in 35 models, deep (66 to 200 metres) in 21 models and very deep (more than 200 metres) in 8 models.

Horizontal resolution of less than 10 grid boxes was used in 7 models all of them having a most detailed vertical resolution with more than 20 layers. The two models of the most detailed vertical resolution (more than 100 layers) did not use any horizontal resolution at all. Horizontal resolution of 10 — 300 grid boxes was used in 12 models.

Horizontal resolution between 301 and 3000 grid boxes was typical for 35 models including 20 models with one layer, 8 models with 5 to 20 layers, 1 model with more than 20 layers and 6 other models (including one two layer model). More than 3000 horizontal grid elements were used in 15 single-layer models, in 6 models with 5 — 20 layers and in 5 other models with number of layers not specified.

The typical time extension of the model applications was expressed to be less than 10 days in 37 models, up to one month in 14 models,  $\frac{1}{2}$  to 8 months in 20 models and more than that (from one year up to centuries) in 26 models.

### 5.2.4 Availability and co—operation aspects

Some documentation was expressed to be available for 47 models, full documentation for 40 models,

partially complete documentation for 5 models and no documentation for 5 models.

63 models were reported to be available for outside users, 9 models were not yet available and 3 models not available. Interest to participate in co-operation was expressed in 71 answers and denied in only one.

The research teams — as far as their sizes were indicated in the answers were typically quite small, most frequently 2 to 4 persons. Eight models had research teams of more than 15 persons. By sizes the model groups were distributed as follows:

Team size of persons	Responsible for models	Working at institutes
1	10	7
2	11	8
3	13	6
4	21	10
5—15	13	5
>15	8	2

## 5.3 Centres of model work

### 5.3.1 Experience and staffs reported

Several important centres for development and utilization of numerical models for water bodies arose from the inquiry, e.g.

- Delft Hydraulics (DHL) from Holland with 22 persons involved in the modelling work and 50 to 60 pwys done so far;
- SOGREAH Consulting Engineers, France, with 50 persons involved and more than 40 pwys work done;
- Danish Hydraulic Institute (DHI) with some 50 applications listed;
- Hydraulics Research Ltd. (HR), Wallingford, England, with considerable number of commercial applications;
- University of Liege (LU) from Belgium with 10 persons staff;
- Institute of Marine Sciences at the University of Hamburg (HU/IfM) with 4 to 6 persons involved and 22 pwys experience;
- National Water Research Institute (NWRI) of Canada (Canada Centre for Inland Waters CCIW) in Burlington, Ontario, more than 6 persons and 20 pwys;
- Institute of Limnology (LLI) at the Academy of Sciences, USSR, in Leningrad with 4 persons involved and 20 pwys experience;

- Institute of Thermophysics and Electrophysics (ITE) at the Academy of Sciences, USSR, in Tallinn, with 5 persons and 16 to 21 pwys;
- Coastal and Oceanographic Department at the Weil Hall University of Florida (FWHU/COD), USA, 5 persons involved and 12 pwys done;
- Swedish Meteorological and Hydrological Institute (SMHI) with 10 to 15 persons and almost 10 pwys work done;
- University of Bradford (BU), England, with 4 persons staff and more than 10 pwys done;
- Civil Engineering Department at the Princeton University (PU/CED), USA, with 7 pwys work; and
- Laboratory of Chemistry at the Royal Pharmacy University of Denmark (RFU/ChL), with 4 to 8 persons and more than 5 pwys.

Most of these institutes are solving both hydraulic and water quality problems. RFU/ChL is concentrated mainly upon ecological, biological and chemical processes while LU, HU/IfM, LLI, PU/CED and SMHI did not mention these water quality aspects in their answers to the questionnaire.

### 5.3.2 Information gaps noticed

The numbers of persons, applications and pwy's given by different institutes need not to be strictly commensurable since no unique rules for calculating these figures were given. Different institutes may have had somewhat different criteria in distinguishing model work from their other research. Nevertheless, the pwy numbers seem to reflect quite well the orders of magnitude of the modelling experience.

It is clear that the list of major institutes based on the inquiry can not cover all of the important model centres. Especially for large countries, like USSR and USA, the list is apparently imperfect lacking e.g. the research institutes of Novosibirsk, Moscow and Kiev, Massachusetts Institute of Technology, University of Rhode Island and other departments than PU/CED from Princeton. Also from Europe, e.g. from Norway, Spain and Italy several institutes are not caught by the inquiry.

In addition, many of the institutes included are not working alone but in close co-operation with several other institutes and authorities. E.g. in the Nordic countries DHI has close contacts to the Water Quality Institute for water quality modelling in Denmark, SMHI to Askö Laboratory with the same purpose in Sweden. Also in Finland the

Reactor Laboratory at the Technical Research Centre of Finland (VTT/REA) has worked for decades together with the National Board of Waters and the Environment (NBWE), Finland, for data acquisition, model applications and interpretation of the flow patterns and the water quality results.

The 15 institutes listed above represent about 50 of the pwys and more than 60 of the personality reported in the answers to the questionnaire. This means that their share from the accumulating experience was increasing. The established co-operation networks may still increase their relative importance.

### 5.3.3 Recent trends in the model work

Commercial applications for solution of practical problems were emphasized especially by Delft Hydraulics, Danish Hydraulic Institute, SOGREAH, VTT/REA and Hydraulics Research Ltd. Most of these institutes — and a few others with fewer applications — had also specified prices for their most conventionally used models. In general, these prices were rather high ranging from about 10 000 US dollars upwards. More important than the models, however, are the skills and experience of using them. A model itself is good-for-nothing without knowing how to use it. Typical periods from one week to a couple of months are needed for appropriate learning of the model use when applied to areas of previous model applications.

In recent years the steeply decreased computer prices have reduced the necessity to work at big institutes with large main-frame computers. Simultaneously, the widely increased interest in environmental impacts with acute need for fast applications has questioned the ability of these institutes for rapid responses to external demands. That may be why separate companies have been formed and detached to carry out and continue the modelling work in several countries.

During the present study at least the following organizational changes have taken place:

- Laboratoire d'Hydraulique de France (LHF) was established by SOGREAH and University of Grenoble among others to continue large share of the model work of SOGREAH;
- Hydromod private company was established by three persons of HU/IfM to carry out part of the applications of the HU/IfM models;
- Two keypersons of modelling tasks have removed from SMHI to private firms in Sweden;
- Environmental Impact Assessment Centre of

Finland (EIA) was established as a spin—off enterprise of the Technical Research Centre of Finland (VTT) to continue and sharpen the model work of VTT/REA at the Otaniemi Science Park.

## 5.4 Model efforts in Finland

### 5.4.1 Backgrounds of the models

Modelling of water bodies in Finland derives its origin from the 1950's—1960's when Sulo Uusitalo was one of the first applying hydrodynamic-numerical techniques to calculation of water levels and flow fields (eg. Uusitalo 1960) quite soon after the pioneering works of Hansen (1956). Thereafter the modelling of flow fields became actual again in the middle of 1970's.

Main reason for the emerged interest in modelling at that time were the discharges and influences of waste waters and cooling waters. Being shallow, the Finnish water bodies had appeared to be quite sensitive to these loading effects. The transport and dilution of discharges were at first widely studied by means of tracer studies using dyes (eg. Hela and Voipio 1960), biological tracers (eg. Niemelä and Kinnunen 1968) and in most cases radioactive isotopes (eg. Kuoppamäki and Kuusi 1973). In more than 60 tracer studies (eg. Virtanen 1984) it became more and more evident that models were needed for proper interpretation of the tracer results.

The basic development of flow field and transport models in 1974—75 was carried out as a co-operation between the Reactor Laboratory at the Technical Research Centre of Finland (VTT/REA) and the Finnish Institute of Marine Research (FIMR) (Kuoppamäki et al. 1977). At both institutes further work was directed according to their special interests (eg. Virtanen 1977, Häkkinen 1979, Myrberg 1990). Gaining experience in flow velocity measurements at the National Board of Waters and the Environment (NBWE) was quite soon coupled to support the model work (eg. Sarkkula and Virtanen 1978).

Simultaneously with the advent of the flow field and transport models the water quality models were started to be developed as well (eg. Kinnunen et al. 1982). These were partly based on original Finnish research from the early 1970s (eg. Lappalainen 1975) and on the more complex EPA models from USA (eg. Kinnunen et al. 1978). Since the end of 1970s some elementary parts of the ecological models were incorporated into the

calculation of the flow velocities, transport and mixing (eg. Juutilainen 1980). The close co-operation between VTT/REA and NBWE soon resulted in the so called VENLA approach (according to the initials of the Finnish words for PRediction OF WATER QUality) (eg. Rautalahti-Miettinen et al. 1981). Further support to the combined transport and water quality models was obtained from the wide biological surveys carried out at those times (eg. Alasaarela 1980).

#### 5.4.2 Development of model types

Till the beginning of 1980's the calculations of transport and water quality were based on one-layer models further developed from that of Hansen (1956). The space-staggered (Arakawa C) grid and explicit solution with fractional time-steps were used together with versatile boundary conditions and strict conservation of water masses and the water quality components (Virtanen 1977). Simple extra assumptions were used to convert the vertical average flow velocities of total depth or epilimnion to the transport velocities of the layer of interest for the water quality.

The necessity of 3D calculation of water currents was tested from the very beginning of the model work. At first the profile type 3D models of Heaps (1971) and Bengtsson (1973) were used. When their results were compared with the measured flow velocities (Rämö 1976), it appeared that the mutual agreement was not significantly improved from that of the Hansen-type 2D calculations. When coupling the water quality aspects into the transport models, the importance of 3D simulation was tested again by using the Swedish-Norwegian version of the 3D multi-layer model developed by Simons at the Canada Centre for Inland Waters (Simons 1973, Tjomsland 1978). For calculation of the dissolved oxygen and nutrient transport, however, the 2D model with extra assumptions still seemed to be satisfactory (eg. Sarkkula and Virtanen 1983), although the assumptions all the time grew more and more complicated.

Finally the transport simulation of algal biomass showed the limits of the 2D single-layer calculations and resulted in persistent efforts for 3D modelling. Based on the principles of Simons (1980) a multi-layer model was programmed using diagonally shifted (Arakawa E) grid for diagonally rotated velocity components and solving the layer velocities indirectly through the the velocity differences between adjacent layers. The effects of gravity waves on the layer velocities were thus

eliminated and — to a great surprise — the 3D solution appeared to be even faster than the old 2D model. Apart from the basic principles, the model structure was completely rearranged from that of Simons and several modifications introduced. These included eg. independent time-steps for each subprocesses, special treatments for narrow channels and straits, arbitrary number of the vertical layers and possibilities for locally refined horizontal resolution (Koponen 1984, Virtanen et al. 1986).

#### 5.4.3 Use of the models

Since 1974 the combined flow velocity, transport and water quality models have been applied in Finland to almost 80 case studies till 1991, often as a co-operation between the National Board of Waters and the Environment and the Environmental Impact Assessment Centre of Finland (EIA, till summer of 1990 the Reactor Laboratory at the Technical Research Centre of Finland, VTT/REA). Total work directly devoted to model development and applications amounts to more than 30 person work years. At the time of the inquiry in autumn 1987, the corresponding figures were 25 pwys for more than 60 applications.

In more than 50 case studies the 2D model — usually with additional approximations — were used but recently for most part the 3D models have been utilized (eg. Sarkkula and Virtanen 1983, Sarkkula 1989, Huttula et. al. 1989). In most of the applications the effects of waste water discharges — mainly from pulp and paper industry, chemical industry, metal industry and from municipal sources — have been considered. In addition, the effects of bridge openings, harbour construction, embankments and dredging have been included in about 20 case studies. Furthermore, the effects of regulation have also been taken into account within the applications.

### 5.5 Conclusions of the model use

The inquiry showed clearly that in the development and use of numerical models there are no big differences between the countries where the national resources and research forces have been successfully collected to work together for a common goal. According to the local conditions and problems, however, the main emphases of the

models may considerably differ between different countries. E.g. in Finland the shallow and irregular water areas with many islands, narrow capes, straits and bays, steep relative depth gradients and unimportance of tidal effects have been taken into account from the very beginning in the model development work.

The sizes of the model teams were not of crucial importance for the experience — partly because the applications always need versatile co-operation and it is to some extent arbitrary which part of the field measurements, laboratory tests and data preparation are included to the model work, but more principally because the applications cannot be carried out mechanically. The success of applications is mainly a question of time, labour, data and putting one's soul into the solution. Larger teams can manage wider spectra of applications but in any specific field the data limitations most often restrict the further development of the model details independently of the size of the model team.

Finite differences (FDM) clearly dominate the applications ever more. Other methods can be used but no reason to reject finite differences has appeared. Explicit algorithms are continuously vital and useful with about 60 share of the models listed. In discussions with Delft Hydraulics it was evaluated that for a constant time step the implicit schemes may be approximately five times as slow as the explicit ones; thus about ten times increase for the time step of each sub-process is needed in order to get the implicit scheme clearly profitable. Anyhow, in the most recent model development the implicit schemes seem to be increasingly preferred.

At the time of the inquiry the three-dimensional (3D) models were coming in several institutes but the two-dimensional (2D) models still dominated the answers. In Finland the 3D models had been in permanent use since 1984 and applied to about ten applications. Everywhere the own models were overwhelmingly preferred to those acquired from other institutes. Almost 90 of the models reported to the inquiry were developed and programmed by the model team using it.

All these facts strongly supported the selection of the Finnish 3D models (the Simons — Koponen models) 3Dwf and 3Dwq (see next chapter) to be used as the basic tools in the interpretation of the Bothnian Bay currents and hydrophysics. These models were to be completed and compared with other models using other approaches, horizontal integration into e.g. vertically one-dimensional temperature and stratification models with layers distinguished by water masses or layer thickness

proportional to local depth (sigma-coordinates) instead of the horizontal layer limits used in the Finnish 3D models.

Information from other sources concerning the distribution of the model types and typical application scales were in agreement with the results of the inquiry. Also most of the most important research institutes and most of the most important model approaches were included among the answers of the questionnaire. Thus the results of the inquiry seem to present a relevant and reliable overview of the state-of-the-art of the model use in general. The time lag spent and the different geographical biases of different sources — Northern and Western Europe emphasized in the inquiry, North America in the literature — still support this conclusion.

For comparisons between different institutes or between different models, however, the inquiry results are far too insufficiently checked, normalized and updated. Thus the results should not be used as a selection guide for real application requests. For this purpose special competitions as organized e.g. in Norway in spring 1989, and in practice the experiences and recommendations of previous customers are much more appropriate basis for model selections.

Altogether, the numerical models are in active use in several countries all over the industrialized world. Big differences in the ways of application and in the know-how between different experienced model teams do not exist. Successful applications call first of all for entering into the essence of the specific case. This is done as a mutual interaction between data and calculations which requires time and labour. Only with them the know-how is accumulated.

Different models, approaches and numerical methods can be used for applications. Their frequency distributions among the inquiry answers do not conflict the impressions received from literature, meetings, visits and personal contacts. This confirms and supports the significance of the inquiry distributions as proper indicators of the state-of-the-art of the numerical models.

## 6 DEVELOPMENT OF THE MODELS AND PROGRAMS

In this chapter the development of the 3D (3-dimensional) flow, temperature and water quality models and the 2D multigrid flow model are

studied. Different models can be specified e.g. with the following nomenclature. bf 3Dwf, bf 3Dwt and bf 3Dwq are the 3D water flow, temperature and quality models and bf 3Dwftq is the totality of the 3D models.

## 6.1 Development of the 3D current model

Development of the 3D current model was divided into the following main tasks:

- inclusion of radiation and heat exchange processes into the model
- local resolution improvement
- direct calculation of the layer velocities
- vectorization of the code
- model comparisons.

The first item will be discussed in the section refwtemp and the last in refcompa1 and refcompa2. Other points will be discussed after the following introductory section. A more detailed treatment will be published in Koponen (1991). For instance the development of terms for the Coriolis and nonlinear factors and new techniques to improve efficiency of the models are studied and the implementation documented in Koponen (1991). Because this discussion is by nature too technical and would take too much space it is not included in this paper.

### 6.1.1 Background

When the well-justified hydrostatic assumption, Boussinesq-approximation and incompressibility of water are taken into account the momentum equations for fluid are:

$$\frac{\partial \mathbf{u}}{\partial t} = f\mathbf{v} - \frac{1}{\rho_0} \frac{\partial p}{\partial \mathbf{x}} + \frac{\partial}{\partial \mathbf{x}} (\nu_{\text{hor}} \frac{\partial \mathbf{u}}{\partial \mathbf{x}}) + \quad (2)$$

$$\frac{\partial \mathbf{v}}{\partial t} = -f\mathbf{u} - \frac{1}{\rho_0} \frac{\partial p}{\partial \mathbf{y}} + \frac{\partial}{\partial \mathbf{x}} (\nu_{\text{hor}} \frac{\partial \mathbf{v}}{\partial \mathbf{x}}) + \quad (3)$$

$$\frac{\partial p}{\partial z} = -g\rho \quad (4)$$

$$\Delta \cdot \mathbf{u} = 0 \quad (5)$$

where

$\mathbf{u}$	is the velocity vector ( $\text{ms}^{-1}$ )
$u, v, w$	are the x, y and z velocity components ( $\text{m s}^{-1}$ )
$t$	is the time (s)
$p$	is the pressure (Pa)
$\rho_0$	is the reference (average) density ( $\text{kg m}^{-3}$ )
$f$	is the Coriolis coefficient ( $\text{s}^{-1}$ )
$g$	is the acceleration of the earth's gravity ( $\text{m s}^{-2}$ )
$\nu_{\text{hor}}, \nu_{\text{ver}}$	are the horizontal and vertical turbulent momentum exchange coefficients ( $\text{m}^2 \text{s}^{-1}$ ).

In the above mentioned equations the momentum advection,  $(\mathbf{u} \cdot \Delta)\mathbf{u}$ , can quite often be ignored. The cases when it can't be ignored are for instance high velocity jets and large depth gradients. The horizontal and vertical momentum diffusion coefficients are indicated separately to stress the usual order of magnitude difference between their values. Pressure  $p$  can be divided into the barotropic (external) and baroclinic (internal) parts:

$$p = p_e + p_i \quad (6)$$

$$p_e = g\zeta\rho_0 + p_a$$

$$p_i = g \int_z^{\zeta} \Delta\rho \, dz,$$

where  $\zeta$  is the surface elevation,  $2p_a$  the air pressure and  $2\Delta\rho = \rho - \rho_0$  the density difference. Quadratic boundary conditions are usually assumed on the surface:

$$\tau_{sx} = \rho_0 \nu_{\text{ver}} \frac{\partial v}{\partial z} \Big|_{z=-\zeta} = K_s \rho_a u_a \sqrt{u_a^2 + v_a^2} \quad (7)$$

$$\tau_{sy} = \rho_0 \nu_{\text{ver}} \frac{\partial v}{\partial z} \Big|_{z=-\zeta} = K_s \rho_a v_a \sqrt{u_a^2 + v_a^2},$$

where  $\tau_{sx}$  and  $\tau_{sy}$  are the surface wind stress components,  $K_s$  is the wind friction coefficient,  $\rho_a$  is the air density and  $u_a$  and  $v_a$  are the wind velocity components. The wind stress is often the most important forcing factor in water circulation and thus the accurate modelling of it is of primary importance. First of all the wind velocity  $u_a$  should be accurate in every point. This would require extensive measurements and a wind model because the wind may vary from one location to another. Also the wind friction coefficient  $K_s$  should be modelled accurately. For instance surface roughness (short waves and ripples) affect the friction coefficient. Often modelling is done however without proper knowledge of the real wind



velocities over the water body. Then the wind friction must be correlated with wind measurements on some nearby locale (usually a weather station or an airport) through the wind friction coefficient. In this case the wind friction coefficient should take into account the wind measurement height, surface roughness (different wind velocities e.g. for water, field, forest), the distance the wind has travelled from the shore (wind fetch), the angle the wind turns on the boundary between land and water etc. In Finland Sarkkula has studied the wind stress and its effects in natural basins based on extensive current and wind measurements and modelling applications (Józsa et. al. 1990).

Bottom stress formulation has been either linear or quadratic. The quadratic form is

$$\begin{aligned}\tau_{bx} &= \rho_0 \nu_{\text{ver}} \left. \frac{\partial u}{\partial z} \right|_{z=-H} = K_{\text{bq}} \rho_0 u \sqrt{u^2 + v^2} \quad (8) \\ \tau_{by} &= \rho_0 \nu_{\text{ver}} \left. \frac{\partial v}{\partial z} \right|_{z=-H} = K_{\text{bq}} \rho_0 v \sqrt{u^2 + v^2}\end{aligned}$$

and the linear one

$$\begin{aligned}\tau_{bx} &= K_{\text{bl}} \rho_0 u \\ \tau_{by} &= K_{\text{bl}} \rho_0 v.\end{aligned} \quad (9)$$

The linear bottom friction coefficient can be a constant or a depth dependent function e.g.

$$K_{\text{bl}} = \frac{r}{H} \quad (10)$$

or

$$K_{\text{bl}} = rH, \quad (11)$$

where  $H$  is the depth. Bottom friction depends also on the bottom inclination and turbulence, see Fisher (1981, pp. 74–75) for the formulations. According to the Delft Hydraulics Laboratory the usual approximation should be replaced with a more accurate one where the profile of the stress is approximated near the bottom, see Fisher (1981, pp. 528–530).

The equations mentioned above can be solved analytically only in some simple cases. Usually the equations must be discretized and solved computationally. The biggest differences between models arise in the discretization (integration) process. The simplest ones are 0D models where the basin is described with only one cell. In 1D models either both horizontal or one horizontal and vertical dimensions are integrated. 3D models describe all the velocity components. There exists also models which describe 3D currents, but where one (usually vertical) velocity component is obtained by

analytical means, e.g. by the use of basis functions. The selection criteria for the model depends on the problem under consideration. As a rule of thumb the 0D model can be used for completely mixed small ponds, 1D model for rivers, 2D model for very shallow lakes and 3D model for any water body. The 3D model can also be used as 0D, 1D or 2D one. The number of dimensions should be kept as low as possible for the sake of effectiveness. On the other hand unnecessary integration should be avoided because it can lead into complications in the calibration of the model.

The principal tool chosen for the Bothnian Bay study was the 3D model introduced by T.J. Simons (Simons 1980; Simons and Kielman 1984; Koponen 1984). The simple idea behind the model is to divide the calculation of the velocities into two parts. First part (vertically integrated currents) contains the free surface elevation calculation. The second part (velocity differences) doesn't contain the free surface equations and is computationally much cheaper. The model is explicit, which implies easy programmability and correct time behaviour. The model was chosen mainly because of the possibility to change the code easily and because of the very reasonable computer costs required by the model. The computer costs were main concern because of the large time spans of the Bothnian Bay simulations. The optimal computer costs of the model were verified by comparing the model computer time consumption with that of two 2D models (explicit Hansen model (VTT) and one implicit model (VITUKI)) and a 3D model (Phoenix).

The actual definition of the relations of the numerical model varies from method to method. These relations may be determined e.g. through the weighted residual method. There the starting points are the continuous functions and the partial differential equations. A space of approximating (trial) or basis functions  $\mathbb{W}_h$  on  $\Omega_h$  is assumed and the solution on  $\Omega_h \times \Omega_\tau$  is written by

$$u(x, t) = u_0(x, t) + \sum_{\beta \in N_h} a_\beta(t) u_\beta(x) \quad (12)$$

where  $u_0$  represents the initial and boundary conditions,  $x = (x_1, \dots, x_n)$  is the space vector and  $N_h$  is the set of the nodes. Note that in this expression the separation of the time and space dependent functions is assumed and the functions  $u_\beta \in \mathbb{W}_h$  are assumed to be known. These solutions are inserted into the differential equations and a residual  $R$  is obtained.  $R$  is normally not zero, because the approximate functions (12) don't usually fulfill the differential equations

exactly. When this residual is integrated over the calculation domain with different weight functions one obtains the equations for the unknowns  $a_\beta$  when the result is required to be zero:

$$\int_{\Omega_h} \phi_\beta R dv = 0, \quad \beta \in N_n \quad (13)$$

where  $\phi_\beta$  is a weight function. The different methods can be enumerated according to form of the weight function:

### 1. Subdomain method

It is required that

$$\begin{aligned} \phi_\beta(x) &= 1, \quad x \in e_\beta \\ \phi_\beta(x) &= 0, \quad x \notin e_\beta \end{aligned} \quad (14)$$

where  $e_\beta$  is the simplicial element of  $\Omega_h$ . This method requires that the average error vanishes over the elementary subdivisions, thus the conservation property is preserved.

### 2. Collocation method

$$\phi_{\beta(x)} = \delta(x - x_\beta), \quad (15)$$

where  $\delta$  is the Dirac delta function.

### 3. Least-squares method

$$\phi_\beta(x) = \frac{\partial}{\partial a_\beta}. \quad (16)$$

Which is equal to the requirement that

$$\int_{\Omega_h} R^2 dv \quad (17)$$

is a minimum.

### 4. Galerkin method

$$\phi_\beta(x) = u_\beta(x) \quad (18)$$

i.e. the weight functions are the same as the approximating functions in (12). (13) indicates that the approximate solution (12) would be the best approximation in the function space  $W_h$ , where the norm  $\|\cdot\|_{W_h} = \int_{\Omega_h} \cdot dv$ . In other words the approximate solution would be orthogonal to the error vector in the  $W_h$  norm.

Other methods for defining discrete numerical models are the finite difference and finite volume methods. In finite difference method the Taylor expansion is used to obtain the discrete dependencies. Finite difference method resembles collocation method, but no explicit assumption of the

form of the solution function (12) is needed. Finite volume method resembles subdomain method but it is similar to finite difference method in the respect that no explicit knowledge about the form of the solution functions is needed. Finite volume method has two advantages: it is by nature conservative (that is it preserves the conservation properties of the original equations) and it allows complicated computational domains to be discretized in a simple (but not necessarily accurate) way. The disadvantage of the finite volume method is that the higher order derivatives required are not easily solved. The porosity method (Versteegh 1990) resembles the finite volume method. The porosity method however requires completely regular grid. In this method partly blocked cells are modelled by making them porous, in other words the blockage is distributed evenly over the cell.

It should be noted that in practice a mathematical model is often obtained through physical considerations directly on the discrete domain. The end result is usually same as from the finite volume method. Because of the easily understood physics behind the finite volume method it is chosen to be the principal tool in this work.

The grids and equations for solving the unknown variables in more complicated divisions of the calculation domains where the boundaries of the subdivisions are curved or the grid is not orthogonal can be solved by transforming the original system into a rectangular one and solving the equations there. The governing equations are expressed in terms of the generalized coordinates as independent variables and the discretization is taken in generalized coordinate space, see Fletcher (1988b, pp. 46—123) for the use of generalized coordinates and grid generation. The use of the generalized coordinates enables adaptive grid generation (grid concentration) for the areas of severe gradients. One disadvantage is that the transformation generates additional terms (transform parameters) which can increase considerably the complexity of the equations to be solved and thus the computational efficiency is decreased. (Often however the orthogonality of the grid is utilized or not all terms in the transformed equations are calculated.) Other disadvantages are the accuracy deterioration especially in the case of non-orthogonal systems, need for complicated grid generation programs and increased geometrical data. The generalized coordinates work well if the curvilinear grid can be chosen along streamlines of the flow, but if recirculating flows are present this is generally impossible. Especially sharp corners pose problems (Versteegh 1990, p. 8.4). For environmental flows the curvilinear grid system

seems to be in most of the cases an unnecessary complication. Cartesian grid systems where the grid is refined in the sensitive areas is an adequate approach for most of the cases.

The finite volume method is suitable for solving the fluxes in irregular divisions and the applications result in particularly simple and efficient methods at least in slightly deformed divisions. But when the pressure gradients and second derivatives must be solved the derivations of the approximate expressions are not that clear. The derivation of the finite volume approximation for the second derivatives can be found in Fletcher (1988a, pp. 107–111). Later on this chapter a simple approximation for the diffusive processes will be suggested. The pressure gradients and diffusive fluxes in varying gridwidth cells will be discussed in the next section.

Often the main reason for using non-Cartesian grid is the fitting of the grid to the boundaries of the calculation domain. Especially the advocates for the finite element method use this argument. When the boundary processes are of vital importance as in the airfoil calculations or the forces act on complicated objects as in structural analysis the use of non-Cartesian grids is understandable. However for environmental processes the rectangular approximation of the calculation domain boundaries seems quite adequate for most of the cases. Probably only the bottom topography modelling would possibly benefit from a boundary fitted treatment because the bottom topography affects strongly the flow.

### 6.1.2 Local resolution improvement

In many practical environmental problems the area of interest is rather limited but is affected by a much larger surrounding area. Places where discharges from rivers, industry and communities cause discernible local effects are typical interest areas. The resolution of the models has to be good near the discharge points because of the steep gradients of the substances released into the water body. Use of large grid widths in these sensitive areas would lead into unrealistically large mixing and dilution of the released substances. On the other hand the required resolution can't be usually applied to larger areas with the current model techniques, because the computation times would become prohibitively expensive.

In the worst case a crude explicit 3D free surface flow model calculation times would be proportional to more than fourth power of the gridwidth. This effect stems from the facts that number of

gridcells is proportional to the third power of the gridwidth, explicit timestep to the first power and additional limitations arise in the free surface flows from the fact that usually improved resolution increases the maximum depth of the grid because less and less averaging is done with increased resolution (e.g. in an explicit 1D free surface model the stability condition is  $\Delta t_{\text{ext}} \leq h/\sqrt{gH_{\text{max}}}$ ).

In the case of the explicit 3D transport models the calculation time is proportional to more than the third power of the gridwidth. This is caused by the unhomogeneous distribution of the flow. When the resolution increases in some cells the detention time ( $V/Q$ ) decreases and the timestep must also decreased accordingly ( $\Delta t_c \leq V/Q$ ).

Typical example of this is the vertical resolution increase. As an example in the wind driven flow the greatest velocities are on the surface and less averaging in the surface means smaller timesteps. In summary it can be seen that the limits to the possible number of gridcells are rather strict. The possibilities to improve efficiency of the models will be discussed later on in this chapter ("Development of the multigrid current model") and in Koponen (1991). This section will be devoted to the idea of local resolution improvement.

Local resolution improvement can be obtained through the generalized coordinate system, finite element method, nested grid systems etc. A typical local resolution improvement method is to use Cartesian grid system and divide the basic elements into smaller units (most popular method seems to be to divide each grid element boundary into three equal parts) in the areas where higher resolution is needed. This type of division however complicates the calculation algorithm considerably compared with a more regular grid. Another disadvantage in the straightforward explicit methods is that the possibly very limiting fine grid timestep must be used also in the coarse grid areas. Nested model systems would allow the solution of sufficiently general systems with easy implementation and with efficient utilization of different timesteps in different areas.

Multigrid method is an example of nested systems. When the numerical method reduces the high-frequency components of the error the resulting smooth error is reduced in a coarser grid. Coarse grid fridlength is typically two times that of the next level,  $h_{l-1} = 2h_l$ , and thus the level index  $l$  indicates also the number of divisions of the sides of the calculation domain with 2 into  $2^l$  divisions. One needs to restrict the error from the finer grid to the coarser one through **restriction** and the obtain the finer grid correction through **prolonga-**

tion. Typical prolongation operator is a piecewise linear interpolation operator. An example of a restriction operator in 1D case would be (Hackbusch 1985, p. 40):

$$u_{l-1}(i) = ru_l(i) = \frac{1}{4} [u_l(i-1) + 2u_l(i) + u_l(i+1)] \quad (19)$$

where the restriction operator  $r$  maps the level 21 values  $u_l$  to the level  $l-1$ . The multigrid method will be discussed more thoroughly later on this chapter.

A simple nested grid algorithm is suggested to calculate the state variables with different resolutions in different areas. The different grids are coupled with each other through the common boundaries. The grids don't have to cover the same calculation area as in the multigrid, that is the finer grid areas can cover only partly the calculation domain. The levels of grids denote the spatial resolution: the highest level  $l_{\max}$  contains the most detailed information about the topography of the calculation domain. In each level there can be more than one grids. Simple algorithm for nested calculations would be:

1. set level number  $l$  to 0
2. set  $l$  to  $l+1$
3. build level  $l$  grids (level 1 grid contains typically the whole calculation area and takes into account the large scale circulation and mass transfer)
4. if  $l > 1$  block in the level  $l-1$  grids the areas corresponding to the level  $l$  grids (not necessary but saves computational time)
5. go to 2 until no more local resolution improvement is needed
6. build a model for all grids
7. set the restriction boundary values (set the blocked area boundary values for the lower level calculation)
8. set level number to 0
9. set level number  $l$  to  $l+1$
10. calculate the values of the state variables in the models corresponding to the level  $l$
11. if  $l < l_{\max}$  prolongate the boundary values for the level  $l+1$
12. if  $l > 1$  restrict the boundary values for the level  $l-1$
13. if  $l = l_{\max}$  and the calculation is not finished go to 8
14. go to 9 until calculation finished.

To simplify this scheme the values are calculated in each grid in each timestep. Because the different grids probably have different limiting timescales it is not necessary to calculate all the values in all the grids in each timestep. The scheduling of different

subprocesses is discussed further in Koponen (1991).

During the Bothnian Bay project a simple change of gridwidths was implemented in the model for local resolution improvement. The change of gridwidth is not free, for instance the number of cells in any row or column is constant and the gridwidth defined is propagated throughout the whole area (see Fig. 9). This restriction is utilized mainly for the simplicity of the model.

The efficient implementation of the varying gridwidths depends on proper formulations for the diffusive terms and the pressure gradients and the use of finite volume method for the fluxes (Koponen 1991). When the grid width varies a four point scheme is used for the pressure gradients. It is however computationally much more inefficient than the two point scheme for regular grids. For this reason there are in the model subroutines for both two point and four point gradients. The user can select the two point module also when the grid width is varying if the accuracy of the result is not deteriorated too much. The justifications for using two point schemes and surface smoothing are given in Koponen (1991).

### 6.1.3 Direct calculation of the layer velocities

As was stated previously the Simons model principle which is used in 3Dwf is to calculate the layer velocities through vertically integrated velocities and velocity differences. This scheme is very efficient in the case of the explicit numerical methods because the effect of the gravity wave propagation is isolated in the 2D part of the model. In the Bothnian Bay project the model was extended to include the direct calculation of the layer velocities for four reasons:

- to test the applicability of the Simons model
- to increase in some cases the computational efficiency
- to limit the vertical mixing — to include processes not easily modelled with the Simons principle.

Unfortunately the change was of such a magnitude that there was no time to include density calculation and varying grid widths in the direct layer calculation. Still the principal characteristics can be obtained already from this limited experiment.

The applicability of the Simons model was tested by calculating the same situation with Simons principle and directly. The solutions were practically identical with small values of horizontal

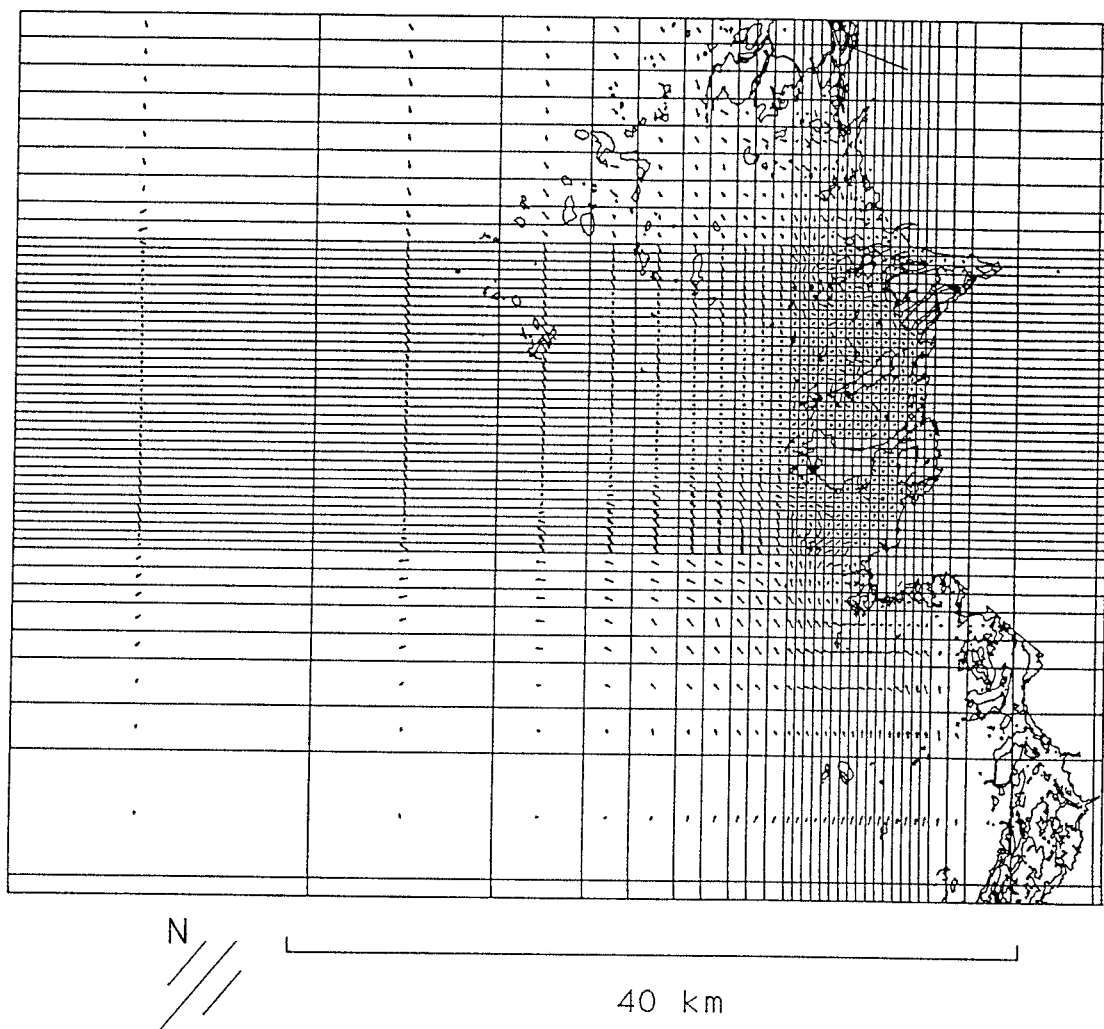


Fig. 9. An example grid on the Bothnian Bay area. Local resolution improvement concentrated off the town Kemi.

diffusion coefficients. The increase of the horizontal diffusion coefficient brought about a slight change between the solutions because the diffusion approximation introduced previously was used in the Simons model.

The increase of the computational efficiency was tested by calculating the nonlinear case with Simons principle (layer velocities were solved at each iteration step) and with directly calculating the layer velocities. The efficiency increase was an hypothesis because in the nonlinear case the layer velocities must be solved in each iteration step for the calculation of the momentum advection. The Simons principle was however about 25 faster than the direct calculation even when the timesteps for the vertically integrated velocities and velocity

differences were the same.

One factor causing increased mixing especially in the vertical direction is the limited resolution both in the vertical and the horizontal direction. It can be easily understood that bigger cells bring about larger mixing and less steep gradients. Especially the closed boundaries of the calculation domain are places where the natural up- and down-welling is exaggerated in the models and thus the vertical mixing tends to be too large. The resolution should be high on the borders and over the steep gradients in order to model the vertical density gradients correctly.

One solution to the unrealistically big mixing is to model the thermocline as nonpermeable boundary whose height is calculated. The difficulty with

this approach is that the natural up- and down-welling must be modelled with some more or less arbitrary mixing coefficient over the thermocline.

In 3Dwf permeability between the layers is used to combat the vertical mixing. It describes the fraction of the flow that passes through a layer boundary freely. The rest builds up pressure. The pressure buildup is positive when the flow is going upwards and negative with downward flow. The upward vertical flow is formed when there is more water coming to the computational cell than leaving it during the time-step. When the pressure builds up it tends to diminish the flow coming into the cell (vice versa for the negative pressure buildup) and the desired effect is obtained. This phenomena is analogous to the density calculation where dense water is transported upwards over the layer boundary. When heavy water is lifted upwards the pressure change tends to diminish the flow bringing water into the cell. The permeability algorithm differs however from the density calculation because no actual advection of water is assumed. The vertical permeability model illustrates a process that is not easily modelled with the Simons principle and for which the layer velocities must be solved.

#### 6.1.4 Vectorization of the code

During the Bothnian Bay project the model was implemented in the new Cray X-MP/416 housed in the Finnish State Computer Centre (VTKK) and run by Center for Scientific Computing (CSC). The purposes of the implementation were

- to test the applicability of the filtered flow fields for the mass transfer calculations
- to calculate flow fields, temperature and salinity in natural conditions for long periods (8 years was chosen for the calculation period)
- to apply the model for grid systems with large number of nodes (20000 nodes with the shortest gridlength in the horizontal direction few hundreds of meters).

The first results were disappointing. The LINPACK test in full precision using all FORTRAN code gives for Cray X-MP/4 an efficiency of 59 MFLOPS while that for the  $\mu$ VAX II is 0.13 MFLOPS (operating system VMS v4.5, observe that f77 in Ultrix 1.1 gives only 0.082 MFLOPS), a 453 fold increase of speed (Dongarra 1988). The obtained speed increase for non-vectorized 3Dwf was however only about 20. This can be understood with the help of the widely cited Amdahl's law:

$$s = \frac{S + V}{S + V/n}, \quad (20)$$

where  $S$  is the time consumed by scalar code and  $V$  in the code which can be vectorized and  $n$  is the speedup obtained with the vectorization (for Cray  $n$  is typically 10). As can be seen from the Fig. 10 the efficient use of the Cray demands large portion of the code to be vectorizable ( $> 80\%$ ).

When the module which calculates the external flow field (vertically averaged velocities) was optimized, a 120 fold increase of speed was obtained compared with  $\mu$ VAX II (the same speedup was obtained also for the water quality model). If we assume that the LINPACK test would vectorize completely this would give for the whole code about 70% vectorization ratio. Dramatic increase would be obtained with small improvements, but the improvements require lot of reprogramming. The most important feature would be to calculate the loops differently.

Cray vectorizes only the innermost loop which happens to be in 3Dwf the  $k$ -loop, that is the loop over the depth, which is generally the shortest one. Due to the register architecture in Cray the innermost loop should be evenly divisible by 64 in order to obtain the best speedup, thus long inner loops would increase the efficiency. (In the external module there was no vertical loop and the optimization was mainly due to the elimination of the IF-clauses.) Even the  $i$ - and  $j$ -loops could be eliminated in the program and the values could be calculated in just one loop. Fortunately the program uses 1-dimensional loops so this would not demand inordinate amount of work, although the boundary values would require special attention. Often it pays also to calculate the zero cells

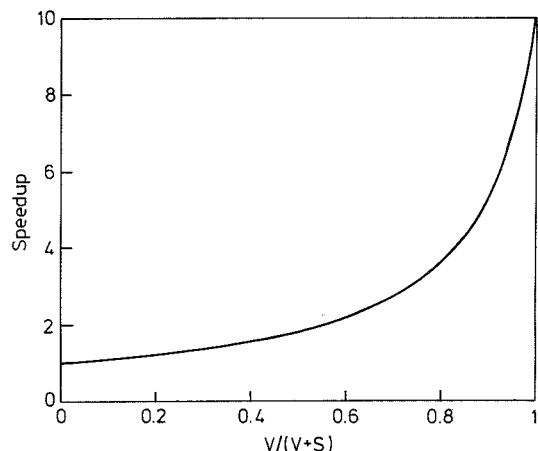


Fig. 10. Speedup as the function of the ratio  $V/(V + S)$  (Karttunen et. al. 1990).

in order to lengthen the inner loops. Preliminary tests indicated that it pays to calculate the values in all points when the number of the zero cells is less than about 35 of all gridcells.

Especially the direct calculation of the layer velocities could be vectorized effectively. The Simons principle requires a solution algorithm which cant be vectorized as easily. For instance the algorithm which calculates the layer velocities from vertically integrated velocities and velocity differences requires the values from the previous loop-step. This would prevent vectorization because the em pipelining could be not utilized.

Pipelining is the simultaneous operand calculation in a "pipe: the operands are fed in each cycle into one end of the execution pipe and the results are obtained from the other. For programming purposes one doesnt normally have to know the hardware implementation of the machine, it is often enough to consider a simple test for vectorization: if an operation can be executed simultaneously to all operands in question the code vectorizes. When the execution of any loop-step depends of the previous execution of the loop this test is not passed.

## 6.2 Development of the multigrid current model

### 6.2.1 Outline of the multigrid method

The multigrid method is a relatively new algorithm for solving elliptic (and to some extent also other) partial differential equations. It is mathematically optimal, as its cost is proportional to the first power of the number of unknowns. This is a great improvement compared to the cost of the classical iterations, which is proportional to the square of the number of unknowns.

The multigrid method is based on the observation, that the classical relaxation iterations produce very quickly smooth residuals, and smooth functions can be approximated well by means of coarser grids. The coarser grid solution is not capable of distorting the high frequency components, but it can reduce low frequency residuals instead. The finer grid smoothing and coarser grid correction have thus complementary properties in reducing the errors. Combined together they give an extremely efficient iterative procedure for solving some classes of equations. The coarser grid correction can be solved exactly (two-grid method) or recursively on coarser and coarser grids

(multigrid method). For complete discussion of the multigrid techniques see Hackbush (1985).

### 6.2.2 Inverse multigrid approach

In most multigrid programs the coarsest grid geometry must be explicitly given as input data, while all the finer grids are generated automatically. On the coarsest grid the exact solution is produced, on all the other grids some relaxation is performed. Although this approach is quite useful in many cases, it can be applied in Finland to very few lakes only.

The geometry of Finnish lakes and coast is mostly very complicated and often even several dozen times connected. The above approach would lead in Finland to large coarsest grid equations, which contain hundreds or even thousands of unknowns, and the exact solution would not be any more reasonable. Because of this fact we have decided to use inverse approach. The finest grid is given to the program, and all the other grids are generated during the calculation by means of simple depth integration. When moving from finer to coarser grid some islands, bays etc. disappear, the geometry becomes simpler and fewer times connected. The simplification of the geometry does not disturb the calculation procedure, it retains the full efficiency of the powerful multigrid technique.

### 6.2.3 The multigrid solver

Consider the following simple set of stationary equations:

$$-\frac{r}{H}u - g\frac{\partial\eta}{\partial x} + \frac{\lambda WW_x}{H} = 0 \quad (21)$$

$$-\frac{r}{H}v - g\frac{\partial\eta}{\partial y} + \frac{\lambda WW_y}{H} = 0 \quad (22)$$

$$\frac{\partial}{\partial x}(Hu) + \frac{\partial}{\partial y}(Hv) = \dot{q} \quad (23)$$

Equations (21) and (22) are simplified two-dimensional Navier-Stokes equations containing only bottom friction, pressure gradient and wind friction. Equation (23) is two-dimensional continuity equation with source term. Using staggered mesh system of Hansen (pressure at cell centre, velocities on cell faces), expressing velocities from the equations of motion and substituting them into the continuity equation, we obtain ordinary diffusion problem of the symbolical form shown in

Table 5.

If we choose natural boundary conditions, we must ensure that the source term  $b_{ij}$  is globally conservative. The set of equations in Table 5 is a perfect one to be solved by means of multigrid technique. In our multigrid program we use Gauss-Seidel smoothing, four-point restriction and four-point prolongation. This preserves the five-point star scheme of the original equation. The velocities are not iterated, but they are computed only once at the end of the calculation. We have applied this multigrid solver to many grids, and it turned out to be even more efficient than we had expected. It has even been possible to compute flow fields on a grid as large as  $512 \times 512 \times 512$  cells (262, 144 unknowns), and it only took less than half an hour to perform the task on MicroVAX II (Table 6).

Table 5. Diffusion problem in symbolical form.

$$\begin{array}{c}
 -D_{ij}^y \eta_{ij+1} \\
 -D_{i-1j}^x \eta_{i-1j} + (D_{ij-1}^y + D_{i-1}^x + D_{ij}^x + D_{ij}^y) \eta_{ij} - D_{ij}^x \eta_{ij+1} = b_{ij} \\
 -D_{ij-1}^y \eta_{ij-1}
 \end{array}$$

### 6.2.4 Kernel correction method

An attempt has been made to include also some other terms in the equations of motion. We ran into difficulties when trying to add the Coriolis term, as it turned out to be dominant over the diffusion in case of varying depth. Even relatively small depth gradient may make the Coriolis term dominant. This can be avoided by making the equations instationary and using sufficiently small time step. Although in this way the program still behaves like multigrid, its efficiency is practically lost due to large proportionality factor of the cost. There is however another remedy. In order to be able to express the velocities from the modified (with the Coriolis term) equations of motion in sufficiently simple manner, we have decided to switch to the staggered mesh system of Simons (velocities at cell centre, pressure in cell corners). Substituting the velocities into the continuity equation, we obtain the diffusive-rotative nine-point scheme (Table 7).

When the Coriolis term equals zero, the set of equations splits into two independent diffusion equation sets. This should be taken into account when correcting the conservativity of the source term  $b_{ij}$ . The Coriolis term matrix  $C_{ij}$  is antisymmetric, has a non-trivial kernel and often dominates over the diffusion matrix  $D_{ij}$ . In another words it is an ill-conditioned problem. In order to

Table 6. CPU times (s) for Bothnian Bay calculations.

L	N = 2 <sup>L</sup> * 2 <sup>L</sup>	INITCPU	ITERCPU	ITERCPU*100
				INITCPU*N
2	4	0.52	0.05	0.31250
3	64	0.52	0.22	0.17188
4	256	0.55	0.84	0.16406
5	1 024	0.96	3.36	0.16406
6	4 096	2.59	13.62	0.16626
7	16 384	9.01	66.58	0.20319
8	65 536	34.87	289.27	0.22070
9	262 144	151.58	1 329.28	0.25354

Table 7. Diffusive-rotative scheme of the kernel correction method.

$$\begin{array}{c}
 -D_{ij+1} \eta_{i-j+1} \\
 -(C_{ij+1} - C_{ij}) \eta_{i-j} \\
 -D_{ij} \eta_{i-j-1} \\
 - (C_{i+1j+1} - C_{ij+1}) \eta_{ij+1} \\
 + (D_{ij} + D_{i+1j} + D_{ij+1} + D_{i+1j+1}) \eta_{ij} - \\
 - (C_{ij} - C_{i+1j}) \eta_{ij-1} \\
 - D_{i+1j+1} \eta_{i+1j+1} \\
 - (C_{i+1j} - C_{i+1j+1}) \eta_{i+1j} = b_{ij} \\
 - D_{i+1j} \eta_{i+1j-1}
 \end{array}$$



get rid of complex eigenvalues let us find the least square solution of the equation in Table 7:

$$(D + C)^T(D + C)\eta = (D + C)^Tb \quad (24)$$

Although this new matrix is even more ill-conditioned, it is a positive definite, and so the equation (24) can be solved iteratively by e.g. Gauss-Seidel method. We may attempt to apply multigrid approach to this equation, but generally it will not work. To understand the reason for this behaviour, we must split each eigenvector of the matrix  $(D + C)^T(D + C)$  into two parts: the one belonging to the kernel of the matrix  $C^TC$ , and the other to the image of the matrix  $C^TC$ . It is plain, that during the iteration of the equation (24) the matrix  $I - O(C)$  cannot influence kernel parts at all, even if it is efficient in reducing image parts. It remains entirely to the matrix  $I - O(D)$  to reduce the kernel parts, but it can do this only at a very low rate, as the  $C$  matrix dominates. For the multigrid to work, the high frequency components must be smoothed entirely, it is not sufficient to smooth only their image parts. Suppose we now solve the following residual equation

$$D^TDx = D^T(b - D\eta - C\eta) \quad (25)$$

The solution  $x$  does contain the lacking kernel parts, but if we corrected  $\eta$  with this  $x$ , the iteration of (24) and (25) together would be a divergent process. This is because  $x$  contains amplified image parts as well, and the iteration of (24) would not reduce them sufficiently. Therefore we have to remove image parts from  $x$  before we perform the correction. This can be achieved by solving the equation

$$C^TCy = C^Tx \quad (26)$$

and computing new  $x$

$$x := x - Cy \quad (27)$$

This correction improves only the kernel parts leaving the image ones unchanged, and thus ensuring stability of the whole process. Image smoothing and kernel correction together reduce high frequency components efficiently enough to be combined with the multigrid technique. It is advisable, but not obligatory — the kernel correction method can be used as a simple iteration as well. It has been applied to several test problems and it has worked efficiently in all cases.

## 6.3 Development of the 3D temperature and salinity model

Mathematically the concentration changes in the water bodies are described by the equation

$$\frac{\partial c}{\partial t} = -u \cdot \Delta c + \nabla \cdot (D_{\text{hor}} \nabla c) + \frac{\partial}{\partial z} (D_{\text{ver}} \frac{\partial c}{\partial z}) + P_c + S_c \quad (28)$$

where  $c$  is the concentration,  $D_{\text{hor}}$  horizontal and  $D_{\text{ver}}$  vertical eddy diffusion coefficient,  $P_c$  biological-chemical-physical processes and  $S_c$  contains the external sinks and sources. This equation is applicable for temperature, salinity and the various water quality factors.

For the temperature modelling the important factor is  $S_c$  in equation (28). This will be studied in the next sections.

### 6.3.1 Temperature model

The principle of energy conservation leads into the following equation

$$\begin{aligned} \frac{\partial}{\partial t}(\rho T) = & - \sum_j \frac{\partial}{\partial x_j} (u_j \rho T) - \sum_j \frac{\partial}{\partial x_j} (\overline{\rho u_j' T'}) \\ & + \sum_j \frac{\partial}{\partial x_j} \left( \frac{\mu_l}{\rho \sigma_l} \frac{\partial}{\partial x_j} (\rho T) \right) + \frac{S_H}{c} \end{aligned} \quad (29)$$

where

- $T$  is water temperature ( $^{\circ}\text{C}$ )
- $\rho$  is density of water ( $\text{kg m}^{-3}$ )
- $c$  is specific heat of water =  $4.2103 \text{ (J } ^{\circ}\text{C}^{-1} \text{ kg}^{-1})$
- $\mu_l$  is laminar viscosity ( $\text{kg m}^{-1} \text{ s}^{-1}$ )
- $\sigma_l$  is laminar Prandtl number
- $u_j$  is velocity ( $\text{m s}^{-1}$ )
- $x_j$  is space coordinate (m)
- $S_H$  is source and sink term ( $\text{J m}^{-3} \text{ s}^{-1}$ ).

The terms in equation (29) are (from left to right) local change, transport, turbulent diffusion, molecular diffusion and source and sink term.

Turbulent heat transfer is modelled analogous to the laminar viscosity:

$$\overline{\rho u_j' T'} = \frac{\mu_t}{\sigma_t} \frac{\partial T}{\partial x_j} \quad (30)$$

where  $\sigma_t$  is the turbulent Prandtl number. Laminar viscosity in environmental flows is insignificant compared to the turbulent viscosity. When water density is assumed to be constant equation (29) is simplified into

$$\frac{\partial T}{\partial t} + \sum_j u_j \frac{\partial T}{\partial x_j} = \sum_j u_j \frac{\partial}{\partial x_j} \left( \frac{\nu_t}{\sigma_t} \frac{\partial}{\partial x_j} (T) \right) + \frac{S_H}{\rho c} \quad (31)$$

where  $\nu_t$  ( $\text{m}^2 \text{s}^{-1}$ ) is kinematic eddy viscosity. See Svensson (1978) for detailed derivation of  $\mu_t$  and  $\sigma_t$ .

### 6.3.2 Source and sink term

The source and sink term  $S_H$  consists of internal absorption of solar radiation and heat discharges and sinks (cooling waters, heat pumps). The infrared part of solar and atmospheric radiation is absorbed within 1 m from surface so that it is taken into account by the boundary values. The incoming shortwave radiation  $R_{SI}$  ( $\text{W m}^{-2}$ ) is absorbed exponentially:

$$S_H = \frac{\partial}{\partial z} (R_{SI} e^{\beta z}) = \beta R_{SI} e^{\beta z} \quad (32)$$

where  $\beta$  ( $\text{m}^{-1}$ ) is extinction coefficient and  $z$  vertical coordinate.  $\beta$  depends strongly on the clarity of the water and can be estimated by secchi disc value  $d_s$  (m) (Lehtinen 1984)

$$\beta = 1.65/d_s \quad (33)$$

The incoming shortwave radiation  $R_{SI}$  depends on the reflectivity of the water surface (Brady et. al. 1969):

$$\begin{aligned} R_{SI} &= (1 - r_s) R_s \\ r_s &= a \alpha_a^b \\ \alpha_a &= \arcsin(\sin \phi \sin \sigma_d + \cos \phi \cos \sigma_d \cos h_r) \end{aligned} \quad (34)$$

$$\sigma_d = 23.45 \frac{\pi}{180} \cos\left(\frac{2\pi}{365} (172 - D)\right)$$

$$h_r = \frac{\pi}{24} \left( h_s + \frac{4}{60} \psi \pm 12 \right)$$

$$a = 2.20 + \frac{C_r^{0.7}}{4.0} - \frac{(C_r^{0.7} - 0.4)^2}{0.16}$$

$$b = -1.02 + \frac{C_r^{0.7}}{16.0} + \frac{(C_r^{0.7} - 0.4)^2}{0.64}$$

$$C_r = 1 - R_S/R_{Smax}$$

where

$R_S$	is shortwave radiation reaching the water surface ( $\text{W m}^{-1}$ )
$r_s$	is reflectivity of the water surface
$\alpha_a$	is solar altitude (rad)
$\phi$	is geographic latitude (rad)
$h_r$	is local hour angle of the sun (rad)
$h_s$	is standard time (h)

$\psi$	is distance between the meridian of the observer and the standard meridian of the time zone (deg); east longitude $\Rightarrow$ -, west longitude $\Rightarrow$ +
$\sigma_d$	is declination of the sun (rad)
$D$	is number of the day (1 - 365)
$R_{Smax}$	is theoretical maximum solar shortwave radiation ( $\text{W m}^{-2}$ ).

In the equation for  $h$  + -sign is taken before noon and -sign after noon. Constants  $a$  and  $b$  depend actually on the cloud cover (Anderson 1954), but the expression in question has the advantage that no cloud information is needed when shortwave radiation is measured. Table 8 gives the averaged values of  $a$  and  $b$  for different cloud covers.

$R_{Smax}$  can be computed by an empirical formula (Kennedy 1944; Klein 1948):

$$\begin{aligned} R_{Smax} &= R_{Se} (0.99 - 0.17 m_0) \\ R_{Se} &= I_0 \sin \alpha_a \\ m_0 &= 1/[\sin \alpha_a + 0.15 \times (\alpha_a + 3.885)^{-1.253}] \end{aligned} \quad (35)$$

where

$R_{Se}$	is extraterrestrial radiation ( $\text{W m}^{-2}$ )
$I_0$	is the solar constant $14.0 \cdot 10^2 \text{ W m}^{-1}$
$\alpha_a$	is solar altitude (rad)
$m_0$	is optical air mass.

When total radiation values are available  $R_S$  can be approximated by

$$R_S = r_s R_t \quad (36)$$

where

$R_t$	is total radiation reaching the ground
$r_s$	$\approx 0.6$ (Dake and Harleman 1969).

$R_S$  can be also calculated from total radiation and amount of longwave radiation (section 6.3.3). Widely used formula is due to Kennedy (1944):

Table 8.  $a$  and  $b$  in equation (34) as functions of high clouds (Anderson 1954).

Cloudiness (%)	$a$	$b$
0— 5	1.18	-0.77
5— 55	2.20	-0.97
55— 95	0.95	-0.75
95—100	0.33	-0.45

$$R_S = R_{Se}(1 - 0.65C_1^2) \quad (37)$$

where

$R_{Se}$  is extraterrestrial radiation  
 $C_1$  is cloudiness (0—1).

### 6.3.3 Boundary values

Boundary values for temperature calculation consist of heat fluxes into the surface water, bottom and banks. Shortwave radiation was discussed on the section refsoursin as it affects the whole water body. Atmospheric longwave radiation is absorbed within the first meter from the surface and can be thus modelled as a heat flux through the surface. According to the Stefan-Bolzman law longwave radiation is

$$R_L = \epsilon_a \sigma_B (T_a + 273)^4 \quad (38)$$

where

$R_L$  is amount of longwave radiation ( $W m^{-2}$ )  
 $\epsilon_a$  is atmospheric emissivity  
 $\sigma_B$  is Stefan-Bolzman constant =  
 $5.67 \cdot 10^{-8} W m^{-2} K^{-4}$   
 $T_a$  is air temperature ( $^{\circ}C$ ), usually measured 2 m above the water surface.

Various empirical relations have been developed for  $\epsilon_a$ . Generally  $\epsilon_a$  is expressed as a function of the air temperature and/or humidity. The frequently used Swinbank formula doesn't depend on the local temperature-humidity regime (Swinbank 1963; Idso and Jackson 1969):

$$\epsilon_a = 0.93710^{-5}(T_a + 273)^2. \quad (39)$$

Brutsaert has proposed theoretical vapour pressure dependent equation which is in good agreement with empirical formulas:

$$\begin{aligned} \epsilon_a &= 0.553e_a^{1/7} \quad (40) \\ e_a &= H_r e_{as} \\ e_{as} &= 6.108 \exp\left(\frac{17.27T_a}{T_a + 237.44}\right) \end{aligned}$$

(Tetons 1930)

where

$e_a$  is the vapor pressure of the air at the temperature  $T_a$  (mb)  
 $H_r$  is relative humidity (0—1)  
 $e_{as}$  is saturation vapor pressure (mb)  
 $T_a$  is air temperature ( $^{\circ}C$ ).

Bolz-formula is often used to take into account the effect of clouds on longwave radiation (Bolz 1949):

$$\epsilon_a = \epsilon_c(1 + k_a C_1^2) \quad (41)$$

where

$\epsilon_c$  is atmospheric emissivity under clear skies  
 $C_1$  is cloudiness (0—1)  
 $k_a$  is factor which depends upon the type and height of the clouds and solar altitude; a mean value of 0.17 can be used.

The reflectivity of the water surface for longwave radiation is 0.030 so the incoming longwave radiation is given by

$$R_{LI} = 0.970R_L \quad (42)$$

The longwave radiation from water body has the largest magnitude among all the heat exchange components. It is given by Stefan-Bolzman law:

$$R_{LO} = \epsilon_w \sigma_B (T_w + 273)^4 \quad (43)$$

where

$R_{LO}$  is amount of outgoing longwave radiation ( $W m^{-2}$ )  
 $\epsilon_w$  is emissivity of the water surface = 0.970  
 $\sigma_B$  is Stefan-Bolzman constant  
 $T_w$  is water surface temperature ( $^{\circ}C$ ).

The evaporative heat transfer can be quite considerable. Evaporation consumes energy according to the following equation:

$$Q_e = \rho LE \quad (44)$$

$$\begin{aligned} L &= 2500 - 2.39T_w \\ E &= (a_c + b_c W)(e_w - e_a) \\ e_w &= 6.108 \exp\left(\frac{17.27T_w}{T_w + 237.44}\right) \end{aligned}$$

where

$Q_e$  is evaporative heat flux ( $W m^{-2}$ )  
 $\rho$  is density of water ( $kg m^{-3}$ )  
 $L$  is the latent heat of vaporization ( $J kg^{-1}$ )  
 $E$  is the volumetric evaporation rate per unit area of the water surface ( $m s^{-1}$ )  
 $T_w$  is water surface temperature ( $^{\circ}C$ )  
 $a_c$  is the free convection factor ( $ms^{-1}ms^{-1}$ );  
 $a_c$  depends on virtual temperature gradient; often  $a_c \approx 0$   
 $b_c W$  is the forced convection factor where  $W$  is wind speed ( $m s^{-1}$ );  $b_c$  depends eg. on the wind fetch, but here  $b_c = 1.13 \cdot 10^{-9} mb^{-1}$

(Marciano and Harbeck 1954) when  $W$  and  $e_a$  are measured 2 m above the water surface; this value is recommended by TVA (Tennessee Valley Authority 1970)

$e_a$  is the vapor pressure of air at the temperature  $T_a$  (mb)

$e_w$  is surface vapor pressure (mb).

The heat flux carried by the evaporated mass of water is insignificant. Heat conduction through surface is regularly given by

$$Q_{ca} = r_B Q_e \quad (45)$$

$$r_B = c_c \frac{p_a}{1000} \left( \frac{T_w - T_a}{e_s - e_a} \right)$$

where

$Q_{ca}$  is heat conduction through water surface ( $W m^{-2}$ )

$r_B$  is the Bowen's ratio

$p_a$  is air pressure (mb)

$c_c$  is constant =  $0.61 \text{ } ^\circ C^{-1}$ .

Heat conduction through bottom can be given as

$$Q_{cb} = {}^3K_t \frac{\partial T}{\partial z} \quad (46)$$

where  $K_t$  is thermal conductivity between water and bottom ( $W m^{-1} \text{ } ^\circ C^{-1}$ ).

### 6.3.4 Realization of the temperature model

The computer realization of the temperature model is divided into two parts. The incoming radiation fluxes are calculated in the other module and radiation, evaporation and conduction in the other in connection with the water temperature changes. This division facilitates optimal use of computational resources: the computationally less demanding terms can be approximated accurately. The atmospheric influence is evaluated only in one point whereas the terms containing water temperature, equations (43), (45) and (46), must be typically calculated in hundreds of gridpoints in each timestep. In practice incoming radiation fluxes can thus be calculated considerably more often than actual water temperature changes.

The surface vapor pressure  $e_w$  is needed in the evaporative and conductive heat flux equations. To get rid of the computationally expensive exponential in the expression for  $e_w$  the exponential is Taylor-expanded around the point  $217.27T_w/(T_w + 237.4)$ ,  $T_w = 10 \text{ } ^\circ C$ . The complete algorithm for water temperature change in the surface layer is:

$$T_1 = T_w^t + 273 \quad (47)$$

$$T_1 = T_1 * T_1$$

$$T_1 = T_1 * T_1$$

$$T_2 = 25 \cdot 10^5 - 2.399 \cdot 10^3 * T_w^t$$

$$T_3 = \frac{17.27T_w^t}{T_w^t + 237.4} - 0.698$$

$$T_w^{t+1} = T_w^t + \frac{1}{\Delta h} (\Delta R_{SI} + R_{LI} - \Delta t (C_1 * T_1 + T_2 * (C_2 * (C_3 * (1 + T_3 + T_3 * T_3 * 0.5) - e_a) + C_4 * (T_w^t - T_a))))$$

where

$T_w^t$  is the old water temperature

$T_w^{t+1}$  is the new water temperature

$T_a$  is the air temperature

$e_a$  is the air vapor pressure

$R_{LI}$  is the time-integrated incoming longwave radiation

$\Delta R_{SI}$  is the time-integrated difference between incoming shortwave radiation on the surface and bottom of the computational cell

$\Delta h$  is the depth of the computational cell

$\Delta t$  is the timestep

$C_1, C_2, C_3, C_4$  are the appropriate coefficients.

The user supplied input parameters are quite simple. In addition to the bottom flux parameters secchi disc value and constants  $a_c$  and  $b_c$  in evaporative term must be fixed. Also geographic latitude and longitude are needed to be given. The weather data consists of air temperature, humidity, pressure and cloudiness. Radiation values are either given from measurements or calculated.

### 6.3.5 Implementation features

The temperature model is put together from various sources as can be seen from the bibliography. It has many common features to the Probe model developed by Urban Svensson and the FINNECO temperature model although e.g. the evaporation part of the model is different. The effect of ice formation and melting was not included in the model at this stage but must probably be taken into account in the future versions.

The problem with the previous temperature

model is that the equations are complicated and the calibration of the model is quite difficult. No actual calibration of the model was done during the project except for the incoming shortwave radiation. It was reduced by 20 % because the model overestimated the shortwave radiation 20—30 % compared to the measurements (The Probe model gave about the same values for the incoming shortwave radiation as the 3D). Otherwise the parameter values were taken from the literature.

The temperature model was first tested without feedback from the temperature model to the currents, that is the density effects were discarded. Later on the temperature model was combined with the flow model. In the flow model there is a feedback from the temperature transport to the flow through the density. It should be noted that the stratification formation is caused by the heat flux in and out of the surface (to a much lesser degree through the bottom), the heat transport and the vertical mixing. If there were no heat flux in or out of the water body the currents would mix the water mass so that eventually no temperature gradients would exist. The salinity gradients are on the other hand due to the salinity of the larger sea areas connected to the calculation domain and the incoming freshwater inflow. In the Bothnian Bay the salinity differences play a significant role to the flow only during the winter when the transport and mixing is reduced due to the ice cover.

The  $k-\epsilon$  turbulence model was implemented and tested during the project. The turbulence model is important especially during the stratified period to obtain the values of the vertical eddy viscosity coefficients. There were however numerical problems and the boundary values were not easily parametrized so that the testing was discontinued after the first preliminary steps.

The implementation of the temperature, salinity and water quality models will be discussed in further detail in the chapter 7 "Application of the models to the Bothnian Bay".

### 6.3.6 Sampling of the statistical characteristics of the simulation

A special procedure was implemented in the water quality model to gain information of the statistical behaviour of the water quality parameters. The following characteristics were calculated:

- mean values
- variances
- probabilities that the concentration exceeds or passes below a certain threshold value.

The statistics are obtained by dividing the possible range of concentrations into equally spaced sections and calculating the concentration frequencies. The accuracy of the statistics suffers somewhat from the sectioning but on the other hand only one calculation is needed to obtain the statistics. The accuracy is not very sensitive to the number of the sections and reasonable numbers were able to give very accurate results.

The statistics sampling can be computationally quite expensive. The calculation of statistics increases the computational load about fourfold in the current model.

## 6.4 Development of the oil and drifting model

A preliminary model to simulate transport and drifting of soluble substances and solid objects was developed as a part of a feasibility study of the present models to describe the fate of chemicals released to sea. The model was planned to be used on a microcomputer in order to have it easily accessible to officials in charge of oil and chemical combatting and sea rescue.

The model does not calculate flowfields but uses those calculated with a 3D flowmodel. These are stored on PCs hard disk thus increasing the speed of computation and reducing memory requirements of the PC. Flowfields caused by any wind is calculated in the same manner as is usually done in the 3D water quality model i.e. as a linear superposition of previously calculated basic flowfields.

A system "memory" was introduced to the model which causes the flowfield to change smoothly from one state to the other as wind direction or speed changes. For the modelled region in the Quark parameters were selected so that 95 of the steady state flowfield is reached in 10 hours from the wind change, 50 is correspondingly reached in 4 hours. These features are in accordance with model and field experiences.

The transport is described using particles which are influenced by advection with the flow velocity, dispersion and wind drift provided that some part of the object is at or above the sea surface. Turbulent dispersion of particles was simulated by random-walk process with random dispersive velocity added for each particle. It has been divided into three components, each being described by corresponding dispersion coefficient. The horizontal components are

- Neutral (isotropic) dispersion, which causes the substance to spread uniformly in all directions.
- Longitudinal dispersion, which determines the amount of dispersion in the direction of the flow velocity
- Transverse dispersion which accounts for the transverse spreading of the substance.

No consideration of turbulence has been taken into account in determining vertical motions. It has simply been assumed that the substance has a constant settling velocity which is then modified by using slightly negatively biased random numbers. This makes it possible for a particle to move either up- or downwards. Vertical velocity calculated by the model can later be incorporated in to the model.

Particles in specified depth are subjected to the average flow velocity of a single model layer. Solid objects are subjected to an average flow velocity which is computed over the vertical range of the object.

The path of each particle is tracked and checks are made each timestep to see whether a particle has stranded or sunk to the bottom. Stranded particles are retained at the shoreline. From the bottom, a particle may be released if the vertical velocity is upwards.

For the particles at the surface a simple method was used to superimpose the effect of wind. To the advection velocity caused by flow velocity, a certain amount of windspeed is added with a possibility of introducing a deviation angle for the direction of wind induced transport to get the final transport velocity and direction of the particle. The amount of wind influence for solid objects is highly dependent on the form of the object and may dominate the transport over flowfields.

## 6.5 Development of the grid generation system

The inverse multigrid approach has one disadvantage: the possibly quite large finest grid must be provided. Sometimes it can be generated manually, but in most practical cases it would be a very energy-consuming task. Furthermore, once you have generated such grid manually, you probably would never try to change it, e.g. translate or rotate to slightly different location or angle. Therefore, it is reasonable to develop an automatic mesh generator program, which can produce grids

out of digitized scattered depth data. Even if a generated mesh is not entirely satisfactory, it is still much easier to correct a few grid cells manually, than to produce them all.

The mesh generator algorithm developed is pretty simple and yet efficient. It is called em binary division and exchange algorithm. During the initialization step the location, angle, size and level of the mesh are chosen. Thereafter all the scattered depth data are placed in a storage vector. Now the mesh rectangle is divided into two new ones in such manner, that approximately half of the data belongs to one rectangle and the rest of the data to the other one. In the storage vector depth points logically belonging to opposite rectangles are exchanged with each other. There are now two independent data sets and storage vectors for both of which the division and exchange is performed again, and so continued recursively, until there is only one depth point in each rectangle.

The above procedure produces a set of disjoint rectangles covering entirely the chosen mesh area. The last simple task consists of dividing the mesh into  $2^L$  by  $2^L$  grid cells ( $L$  is the mesh level) and computing their depths as weighted averages over the disjoint rectangle set. The cost of the described algorithm is  $O(M \times \log M) + O(N)$ , where  $M$  is the number of scattered depth points and  $N$  is the number of grid cells. The reason for the efficiency requirement is the large amount of the digitized data. For instance the Bothnian Bay datafiles contain over 60 000 depth points. Should any neighbour searching algorithm be used, which costs  $O(M^2)$  operations, it would take several days to process all the Bothnian Bay files on a 1 MFLOPS computer.

Despite its simplicity the binary division and exchange algorithm performs quite well in practice, especially when there is enough and correct data available. There are very many other important sources of errors (e.g. inaccurate foreign data, imperfect mathematical models, depth and grid cell averaging etc.), but if a few metres mislocation in depth value (which is anyway inaccurate) should particularly disturb anyone, the generated mesh may be viewed and corrected on a graphic terminal by means of a simple mesh editing program.

Usually good resolution is needed for some sensitive area or the area under special study while the influence of the whole water body should also be included in the model. Because the possibilities for large grid systems is limited (the curse of dimensionality) a locally refined grid must be often used while rest of the water body is modelled with coarser grid. That is why an interactive post-

processing program was devised for the basic grid generation program. After the basic dense regular grid is created with the grid generation system it is integrated in desired areas with the secondary program. The grid to be integrated and the map of the area are drawn on the computer terminal screen and the user selects in with a cursor the boundaries of the final grid. The program gives as a result the grid depths and widths which can be used directly in the models.

The grid generation system suffers from some problems:

- digitization requires lot of work
- maps of different scales usually dont fit well together
- parts that are digitized at different times possibly dont fit together
- errors are tedious or impossible to correct
- storage is required for large amounts of data
- the depth determination algorithm is biased.

In Fig. 11 is an example of the biased depth determination algorithm. The reason for the bias is the different resolution by which data is usually digitized. Usually the depth contours are digitized much more accurately than the single depth points. The depth determination algorithm can also run into problems e.g. in narrow straights when there are not enough depths to indicate water areas.

Despite of the problems the grid generation system can be flexible and useful tool to generate grids especially at the open sea and less important areas of the calculation domain. The grid generation system could be developed further by:

- taking into account the different resolutions data is entered
- building a graphical interface where the depth generated by the program is shown with the raw data used and where the user can correct the depth when needed
- by devising ways to fit the data digitized from different maps and at different times
- by devising an interactive program to correct the erroneous data on a graphics screen.

## 7 APPLICATION OF THE MODELS TO THE BOTHNIAN BAY

### 7.1 Hydrodynamics

#### 7.1.1 3D flow model compared with observations

The hydrodynamics of the Bothnian Bay were studied with the aid of the 3D flow model described in the previous chapter. Several different grid systems were used in order to get required resolution in various areas and to solve different problems. The grid generation system was used in most of the cases to generate the grid from digitized depth information.

The current information was used in the model verification in two ways: firstly regression equations based on the current measurements and wind data were devised mainly for steady state comparisons and secondly time dependent field data was compared with model time-series. The regression equations are useful because they filter out the oscillations of currents and yield a simple dependency of the currents on the wind. In Figure 12 is shown the flow field over the whole of the Bothnian Bay when the wind is from the south-west. The general tendency of the wind generated fields can be seen in the figure: near the surface the flow tends to be aligned more or less along the direction of the wind although there can be regions where the flow may be even against the wind. The flow turns in the deeper parts gradually into a return current. This can be already seen in the pictures from 2—5 m and 5—10 m. Regression equation flow (thick circled arrows) is in good agreement with the model results in respect with the flow direction. This can be seen even more clearly in the Fig. 13, where the flow has more regular pattern in the northern part than in the Fig. 12.

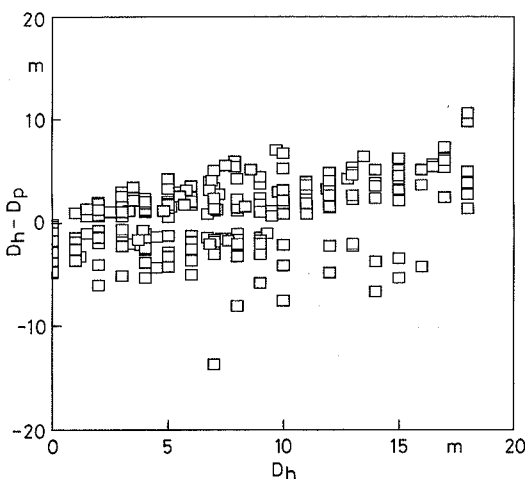


Fig. 11. Comparison of depths generated by the two methods.  $D_h$  is the depth generated by hand and  $D_p$  by the grid generation program.

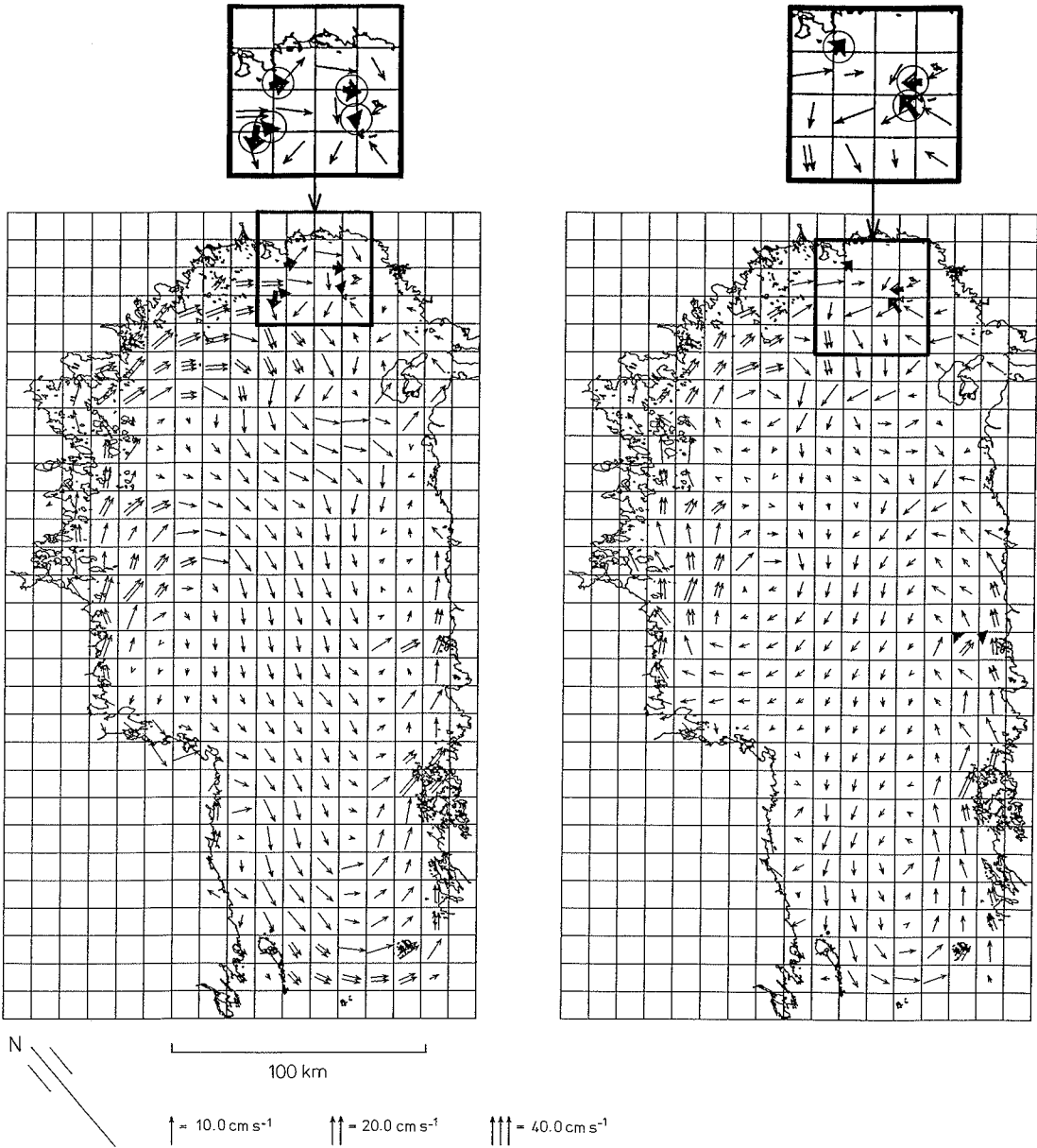


Fig. 12. Steady state flow fields from the 2–5 m (left) and 5–10 m (right) depths. Wind 5 m s<sup>-1</sup> from the south-west. Regression analysis results shown with the thick circled arrows.



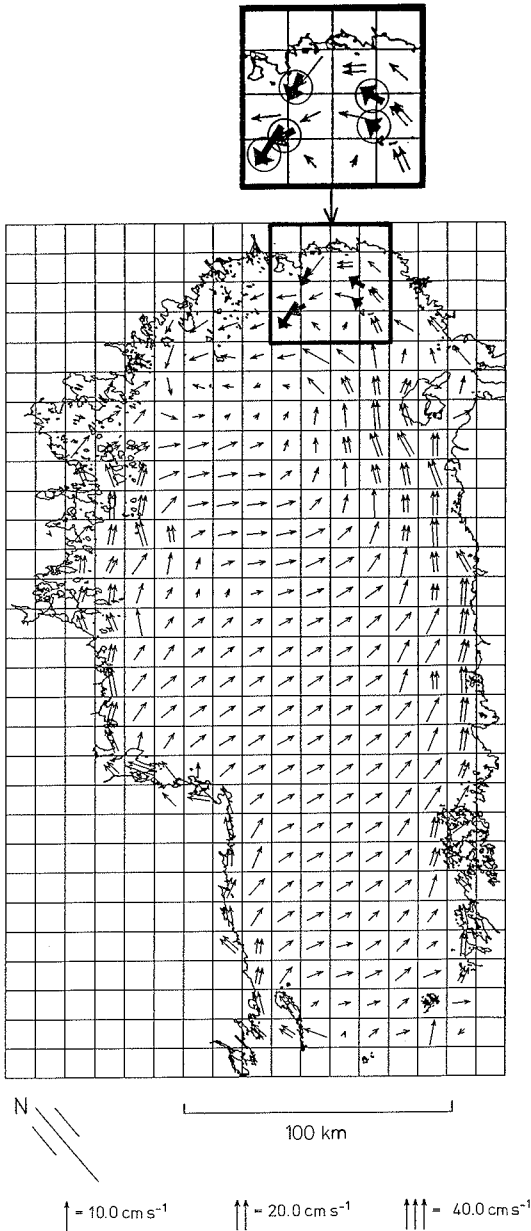


Fig. 13. Stationary flow fields from the 2–5 m depth. Wind  $5 \text{ m s}^{-1}$  from the south. Regression analysis results shown with the thick circled arrows.

When comparing the results between the regression equations and the mathematical model it should be kept in mind that:

- the agreement between the mathematical model and regression is usually good when the latter model has a high explanation degree ( $r^2$ )
- flow model results are averages over certain areas, regression equations apply to one point

- regression equation is the result of a statistical analysis and the bias in the wind conditions during the measurement period can affect the results
- when filtered currents are used the regression equation tends to give smaller velocities than are encountered in reality.

In the Fig. 14 is shown a grid where the resolution is concentrated off the town Kemi. The grid consists of  $36 \times 62 \times 9$  gridpoints. The smallest grid widths are 500 m and the largest 63 000 m. In the Fig. 15 there is a part of a flow field off the town Kemi and in Fig. 16 of the region east of Kemi. The general agreement between the coarser flow fields (Figs. 12 and 13) and the solution in the fine grid is quite good especially with the southern wind. There is however an interesting feature different in the different grid systems: the flow near the coast east of cape Maksniemi when the wind blows from west is in the coarser grid to the east and in the finer one to the west. In the westerly wind the denser model shows a strong current off the Cape Maksniemi to the south. According to measurements there are quite strong currents off the Cape Maksniemi to the south. The model result suggests that they are due to two large scale eddies which converge at the region.

As a last example of wind induced currents, the flowfields in a region between the towns Kokkola and Raahe are shown in Fig. 17. The bathymetry of this region is quite simple. The flow model results are from a quite coarse grid (in this region grid size  $19 \times 71 \text{ km}$ ), but they show relatively good agreement with the regression model results.

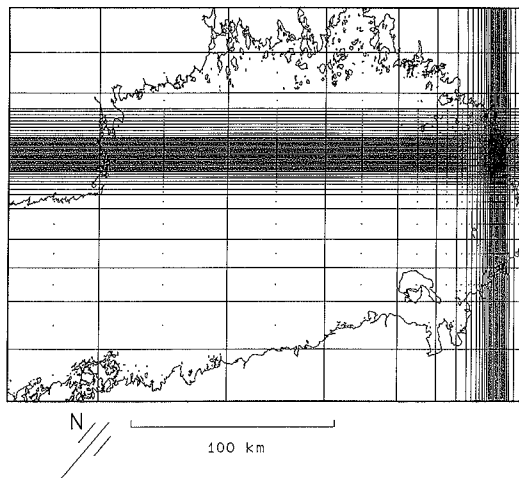


Fig. 14. Locally refined grid used in computation of flow fields off the town Kemi.

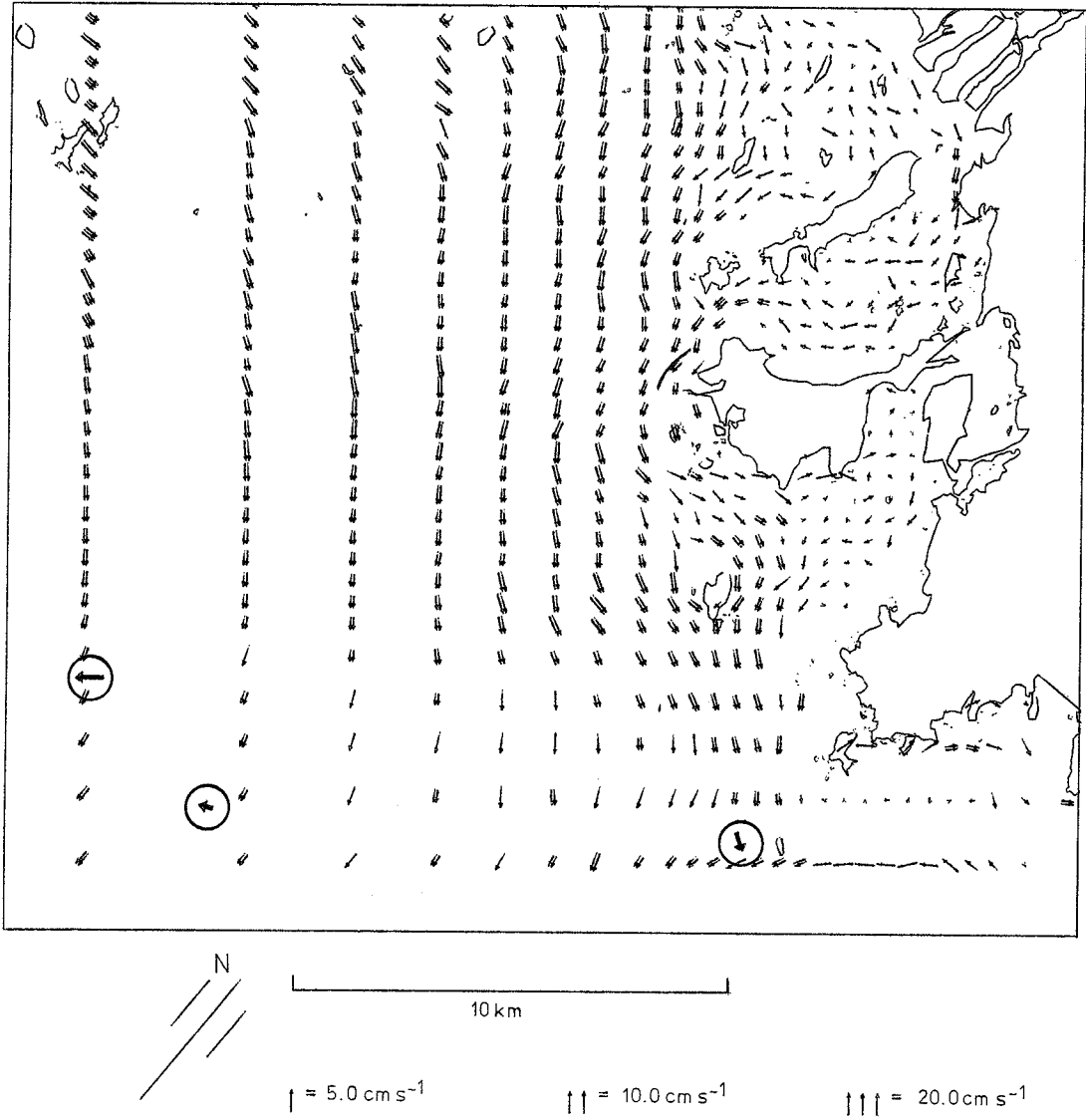


Fig. 15. Flow in 2–5 m depth off the town Kemi. Regression analysis results shown with the circled arrows. West wind  $5 \text{ m s}^{-1}$ .

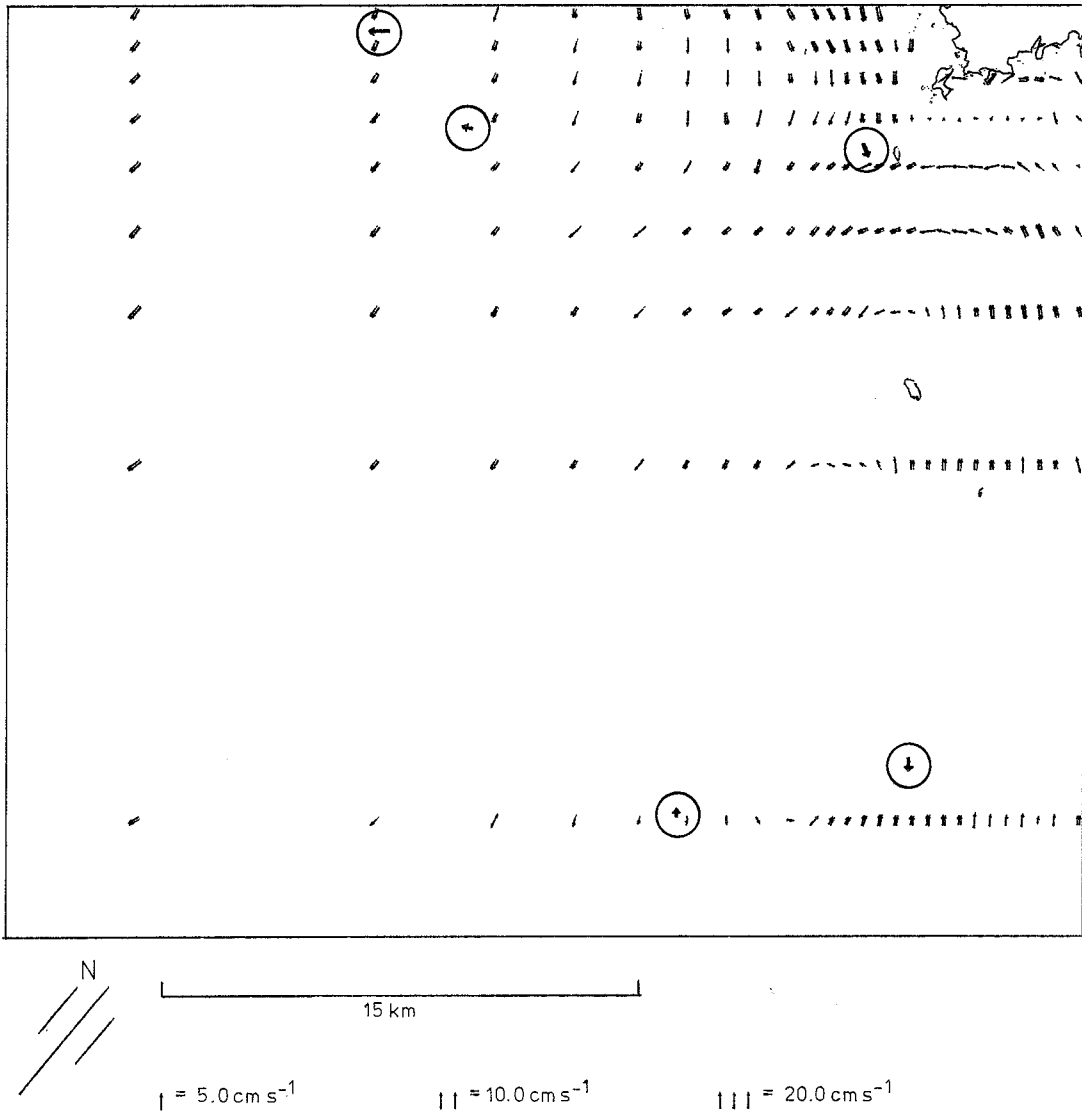


Fig. 16. Flow in 2—5 m depth in a region east of the town Kemi. Regression analysis results shown with the circled arrows. West wind  $5 \text{ m s}^{-1}$ .

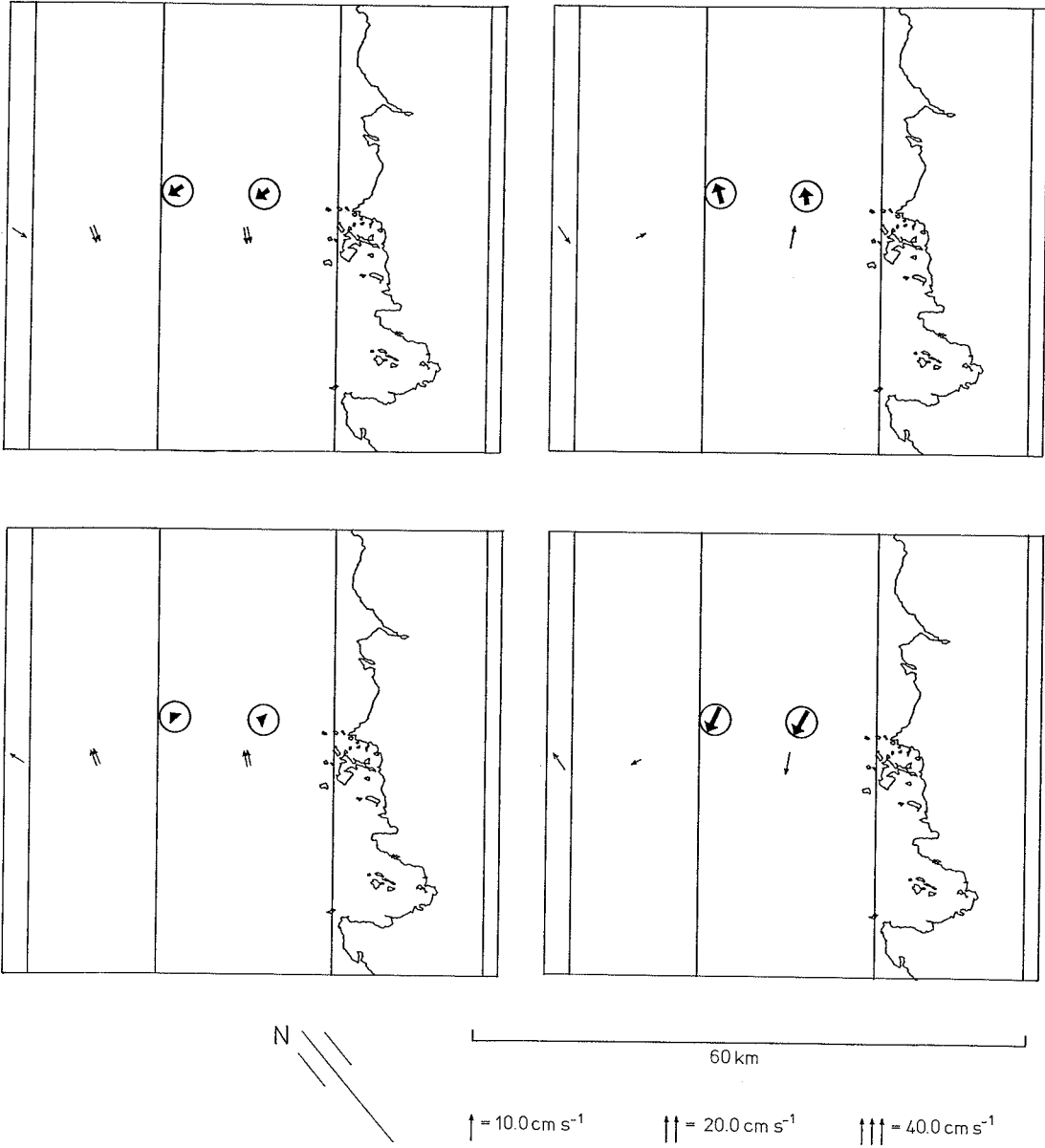


Fig. 17. Flow in the region of the towns of Kokkola and Raaha. Wind  $5 \text{ m s}^{-1}$  from east (upper left), south (upper right), west (lower left) and north (lower right). Regression analysis results shown with the circled arrows.

### 7.1.2 3D flow model compared with other models

A joint project for comparing two 3D models was established with the Swedish Meteorological and Hydrological Institute (SMHI). SMHI used a widely known Phoenix model for their calculations. It is quite different from the Finnish model. For instance the grid system is different, there is no explicit water elevation calculation and the vertical velocities are solved explicitly. Because the grid system was so much different especially in the vertical direction (the so called sigma-coordinate system) the comparison of the velocities in other layers than the surface one is difficult. There was a plan to devise an interpolation program for the Phoenix results but that was not realized because of the staff departures from SMHI.

Two grids were used in the comparison runs for the Bothnian Bay: one had a flat bottom topography (depth was equal to the mean depth) and the other one had natural depths. The results from the flat bottom topography calculation are shown in the Fig. 18. It can be seen that the flow magnitudes and flow directions agree quite nicely in both models especially when it is taken into account that the points where the velocities are defined don't completely agree in both models and that the Phoenix results are not completely stabilized.

In the Fig. 19 are shown the comparison in the natural depth grid. The velocities shown are the top layer velocity and the vertically integrated velocity. It can be seen that the flow direction is very much the same in both of the models but that the flow velocity is much more higher in the Finnish model near the coast. The comparatively short Phoenix calculation time might be the cause for this difference because from the time-series we can see that the velocities still rise in some points after the 48 h Phoenix calculated the result.

In Fig. 20 are shown time-series of flow speed and direction in one selected point when the wind is constant and the natural bottom topography is used. The exact comparison of the time-series is not meaningful because of the basic differences in the depth ranges and points these series represent, but the general impression is that the magnitudes of the flows, the directions and the stabilization times are not very much different in the models.

The multigrid results in Fig. 21 show the depth integrated fields over the Bothnian Bay and the vertically integrated 3D field. The multigrid results might be somewhat influenced by the grid direction because the Hansen grid used in the multigrid method aligns the flow along the x- or

y-directions. Quite an interesting result of the multigrid calculations is that flow fields calculated with anyone of the coarsest grids seem to be about the same as would be obtained by integration from the denser grids. What is missing from the coarse grid are of course the small scale eddies described by the denser grids. This is quite a reasonable result and increases the assurance of the consistency of the models. It can also be seen from the grids  $124 \times 124$  and  $256 \times 256$  that the denser grid doesn't increase appreciably information about the flow at this digitization resolution, that is the flow in the denser grid can be approximated well by interpolation from the coarser grid. A more systematic study where the depth data resolution would correspond to the flow field grid resolution in the smallest scales would offer quite interesting results about the behaviour of the flow models. It should be noted, that the depth integrated flow fields from 2D models can't be easily compared with the layer velocities from the 3D model because the velocities can change quite appreciably in the vertical direction. However when the 3D fields are integrated over the whole depth the results are quite near the fields calculated with the 2D models as can be seen from the Fig. 21.

### 7.1.3 3D flow model compared with observed wind induced time series

More or less stable flow is reached in the model after 4 days in most of the points under steady meteorological conditions when the stratification effects are discarded. Of course so long stable meteorological conditions are quite exceptional in nature. Therefore long periods of constant wind direction were selected for comparisons between the model and measurement results. The measurements were not averaged, but the sampling frequency was reduced from the original one.

In Fig. 22 is shown the wind during the flow measurement period in 1987. It can be seen that there was a relatively stable wind period from september 25 to 29 when the wind blew from north ( $25^\circ$ ) and the wind speed was typically  $8 \text{ m s}^{-1}$ . In Fig. 23 are shown the model and measurement time-series from the Maksniemi point (point 2 in Fig. 3) from 3.5 m and 9.5 m depths. The Ulkokrunni point (point 6 in Fig. 3) is not shown here because  $r^2$  was rather poor (on the average 0.29) in these points. The measured flow direction is between  $270^\circ$  and  $45^\circ$  and the model one about  $45^\circ$ . Especially at the end of the shown period the measured and modelled flow directions are in good agreement with each other.

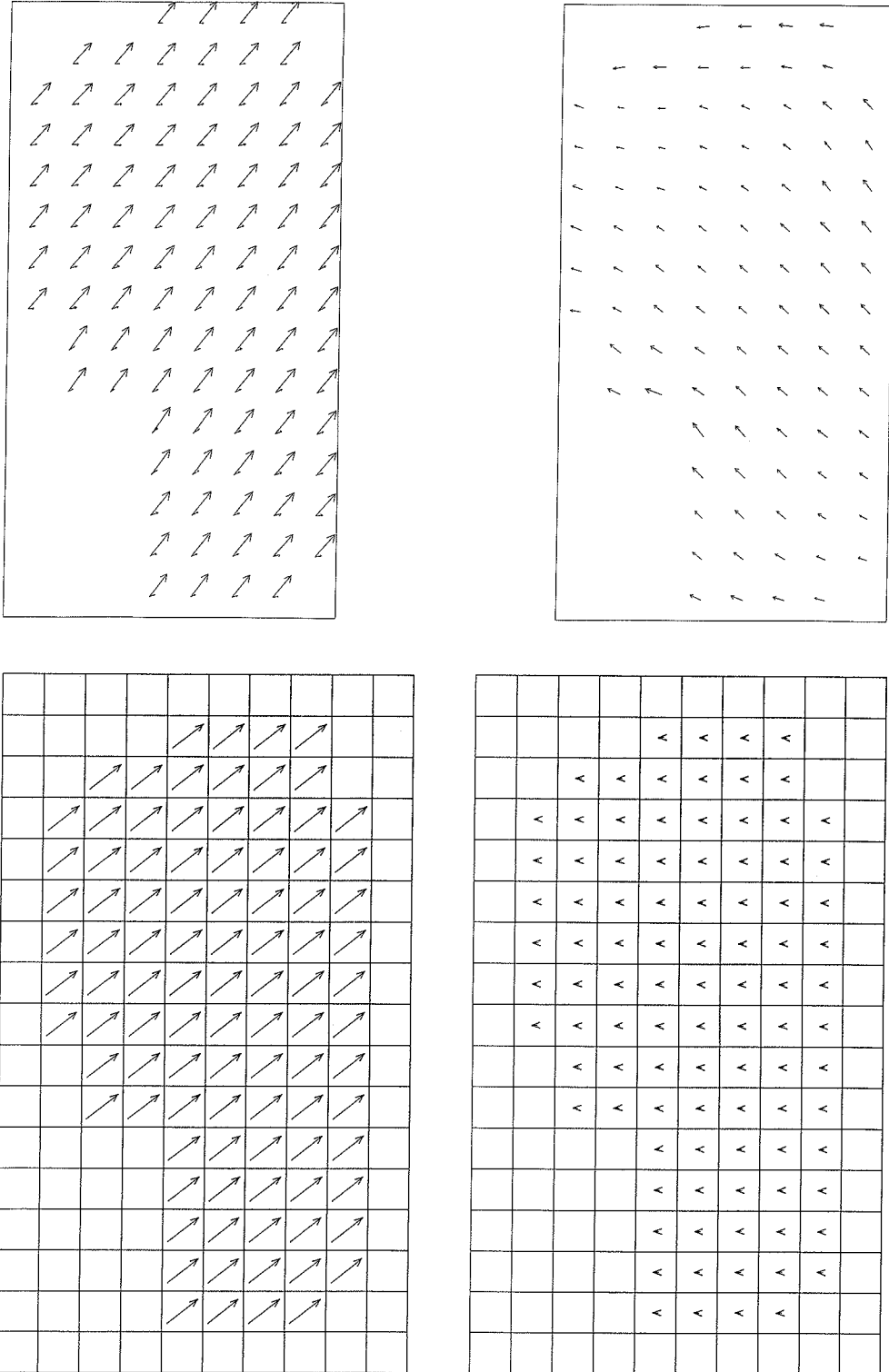


Fig. 18. Phoenics (upper figures) and Finnish (lower figures) model results from the surface (left side) and the bottom (right side). Flat bottom topography. Wind  $5 \text{ m s}^{-1}$  from SW (parallel to the y-axis).

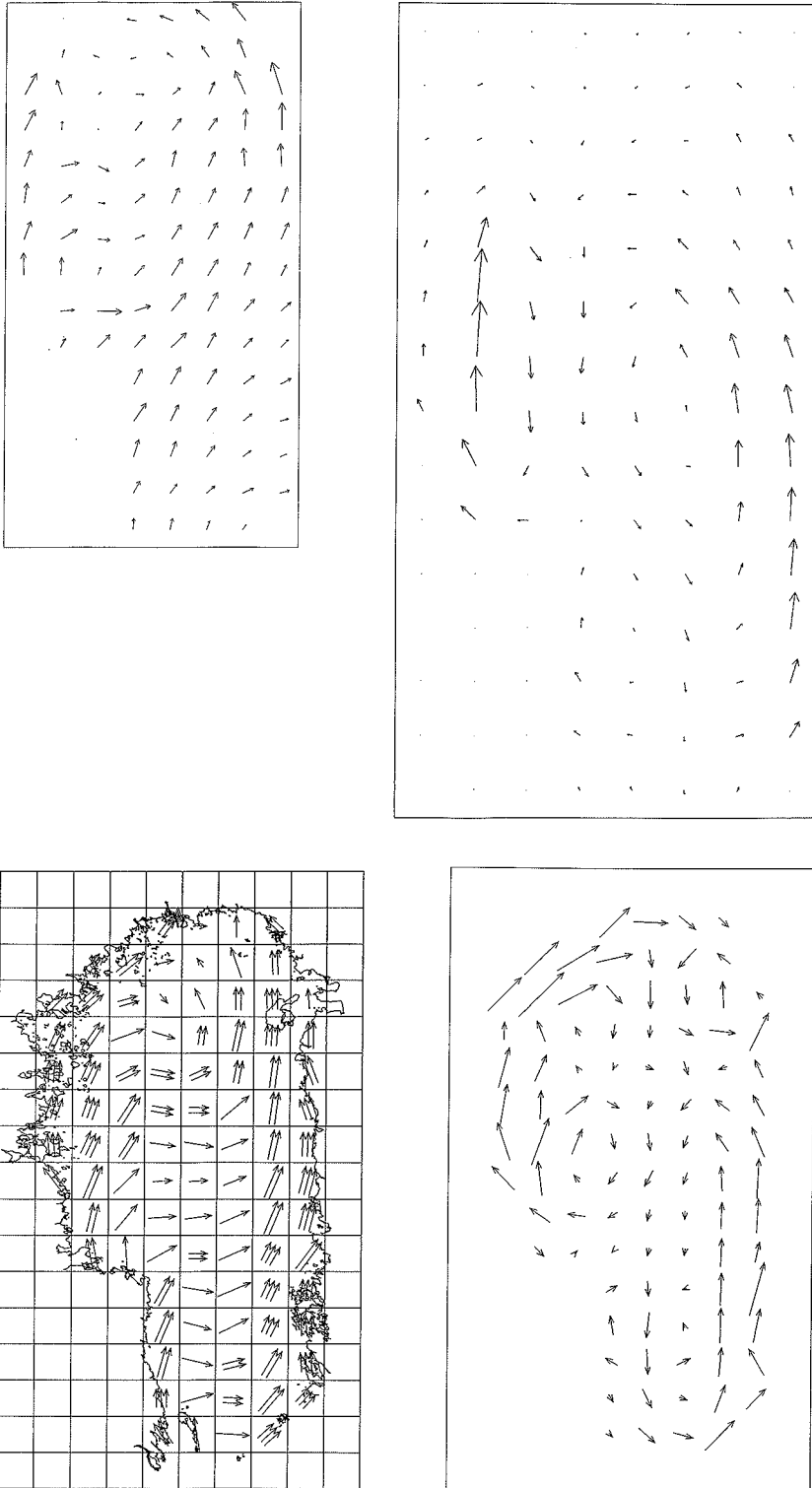


Fig. 19. Phoenix (upper figures) and Finnish (lower figures) model results using natural depths. Left side: the top layer velocities, right side: vertically integrated velocities. Wind  $5 \text{ m s}^{-1}$  from SW (parallel to the y-axis).

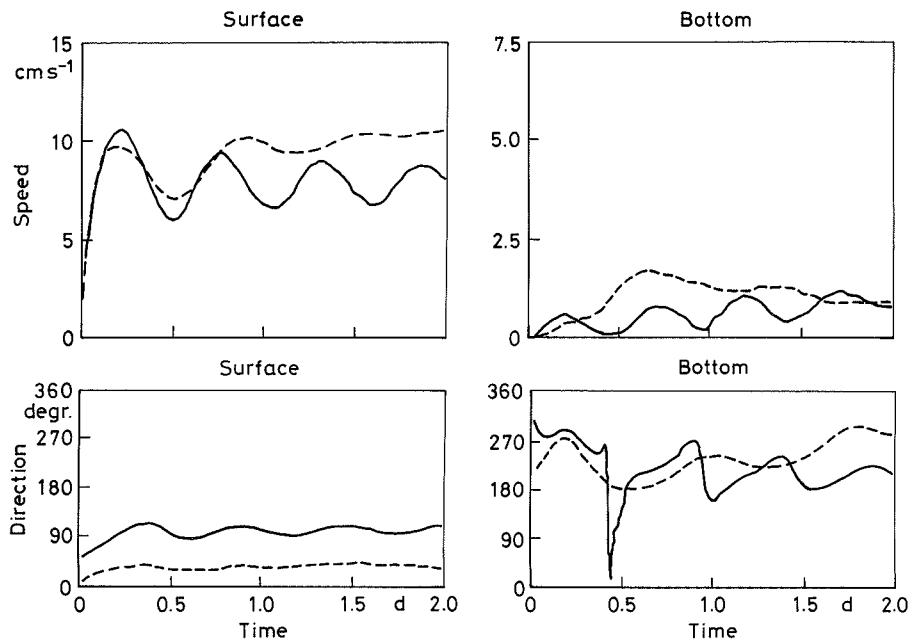


Fig. 20. Phoenix (broken line) and Finnish (solid line) model time-series from one point at two depths.

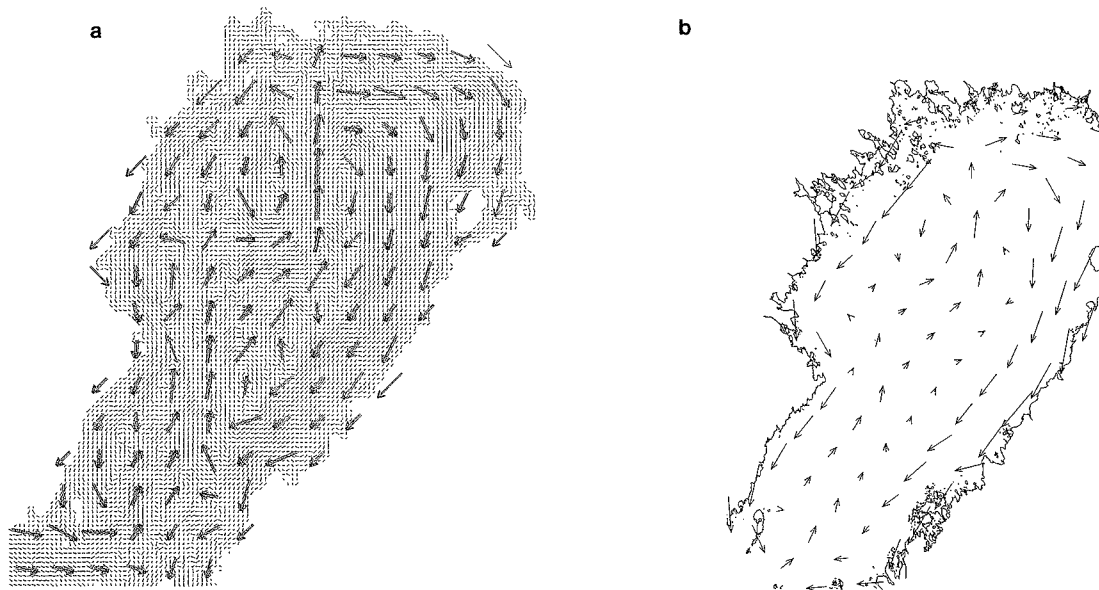


Fig. 21. a) Multigrid and b) 3D vertically integrated field when the wind direction is from north (observe that the ratio of the x- and y-scales in the multigrid figure is not 1).



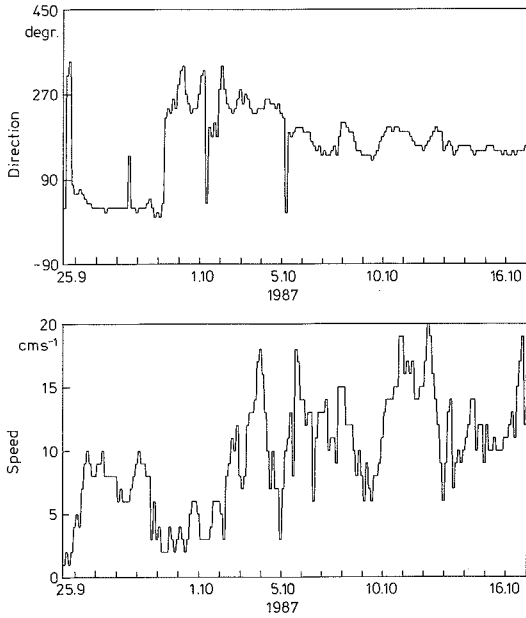


Fig. 22. Wind direction and speed from Kemi Ajos wind station during the 1987 current measurement period.

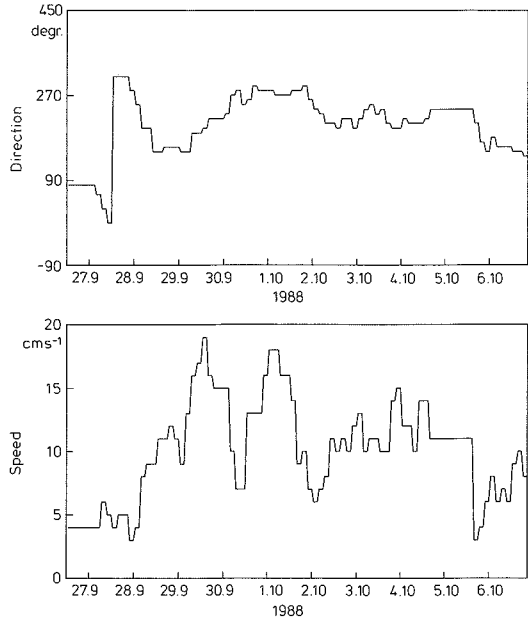


Fig. 24. Wind direction and speed in Kemi (Ajos) in 1988.

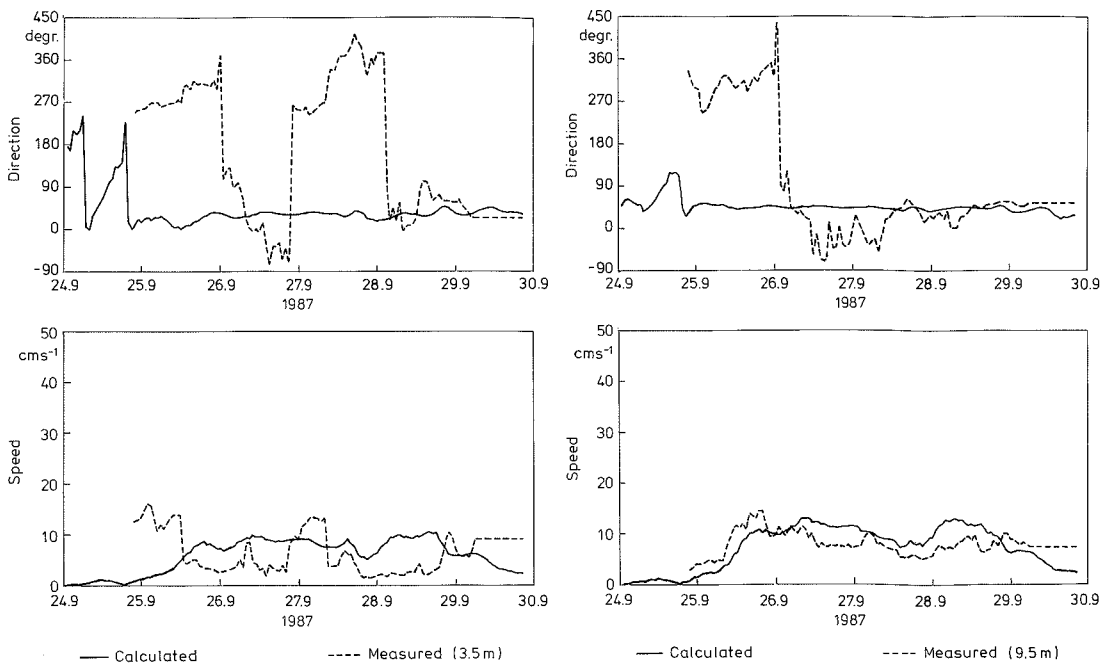


Fig. 23. Current time-series from 3.5 m and 9.5 meters depths from Cape Maksniemi (point 2 of Fig. 3).

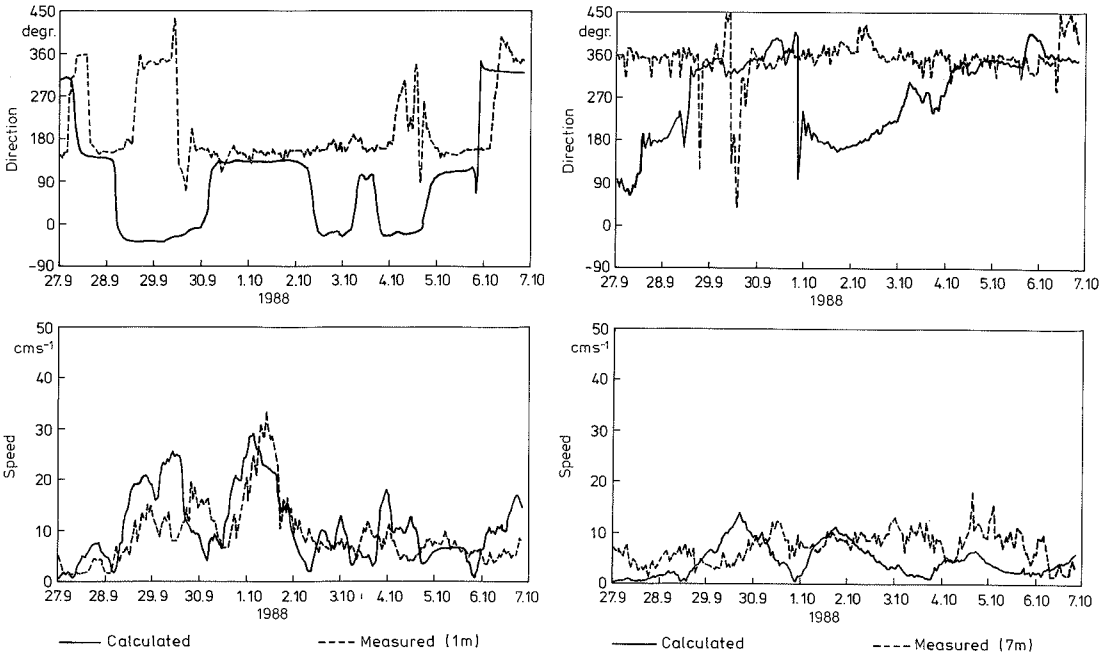


Fig. 25. Current time-series from Kemi harbor (left, point 1 of Fig. 3) and Ulkokrunni (right, point 5 of Fig. 3).

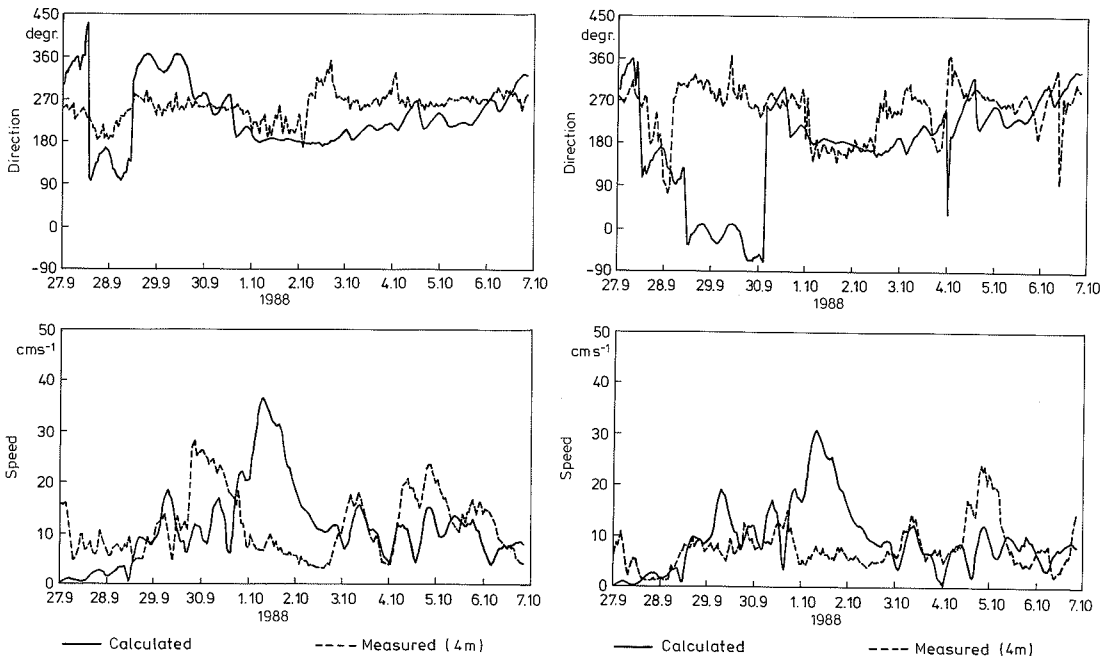


Fig. 26. Current time-series for two points at the open sea south-west from Cape Maksniemi (points 3 and 4 of Fig. 3).

In the Fig. 24 is shown the wind during September 27–October 6 1988 in Kemi (Ajos). In Fig. 25 are time-series from Kemi harbor (point 1 in Fig. 3) and Ulkokrunni (point 5) and in Fig. 26 from two points further out in the open sea southwest from Cape Maksniemi (points 3 and 4). An interesting anomaly in these series can be seen around October 1–2 when there is a significant peak in the flow velocities in the modelled results in all of the points. This peak is however missing from measurements in the Cape Maksniemi points. The wind from Ajos shows at this time a peak  $18 \text{ m s}^{-1}$ . A simple explanation for the results might be the local wind variations which were not taken into account in the model runs. Other explanations might be the influence of large scale circulation, nonlinear effects or thermocline oscillations that the model does not take into account. It would seem however probable that the wind was weaker at the open sea during this period than at the coast because the measurements were quite near the surface (4 m depth) and the effect of high wind velocities should be strongly seen in the current velocities. Combined current and model studies, wind measurements in various locations and use of wind models would be needed to clarify the extent of spatial variations in windstress.

#### 7.1.4 Observed and calculated wintertime flow characteristics

Fig. 27 shows the advance of the river Kemijoki plume during the ice covered period. The significant factor in the dynamics of the wintertime river plume is the density difference between the fresh river water and the saline sea water (of the order 3 ‰). In the figures it can be seen that large scale eddies can be formed when the river plume advances.

In the Fig. 28 is shown a time-series from a point off the town Kemi during a ice covered period in 1985 (Forsius 1985). Altogether 5 Aanderaa RCM4-meters were employed in the region, but only in one point that is shown the threshold velocities were significantly over the threshold velocity  $2 \text{ cm s}^{-1}$  of the meters. In the others the velocities exceeded the threshold velocity in 0–3 % of the time. It is interesting to note that the current is governed largely by oscillations but there seems to be an average component that is toward the coast and that is associated with the rise of the sea level that occurred during the shown period. For the wintertime water quality modelling these results would suggest that beside the river flow the water level changes and the (seiche) oscillations

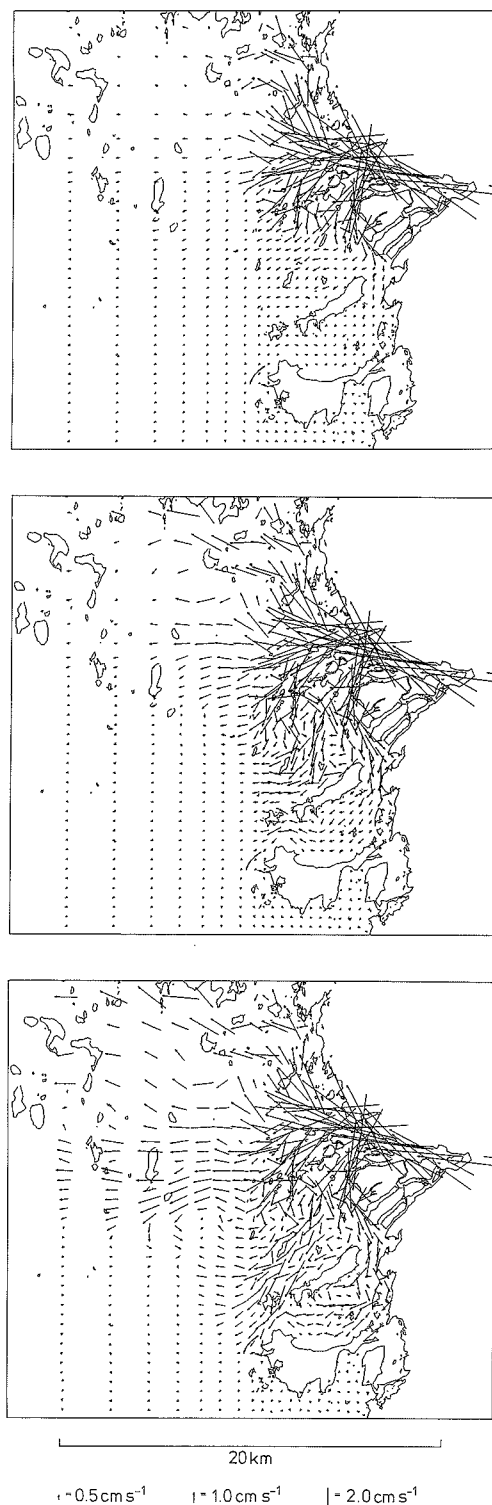


Fig. 27. Advance of the river Kemijoki plume. Flow fields after 50, 100 and 200 hours calculation time.

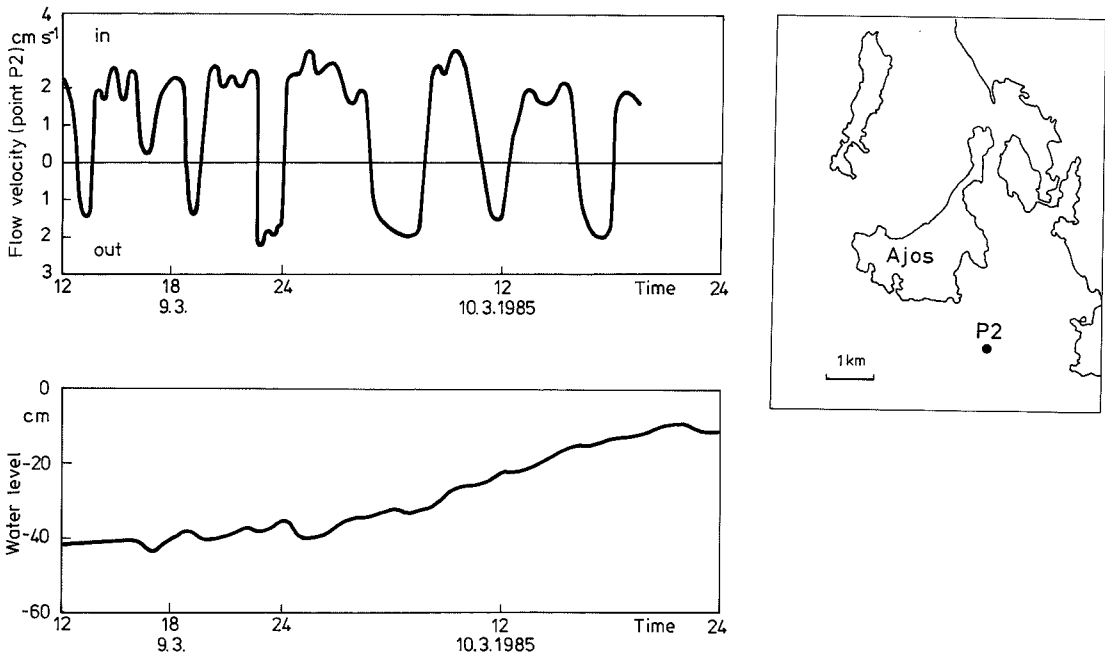


Fig. 28. Location of the measurement point and time-series of the current and sea level off the town Kemi (Forsius 1985).

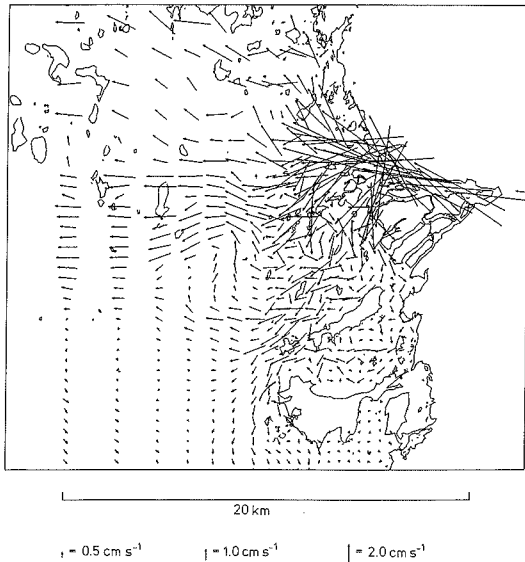


Fig. 29. Modelled river flow at the end of the winter off the town Kemi.

should be taken into account. In the Figure 29 is shown the flow field induced by the river Kemijoki at the end of the winter. As can be seen the velocities especially in the bay of Veitsiluoto (east of Ajos) are very small and are not sufficient to cause the observed pollution transport off the coast.

The effect of the following factors were tested in connection with the wintertime flow calculations: density difference between the fresh and sea water, vertical momentum diffusion, difference schemes for density gradients, surface friction, Coriolis-coefficient, calculation time-steps. The importance of the factors to the flow direction diminishes from the beginning of this list to the end and the importance to the stability and vertical mixing behave approximately in a reverse order. It was found out that the minimum vertical mixing was obtained with small timesteps (20 s for the external field), no Coriolis term and zero surface friction. The important point in the flow direction is the ratio between the density difference and the vertical momentum diffusion. The closest agreement between the measured and calculated phosphorus values was obtained with  $10 \text{ cm}^2 \text{ s}^{-1}$  vertical momentum diffusion and  $1000 \text{ mg l}^{-1}$  salinity difference.

A subjective evaluation of the agreement was used instead of any statistical measures because it was found out that the  $r^2$  method described in Koponen (1991) would give quite erroneous results regarding the general distribution of the phosphorus in the whole study area (values near the outlets improperly dominated the results). The density gradient scheme that was chosen was one assuming regular distances between the gridpoints. Another tested one was scheme that used 4 points and the real distances.

It should be noted that the comparisons between the cases were done using the stable fields at the end of the calculation period (a typical ice covered situation) and were not realistic because the transport in reality is not stable due to the advance of the plume and the factors causing oscillations (e.g. atmospheric pressure dynamics). Altogether 26 cases were studied, but the further testing was limited by the extremely long calculation times these calculations required (imagine 5 month calculation period, 20 s timestep,  $36 \times 62 \times 9$  grid, continuous flow and density calculation!).

### 7.1.5 High resolution flow fields

Using the mesh generator program described in section 6.5, it has been possible to produce high resolution grids of the Bothnian Bay. Axonometric pictures of the bottom geometry for grid sizes  $128 \times 128$ ,  $256 \times 256$  and  $512 \times 512$  are shown in Fig. 30 to 32. As expected, the number of visible local details increases with the resolution. Particularly the growing amount of inactive land areas makes the domain more times connected on higher mesh levels. This visualizes the need for inverse approach in the multigrid model. It is just not possible to describe all the necessary formations in only a few grid points, so the geometry has to be simplified on the coarser levels. Flow fields on the generated grids were also computed (see Fig. 30 and 31). Again, on denser mesh more details can be seen, but otherwise there is no contradiction between the results. The differences are mainly due to the absence of high frequency components from the coarser grid solution. This is also true for Figure 32, where two different resolution flow fields

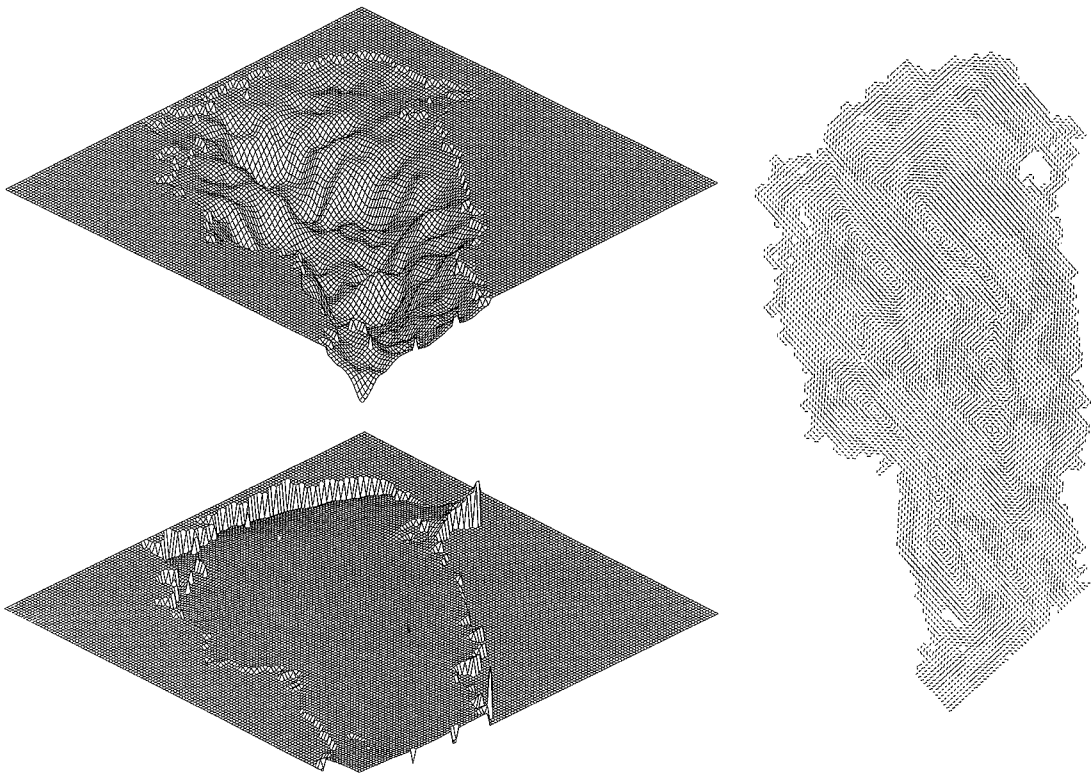


Fig. 30.  $128 \times 128$  mesh (upper), pressure (lower) and flow (right).

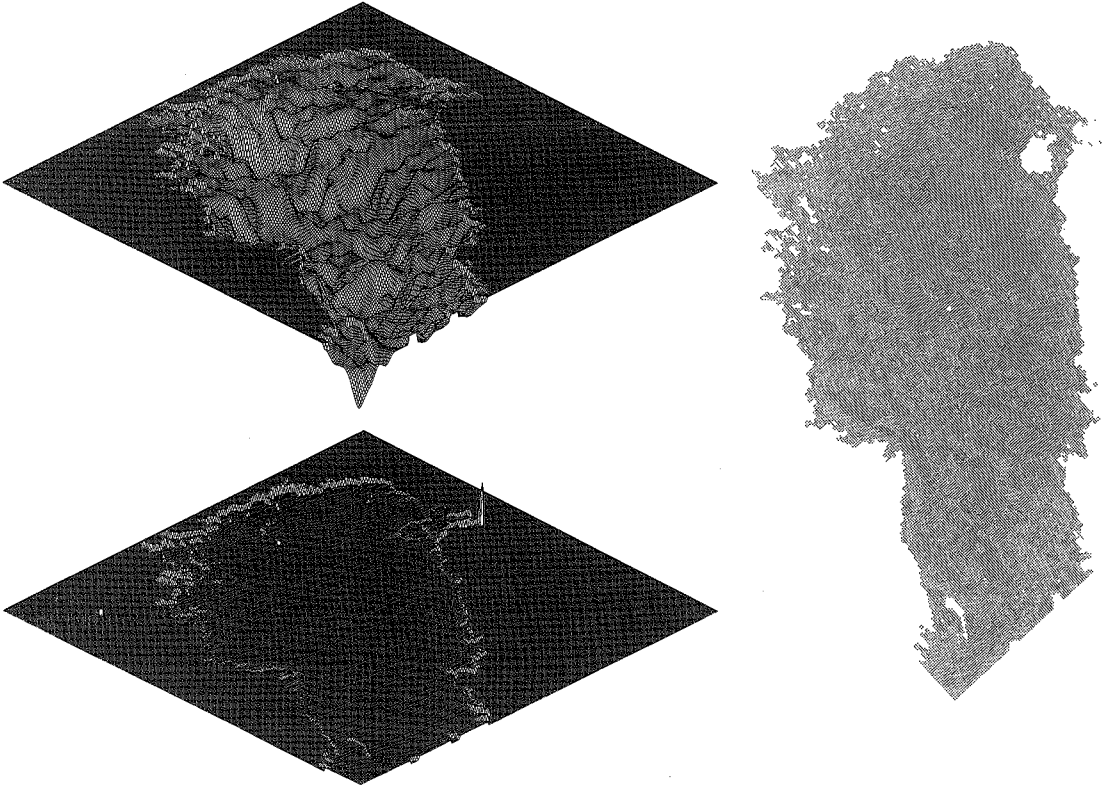


Fig. 31.  $256 \times 256$  mesh (upper), pressure (lower) and flow (right).

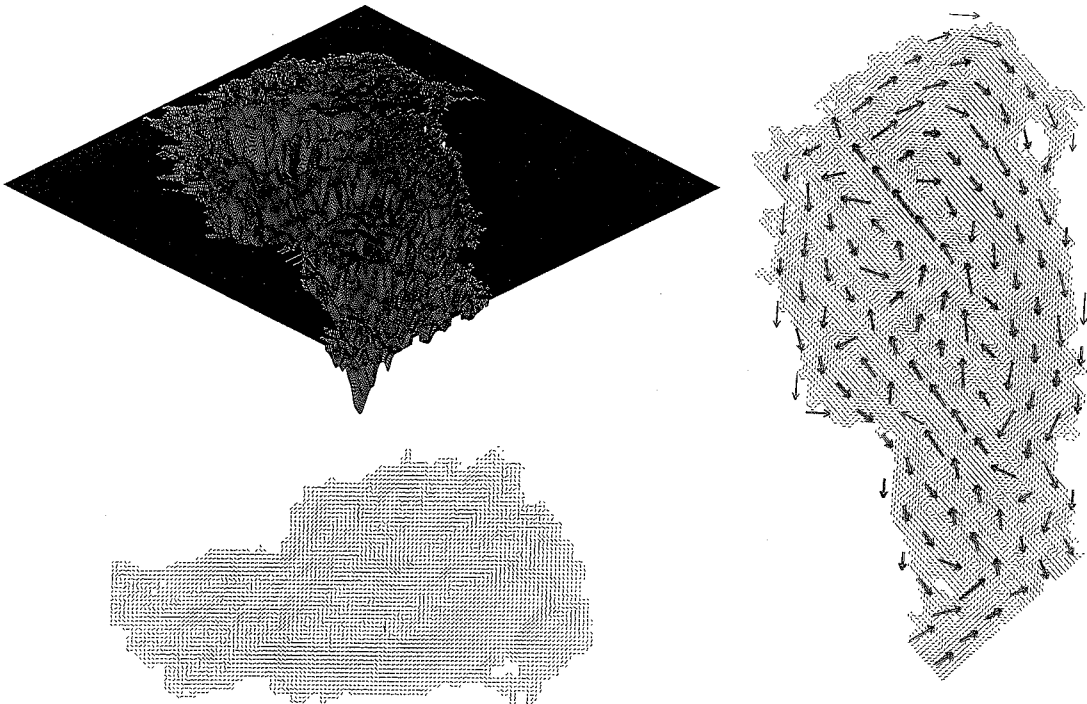


Fig. 32.  $512 \times 512$  mesh (upper), influence of different mesh angles (lower and right) and grid resolution (right).

(128×128 and 16×16) are plotted on top of each other. Finally, the influence of the mesh angle on the flow field was tested. The two 128×128 flow fields in Fig. 32 have been computed on grids of different angles between the x-axis and north direction. Due to the way the binary division and exchange algorithm works, the generated grids are slightly different from each other. Nevertheless the flow fields seem to be quite similar. This would mean, that the computed flow fields are not very sensitive to minor errors in the generated depth geometry, what could be considered an argument for the usability of the mesh generator program.

## 7.2 Comparison of measured and calculated incoming short wave radiation

Usually one doesn't have measured values for incoming short wave radiation, which is a very important part of heat energy simulation of water bodies. One way to get an approximation is to calculate those values. In the following, a comparison of radiation calculated with two different equations with each other and with measured values is presented.

Heat energy equation for a closed water body may be written in the form

$$RSI + RLI - RLO - QE + QCA + QCB = 0 \quad (48)$$

where

**RSI** is short wave radiation reaching the water surface. It may be written as  $RSI = (1 - r_s)RS$  where  $RS$  is incoming short wave radiation and  $r_s$  is reflectivity of the water surface. The instant values of radiation may vary from  $0 \text{ W m}^{-2}$  to  $1000 \text{ W m}^{-2}$ . The daily mean values of  $RSI$  may vary between  $60\text{--}300 \text{ W m}^{-2}$

**RSI** is atmospheric longwave radiation, the daily mean values of which may vary between  $200\text{--}450 \text{ W m}^{-2}$

**RLO** is longwave radiation from water body to the air. It has the largest magnitude among the heat exchange components. The daily mean values vary between  $250\text{--}500 \text{ W m}^{-2}$

**QE** is evaporative heat transfer. The daily mean values vary between  $-5\text{--}350 \text{ W m}^{-2}$

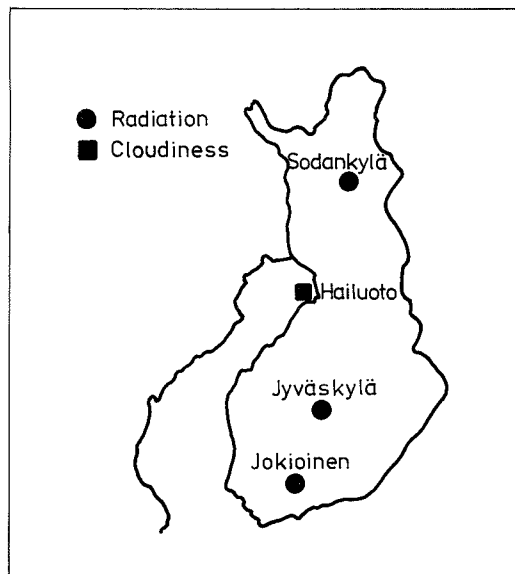


Fig. 33. Location of incoming short wave radiation measurement stations and observation site of cloudiness.

**QCA** is heat conduction through the water surface. The daily mean values vary between  $-7\text{--}200 \text{ W m}^{-2}$ .

The heat exchange between water body and bottom (**QCB**) is negligible in summer but it may have considerable influence for heat budget during the winter. In the lake Prästkonselet in Sweden the heat flux from the bottom to the water was about  $2 \text{ W m}^{-2}$  in mid winter.

Two different equations for calculation of incoming short wave radiation were used. The first equation, used in PROBE model developed in SMHI, is described below. The equations used in the 3D-model were discussed in section 6.3.2. Three meteorological stations were used to compare calculated values with measurements. Although these stations were situated inland (Fig. 33) they gave an approximation on the magnitude of incoming short wave radiation.

The equation for incoming short wave radiation used in PROBE is

$$R_s = I_o \cos(\beta)(T_r - A_w) \times \quad (49)$$

$$(1 - c_1(0.55 + 0.01saz)) \quad (50)$$

where

$$\beta = \arccos(sz + cz)$$

$$sz = \sin(\text{dekl}) \sin(\theta)$$

$$\begin{aligned}
cx &= \cos(\text{dekl}) \cos(h) \\
\text{dekl} &= 23.5(\pi/180) \times \\
&\quad \sin(2\pi(\text{DAY} - 180)/365) \\
h &= 15\pi(h_s - 12.00)/180 \\
T_r &= 1.041 - 0.16\text{saz}^{0.3} \\
A_w &= 0.077(1.25 + 0.75 \sin(\text{FA}))\text{saz}^{0.3} \\
\text{FA} &= 2\pi(\text{DAY} - 120)/365 \\
\text{saz} &= \frac{1}{sz + cz}
\end{aligned}$$

Calculated weekly values for incoming short wave radiation compared with measured values are given in Table 9. Both models seem to give about 20 % too large values for incoming short wave radiation. The difference between the two models is only 4 %.

### 7.3 Comparison of 3D and 1D temperature models

This section presents water temperature simulations of the Bothnian Bay calculated by one dimensional PROBE model and three-dimensional 3Dwt model. The structure of 3D temperature model has been discussed in detail in section 6.3.1.

In PROBE model the heat energy conservation law can be expressed in the form

$$\frac{\partial}{\partial t}(\rho c_p T) = \frac{\partial}{\partial z} \left( \frac{\mu_{\text{eff}}}{\rho \sigma_{\text{eff}}} \frac{\partial}{\partial z} (\rho c_p T) \right) + S_H \quad (51)$$

$$\frac{\mu_{\text{eff}}}{\sigma_{\text{eff}}} = \frac{\mu}{\sigma} + \frac{\mu_T}{\sigma_T} \quad (51)$$

where

$\mu_{\text{eff}}$  is effective viscosity  
 $\mu$  is laminar viscosity  
 $\mu_T$  is turbulent viscosity

$\sigma_{\text{eff}}, \sigma_T, \sigma$  are effective, turbulent and laminar Prandtl numbers  
 $S_H$  is source and sink term

Source term which embodies energy exchange between the water body and its surroundings is about the same order of magnitude in both models.

The basic difference between the two heat energy conservation equations is heat energy advection and constant kinematic eddy viscosity in 3D model. PROBE model contains k- $\epsilon$  turbulence model where the dynamical eddy viscosity is calculated from the turbulent kinetic energy, k, and its dissipation rate,  $\epsilon$ , by the Prandtl/Kolmogorov relation:

$$\mu_T = C_\mu \rho \frac{k^2}{\epsilon} \quad (52)$$

where  $C_\mu$  is an empirical constant. A PROBE version where the k- $\epsilon$  model contains an extra term was also tested:

$$\mu_T = C_\mu \rho \frac{k^2}{\epsilon} + DM \quad (53)$$

$$DM = C2 + \min \left( \frac{C1 \rho_{\text{ref}}}{BR + 10^{-10}}, 0.1 \right)$$

$$BR = \sqrt{\frac{|-\mathbf{g}(\rho_{i+1} - \rho_{i-1})|}{\rho_{\text{ref}} z}}$$

where

$C1$   $10^{-7}$   
 $C2$   $10^{-6}$   
 $\rho_{\text{ref}}$  is reference density of water  
 $\rho_{i+1}$  is density above the layer concerned  
 $\rho_{i-1}$  is density below the layer concerned  
 $z$  is thickness of the layer  
 $\mathbf{g}$  is acceleration due to gravity.

Table 9. Calculated and measured values for incoming short wave radiation.

Time 1976	Model (J m <sup>-2</sup> )		Measured (J m <sup>-2</sup> )		
	Probe	3D	Jokioinen	Jyväskylä	Sodankylä
3.—9.6	15 411	16 180	13 110	13 624	12 243
10.—16.6	17 763	18 859	14 402	14 620	17 252
17.—23.6	15 077	16 416	10 988	10 258	11 079
24.—30.6	15 946	16 475	16 059	13 594	11 599
1.—7.7	15 299	16 246	14 815	12 805	11 860
8.—14.7	15 420	16 042	13 853	11 802	12 746
15.—21.7	14 737	15 059	12 906	10 721	13 225
22.—28.7	14 488	14 796	9 296	11 032	12 343
total	124 141	129 573	105 429	98 456	102 447



First, a comparison between these two PROBE versions was made. Calculated space-time temperature distributions of the Bothnian Bay are shown in Fig. 34 and measurements in Fig. 35. The best result was carried out by PROBE version where  $k-\epsilon$  turbulence model contained the extra term. Probe version with  $k-\epsilon$  model builds up too steep

thermocline. In both cases temperatures in epilimnion and hypolimnion are too high.

Usually a special pressure filtering term has been used to get a more economical time-step. The pressure gradient formula for lakes and reservoirs simulates seiches with periods based on the dimensions of the water body. Pressure gradient

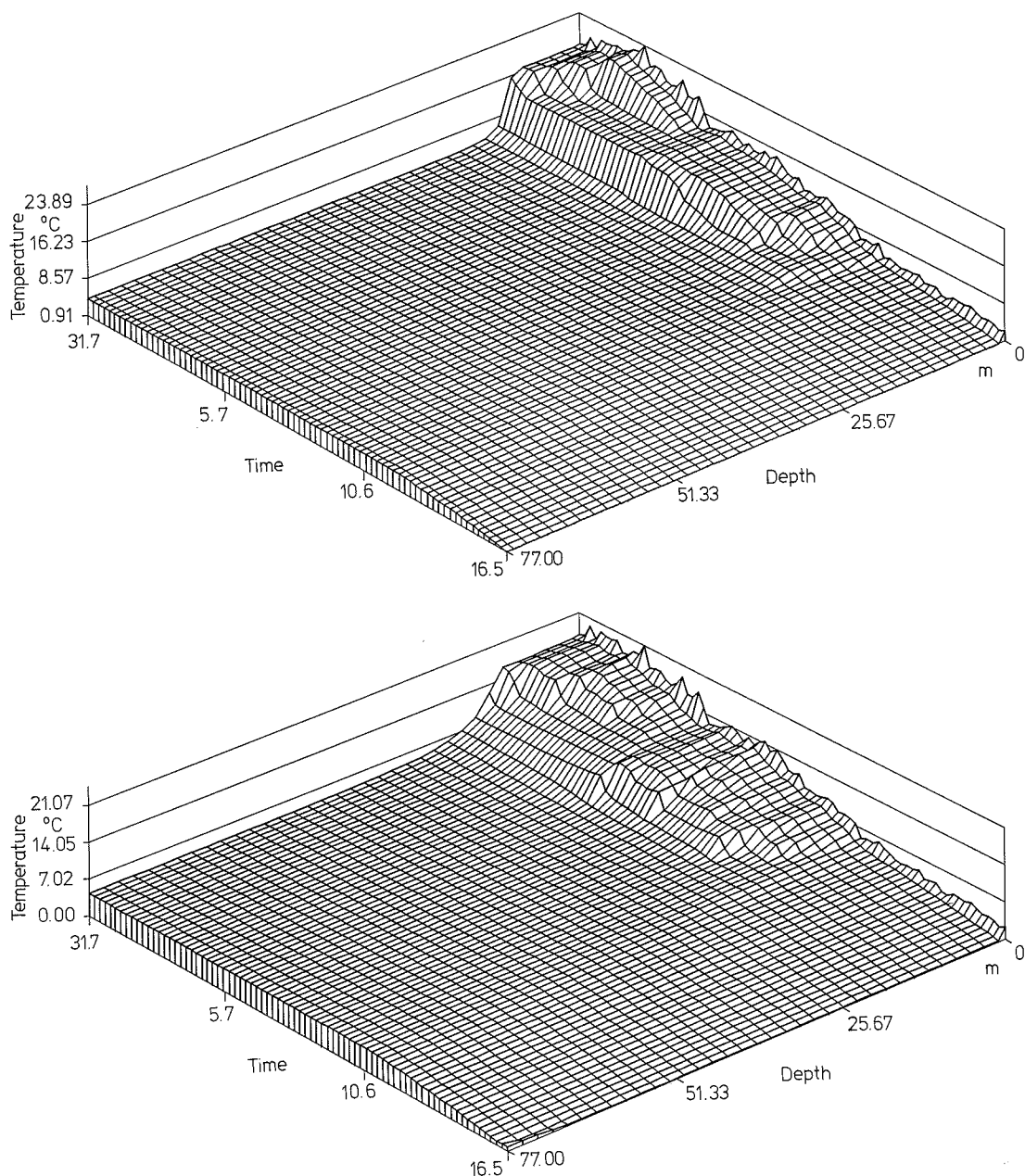


Fig. 34. Calculated temperature distribution with the original PROBE-model (upper) and PROBE with extra term DEEPMIX (lower).

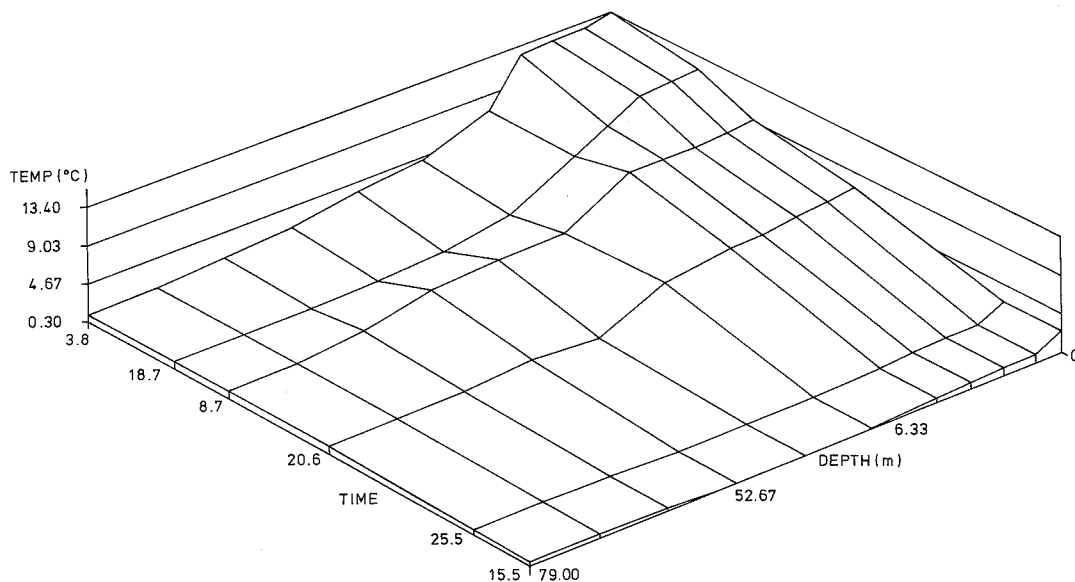


Fig. 35. Measured temperature distribution.

equations in x- and y-directions in PROBE are

$$\frac{\partial p^{i+1}}{\partial x} = \left( \frac{\partial p^i}{\partial x} + p_f^2 + \frac{\Delta t \rho g \pi^2 u D}{L_x^2} \right) \times \frac{T - T_b}{T_s - T_b} \quad (54)$$

$$\frac{\partial p^{i+1}}{\partial y} = \left( \frac{\partial p^i}{\partial y} + p_f^2 + \frac{\Delta t \rho g \pi^2 u D}{L_y^2} \right) \times \frac{T - T_b}{T_s - T_b}$$

where

- $i$  is time level
- $\Delta t$  is time step
- $g$  is acceleration due to gravity
- $u, v$  are mean velocities
- $D$  is the depth
- $L_x, L_y$  are horizontal dimensions of the water body
- $T$  is temperature.

By using pressure filtering ( $p_f$ ) values smaller than 1.0 a more economical time-step can be used. However, when pressure filtering is used it changes the horizontal pressure gradient thus affecting horizontal velocities. This in turn has influence on the magnitude of the dynamical eddy viscosity. Because the estimation of the influence of pressure filtering factor is so complex, test calculations should be carried out before the use of filtering. In the simulations of the Bothnian Bay temperature the use of pressure filtering is not correct (Fig. 36).

The temperature calculations by the 3D model

were carried out in a point where water depth was 80 m. Calculated temperature distribution for that point is shown in Fig. 37. It can be seen that no clear epilimnion exists. Also the temperature in hypolimnion is too high.

Altogether, the best result was achieved with 1D PROBE model which included k-epsilon turbulence model with the extra term.

## 7.4 Salinity and temperature

Salinity and temperature are the main factors that determine the density of sea water. In the Bothnian Bay salinity plays a minor role during summer compared with the temperature while during the ice covered period salinity differences are the main density factor. Because of this the salinity effects are discussed in this section mainly in the ice covered period and the temperature effects during the summer.

The focal point of the temperature and salinity model verification were the years 1976 and 1977 when a large measurement program was realized in the Bothnian Bay in a line reaching off the town Oulu about 85 km to the open sea. The measurement points are shown in the Fig. 38. Simulations were done in a grid shown in the Fig.

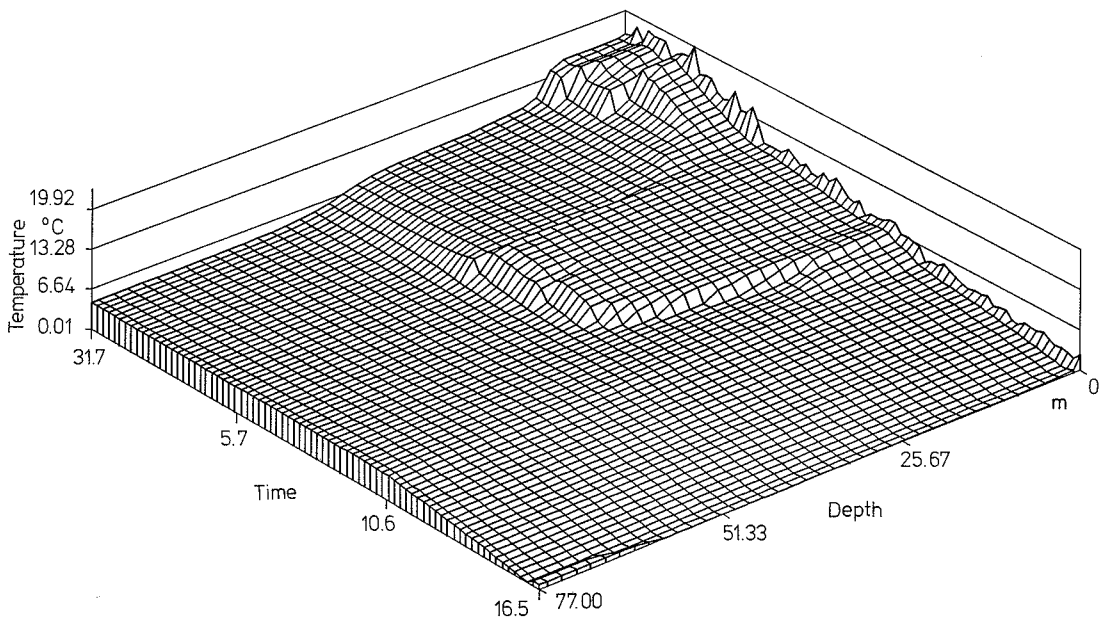
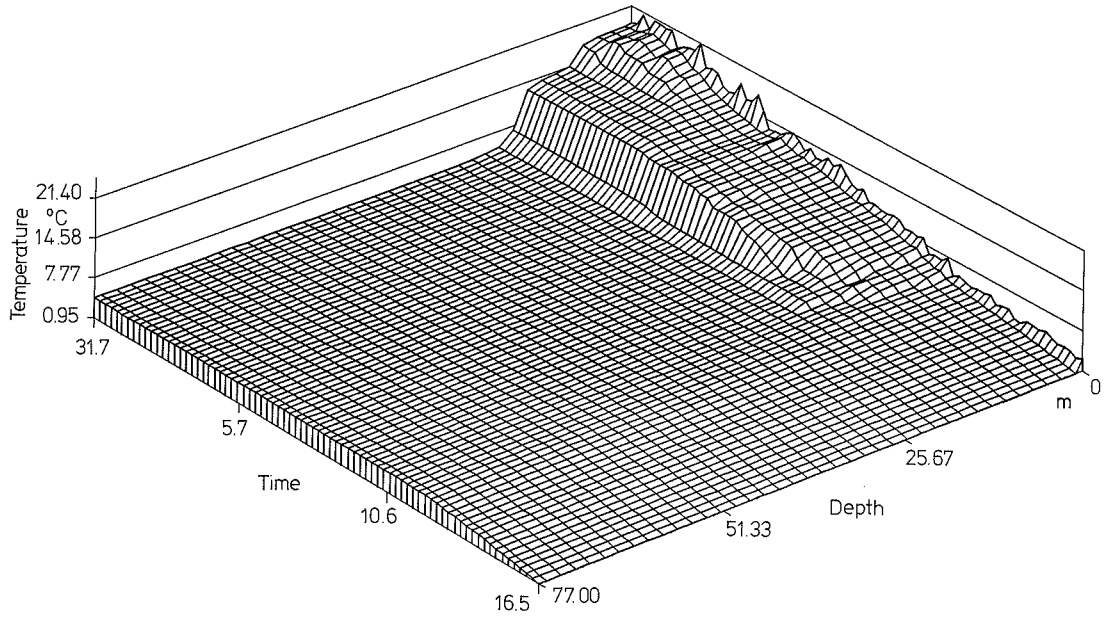


Fig. 36. Calculated temperature distribution with the original PROBE-model (upper) and PROBE with extra term DEEPMIX (lower). Pressure filtering value 0.2.

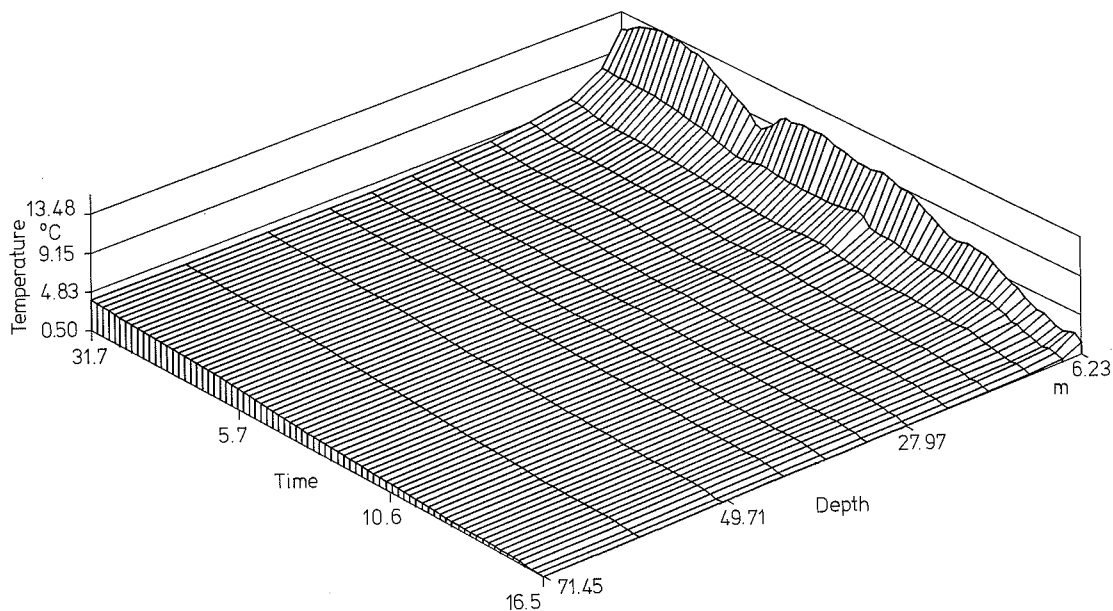


Fig. 37. Vertical temperature distribution in the point V of Fig. 38, 3D model result.

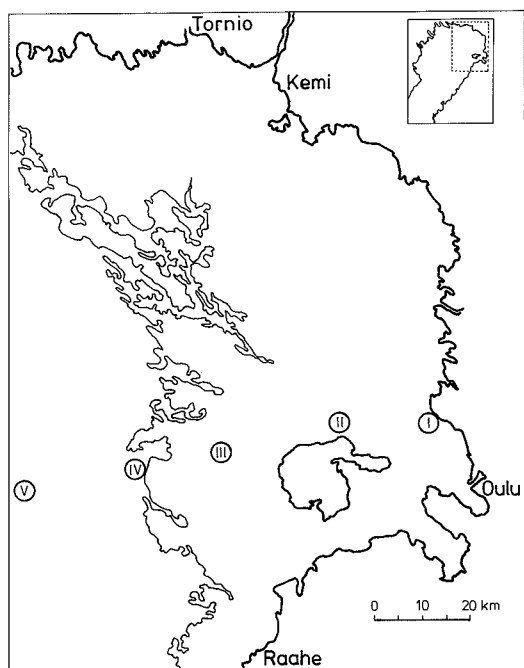


Fig. 38. Measurement stations I—V during the 1976—1977 special measurement program.

39. The measured and modelled temperature profiles as the function of time are shown in the Figs. 40—42. The most obvious feature about these figures is that the vertical profiles are not modelled very accurately. The model gives near the coast too high vertical mixing and at the open sea too low. Near the coast the water warms up too much and at the open sea the thermocline is located too high and it is too steep. On the other hand the bottom water at the open sea is too warm probably because the too warm coastal hypolimnic water warms up gradually also the offshore hypolimnic water. Three main factors which affect the vertical mixing were identified in the model:

- area of the gridcell
- amount of filtering in the flowfields
- vertical temperature diffusion coefficient.

The first factor is the most troublesome because it is the most difficult to control. It is due to the discretization of the calculation domain. The correction of this effect would probably require the use of a vertical diffusion coefficient that depends on the grid size. The effect of the third factor is quite obvious and it can be used to parametrize the small scale eddies or oscillations. The second factor is also very important. When oscillations in the

flowfields are filtered out also the vertical mixing diminishes and the effect of oscillations must be parametrized.

One additional problem with the temperature calculation is associated with the overestimated up- and down-welling near the coast. Fig. 43 illustrates this fact. In the figure two different flowfields are used to study the vertical mixing of water that initially lies in the upper layers from 0 to 5 m. Both of the flowfields are started with the same initial stratification, parameters and total calculation time but in one the calculation time for the thermocline tilting is 6 hours and in the other 12 hours. After the currents have been stabilized the concentration

calculation is started from value 8 in the upper layers and 0 in the lower ones. It can be seen that the 6 h tilted field maintains the material much better in the upper layers whereas in the 12 h tilted field there is much more vertical mixing.

These considerations led to the development of a new model where the layer velocities are calculated explicitly (see section 6.1.3). Unfortunately there was not enough time to include the density effects in the new model. The new model can be utilized in two ways: direct calculation of the vertical velocities and use of "permeabilities" across the layer boundaries. Increased vertical and horizontal resolution would also help to describe better the stratification effects. The parametrization of the vertical diffusion coefficients as a function of the gridsize should be also studied in order to describe the vertical mixing better.

Usually temperature modelling is done by using vertical 1D models. For instance in the Canada Center for Inland Waters there has been done a lot of work with Great Lakes measurement program, 3D hydrodynamic modelling and temperature modelling. In their opinion it would be almost impossible for the 3D temperature models to give right answers (personal communication). Their strategy is to combine all the temperature measurements from a basin and compare the result with a 1D vertical temperature model. With right parametrization it is possible to get very good agreement between the model and averaged measurement results. The 3D temperature modelling is however quite essential for the understanding and development of the 3D models and should not be discarded.

The 3D temperature model and the 1D Probe temperature model were compared to gain information about the differences between the model results and to test the model equations. In Fig. 44 are shown temperature profiles from points V and III which are calculated with the 3D models. A Probe result corresponding to the point V depth is shown in Fig. 45. Vertical mixing in the 3D case is clearly too large. The 1D obtains much better results but it must be kept in mind that the processes the model describes are much more simpler than in the 3D, only one point is calculated and the good results can be obtained by hand adjustment of the vertical mixing coefficients. Undoubtedly also the 3D would have given better results when the vertical mixing coefficient would have been adjusted, but because the purpose of the study was an improved understanding of the dynamics of the Bothnian Bay and model behaviour no time was devoted for that task.

The river water distribution near the town Kemi

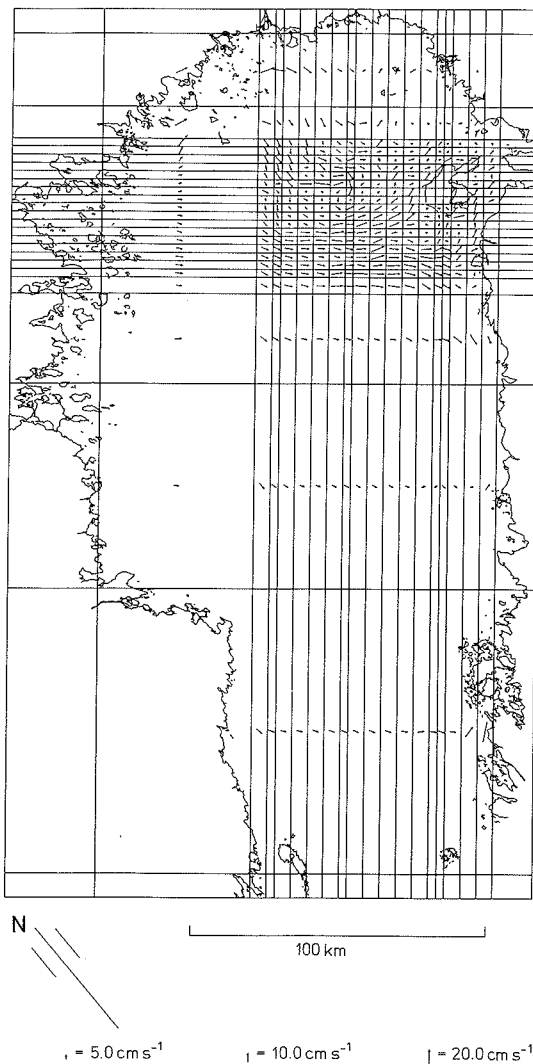


Fig. 39. Grid used in the temperature model verification.

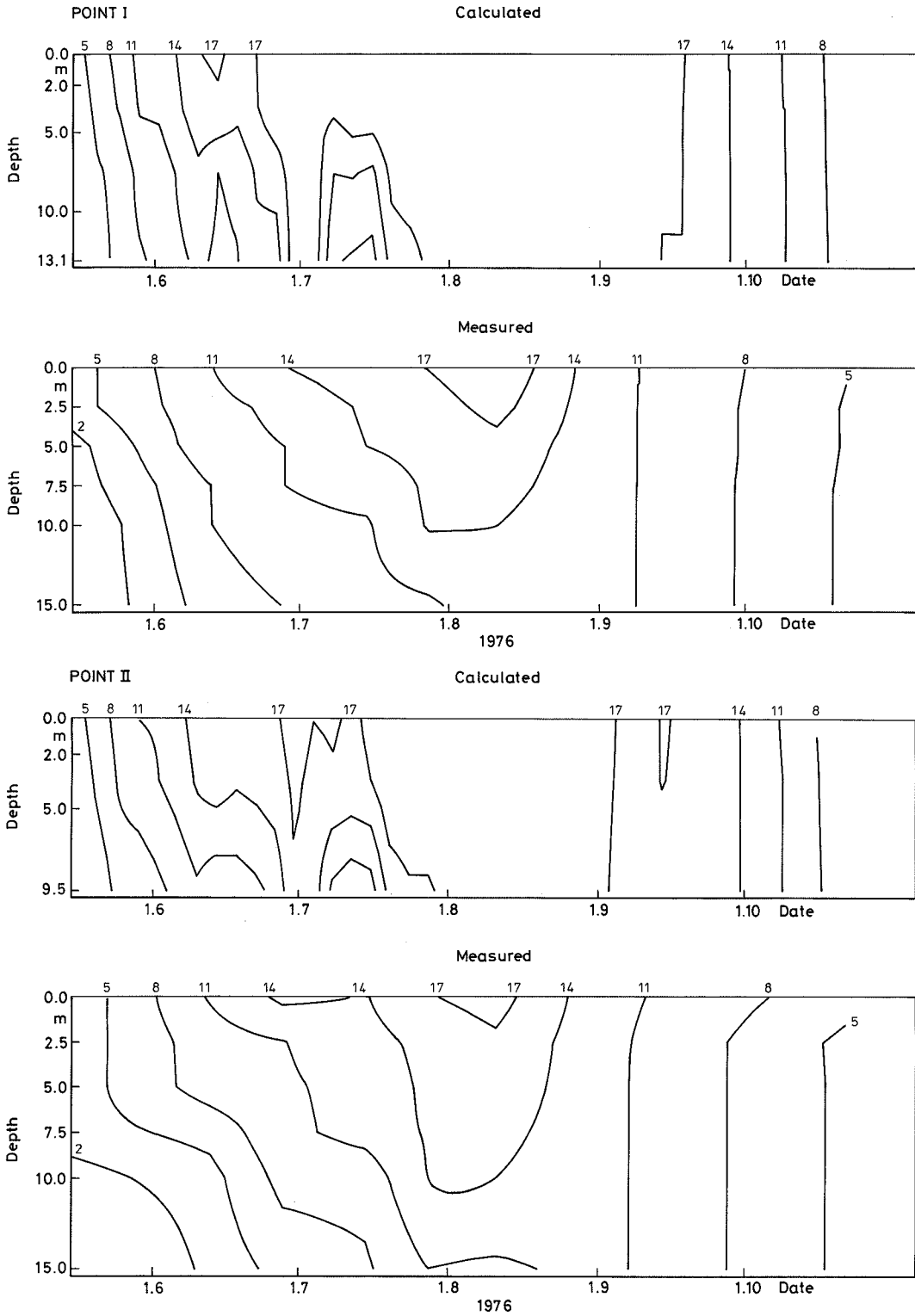


Fig. 40. Temperature profiles from the point I (on the coast) and II ( 20 km off the coast) of Fig. 38.

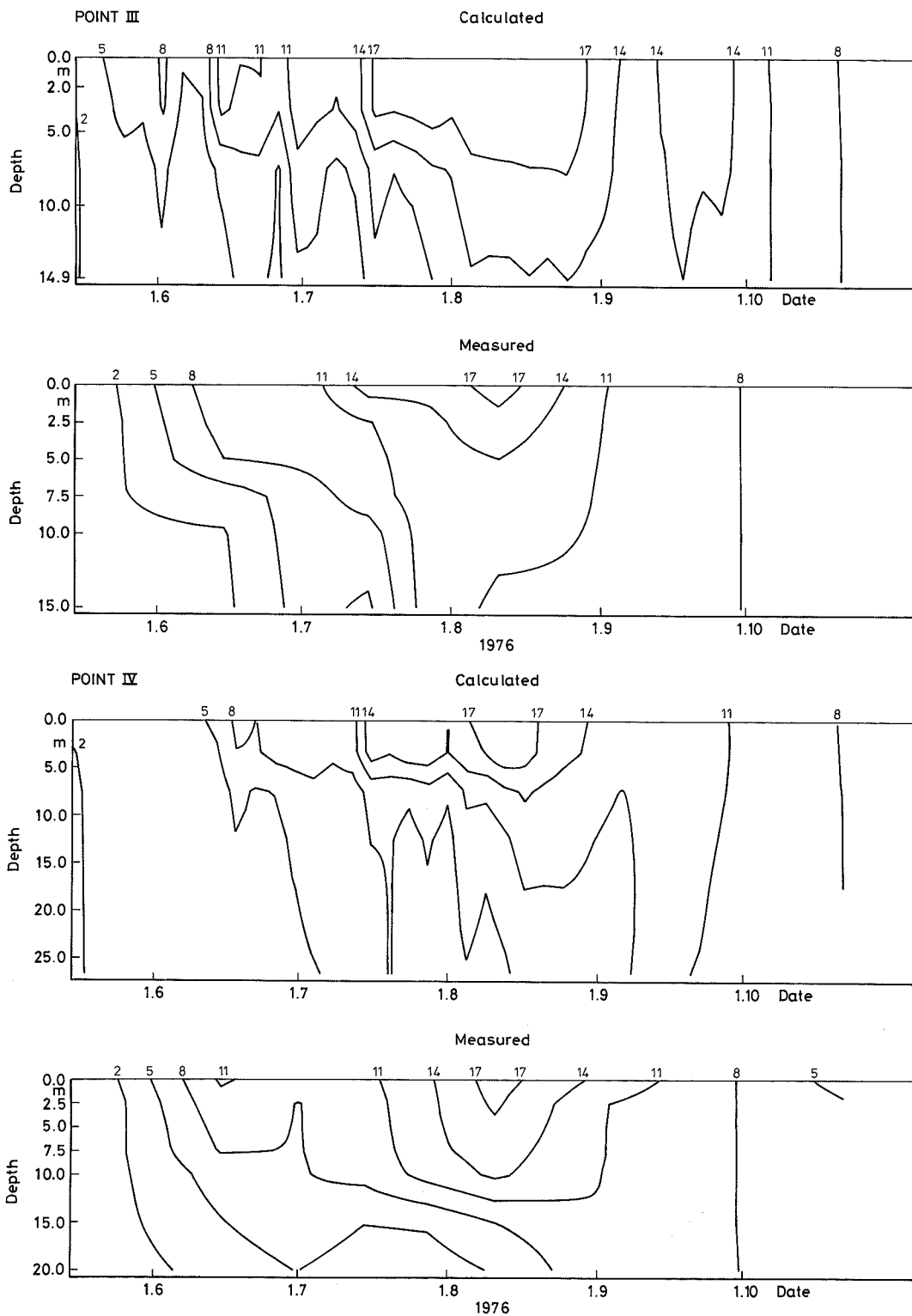


Fig. 41. Temperature profiles from the point III (45 km off the coast) and IV ( 60 km off the coast) of Fig. 38.

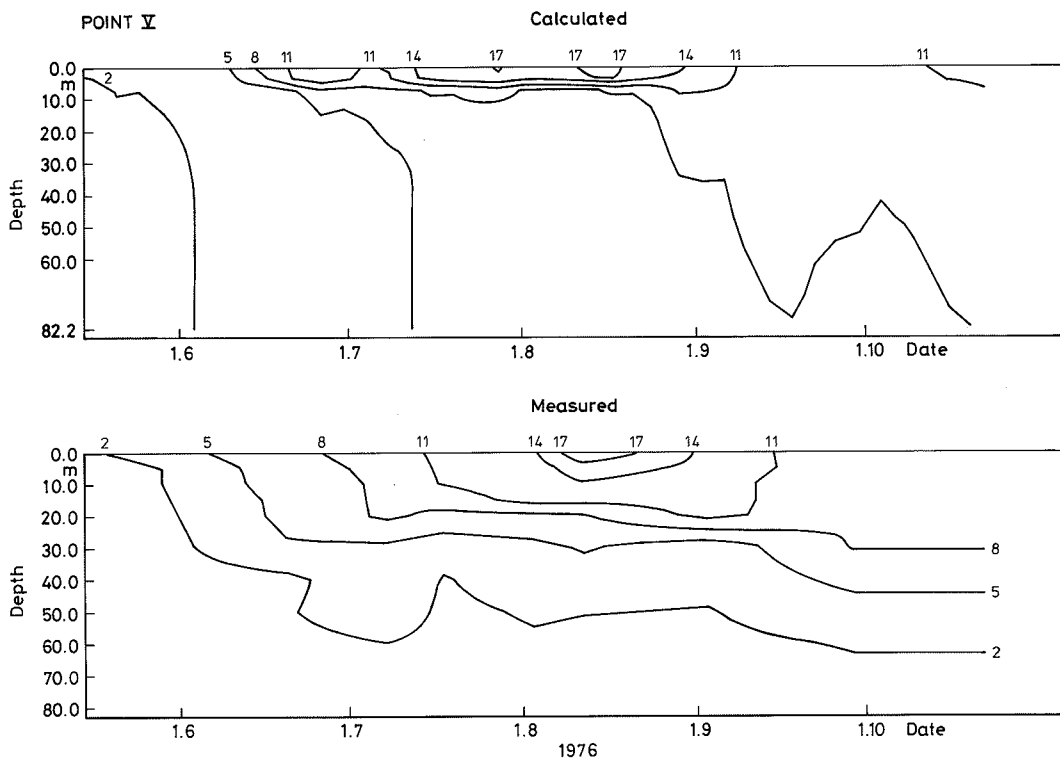


Fig. 42. Temperature profiles from the point V ( 80 km off the coast) of Fig. 38.

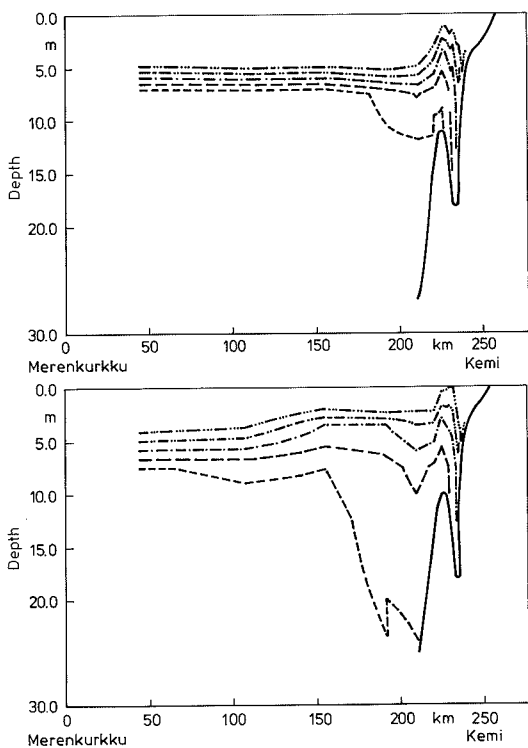


Fig. 43. Longitudinal vertical concentration profile from Quark to the north when the thermocline tilting is calculated for 6 h (upper figure) and for 12 h (lower figure).



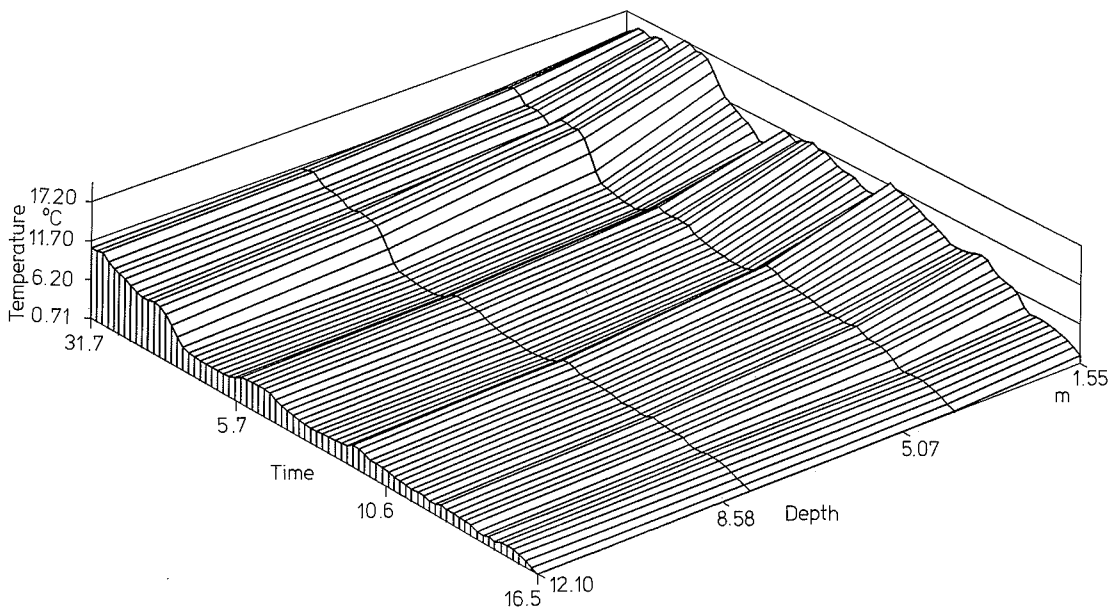
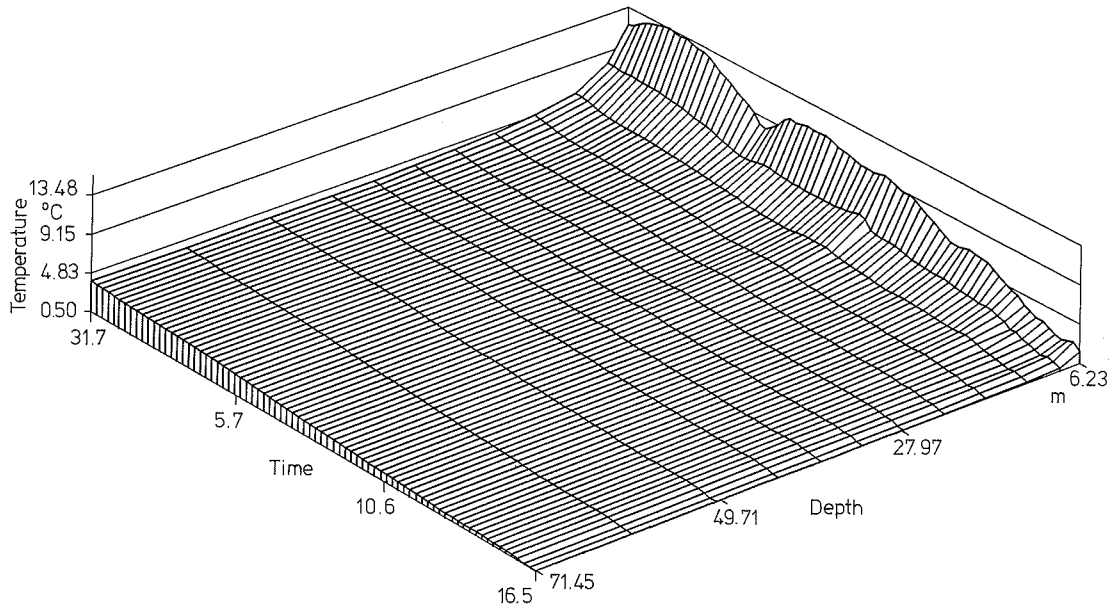


Fig. 44. Temperature time-series. 3D results from the points V and III of Fig. 38.

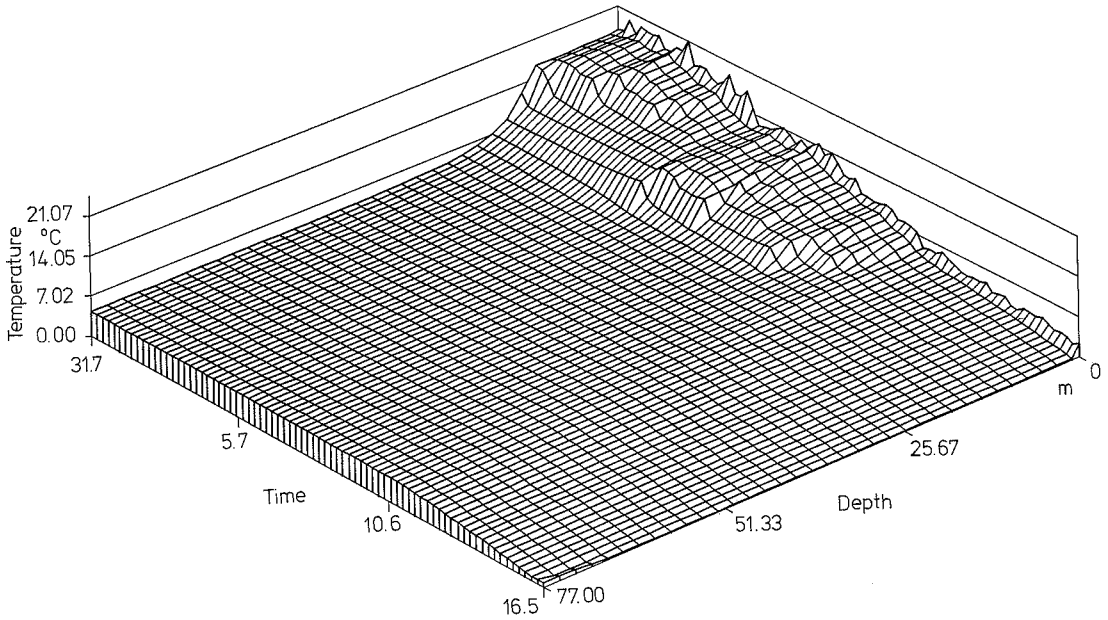


Fig. 45. Temperature time-series. 1D results corresponding to the depth of the point V of Fig. 38.

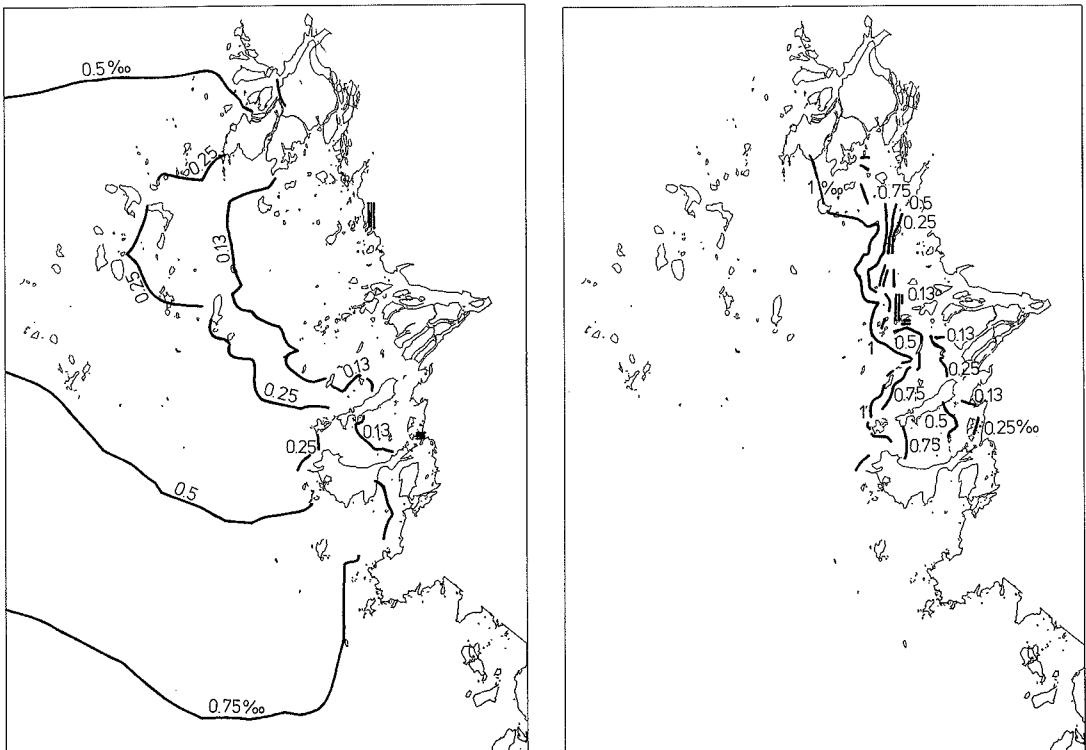


Fig. 46. River water distribution near the town Kemi at the end of the winter from 0.5 (left) and 3.5 m (right) depths.

at the end of the winter is shown in the Fig. 46. There is a very strong stratification of the river water both in the model and in the nature. In the northern Bothnian Bay the river water forms a layer 1 to 3 meters thick just below the ice. The strong stratification of the river water in the model was obtained only after lengthy tests using different parameter values and difference schemes. These were discussed in the previous section. The distribution of the river water for the whole of the north-eastern part of the Bothnian Bay is studied in the next section.

The temperature and salinity model was used to calculate the salinity and temperature development in the Bothnian Bay during the period December, 1 1975 — December 30, 1983. The full equations were solved, that is all the current components, temperature, salinity and density were calculated continuously. The eight years took about 40 min. with Cray X-MP which corresponds about 80 hours calculation time with MicroVax II. The temperature time-series in three points corresponding to the measurement points indicated in Fig. 38 are shown in Fig. 47. The effect of ice formation and melting is not taken into account in the model runs.

The variation of the temperatures between different years is greater at the coast than at the open sea. The mean temperatures grow as one moves from the open sea toward the coast. There is also a larger difference between the surface and bottom values at the open sea than at the coast. The peak temperature in the bottom layer is delayed in comparison with the surface values because of the time required to propagate the temperature to the deeper layers. Because of the reasons explained above the open sea bottom temperatures are about 5 °C greater in the model than in reality during the summer months. The wintertime bottom temperature at the open sea near the bottom rises throughout the whole simulation period. This effect suggests that there is not enough vertical mixing during the wintertime in the model and the atmospheric pressure gradients or vertical diffusion should be added to the model.

The salinity time-series corresponding to the temperature ones in the previous paragraph are shown in the Fig. 48. The salinity variation between different years is greater than the temperature variation near the coast. There is a very big difference between the bottom and surface salinities near the river Oulujoki during the wintertime. This difference can be also seen in the measurements conducted in the area. The salinities especially at the open sea tend to be too high

because the effect of the Swedish rivers is not taken into account in the model.

## 7.5 Water quality simulation in the northern Bothnian Bay

Previous water quality model applications in the Bothnian Bay have been (application area, model type, project years):

1. Kemi 2D 1981
2. Kuivaniemi 2D 1981
3. Hailuoto—Siikajoki 2D 1982
4. Tornio—Kemi 2D 1983
5. Raabe 2D 1984
6. Oulu 2D 1978—1986
7. Hailuoto 2D and 3D 1981—1987
8. Kokkola 2D 1983—1987
9. Kalajoki 2D 1987
10. Pietarsaari 2D 1987—1989

In contrast to the Bothnian Bay project where a large sea area is modelled all of the previous flow and water quality model applications have been regional ones, that is calculation area has been covered only small coastal part of the Bothnian Bay.

In the Bothnian Bay project the original project plan didnt include water quality modelling but because there was a need to study the effect of loading alternatives off the town Kemi during the project period considerable amount of work was devoted to make up a water quality model to this area. The work has been published in a report (Alasaarela et. al. 1989). The results which are relevant to the verification of the model and to the water quality dynamics in the Bothnian Bay will be shown in this work. Some results concerning the water quality modelling in the north-eastern part of the Bothnian Bay will also be shown (previously appeared in Alasaarela and Koponen 1989).

The average phosphorus distribution during an open water period in the north eastern Bothnian Bay is shown in the Fig. 49. The calculated phosphorus distribution at end of the ice covered period is shown in the Fig. 50. The phosphorus calculation was started from a completely mixed basin with small phosphorus concentration. This gives too small phosphorus values also at the end of the calculation period.

The pattern of calculated phosphorus distribution agrees amazingly well with the measured river water distribution (most of the phosphorus in

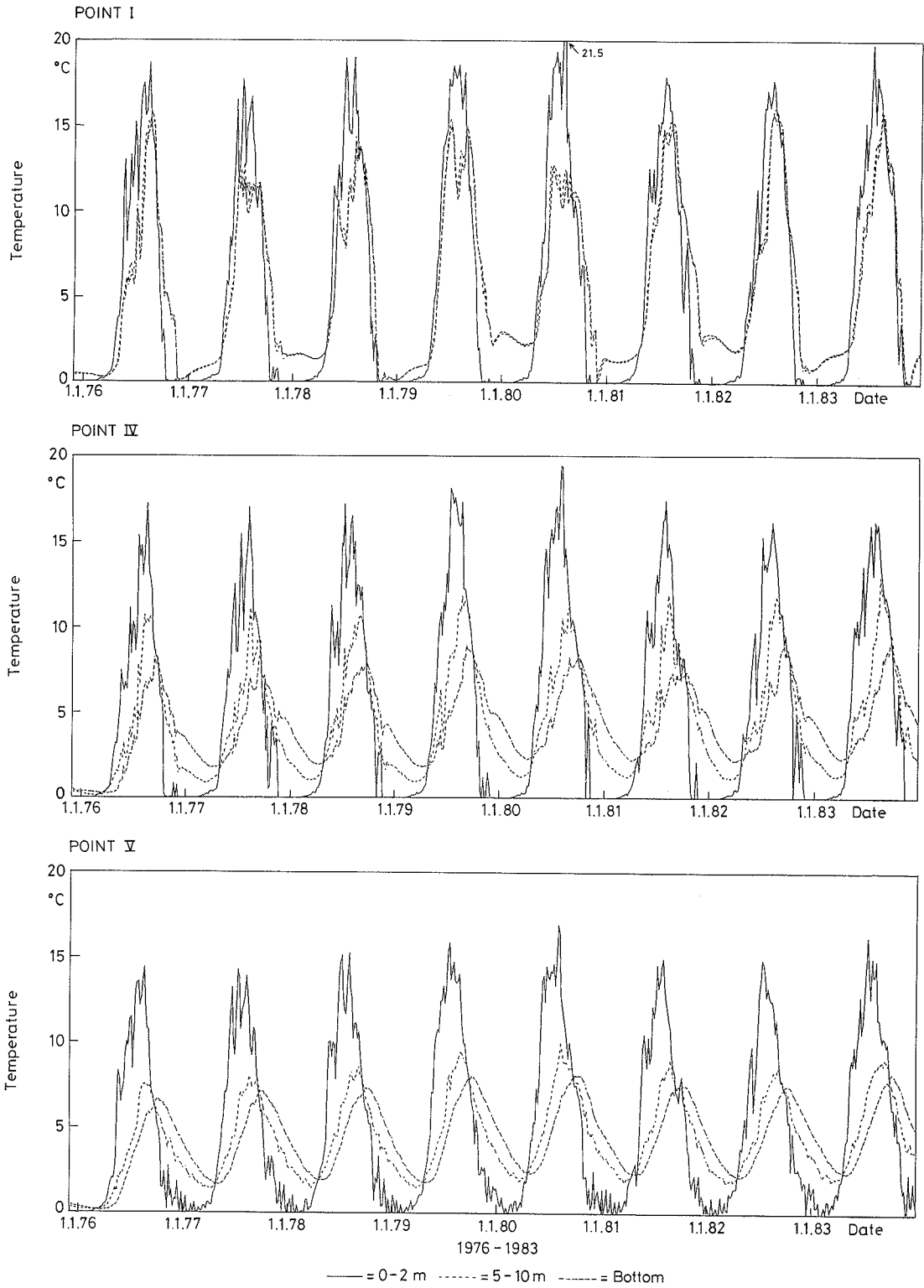


Fig. 47. Temperature time-series from the 1 m, 7.5 m and bottom depths in the points I, IV and V of Fig. 38.

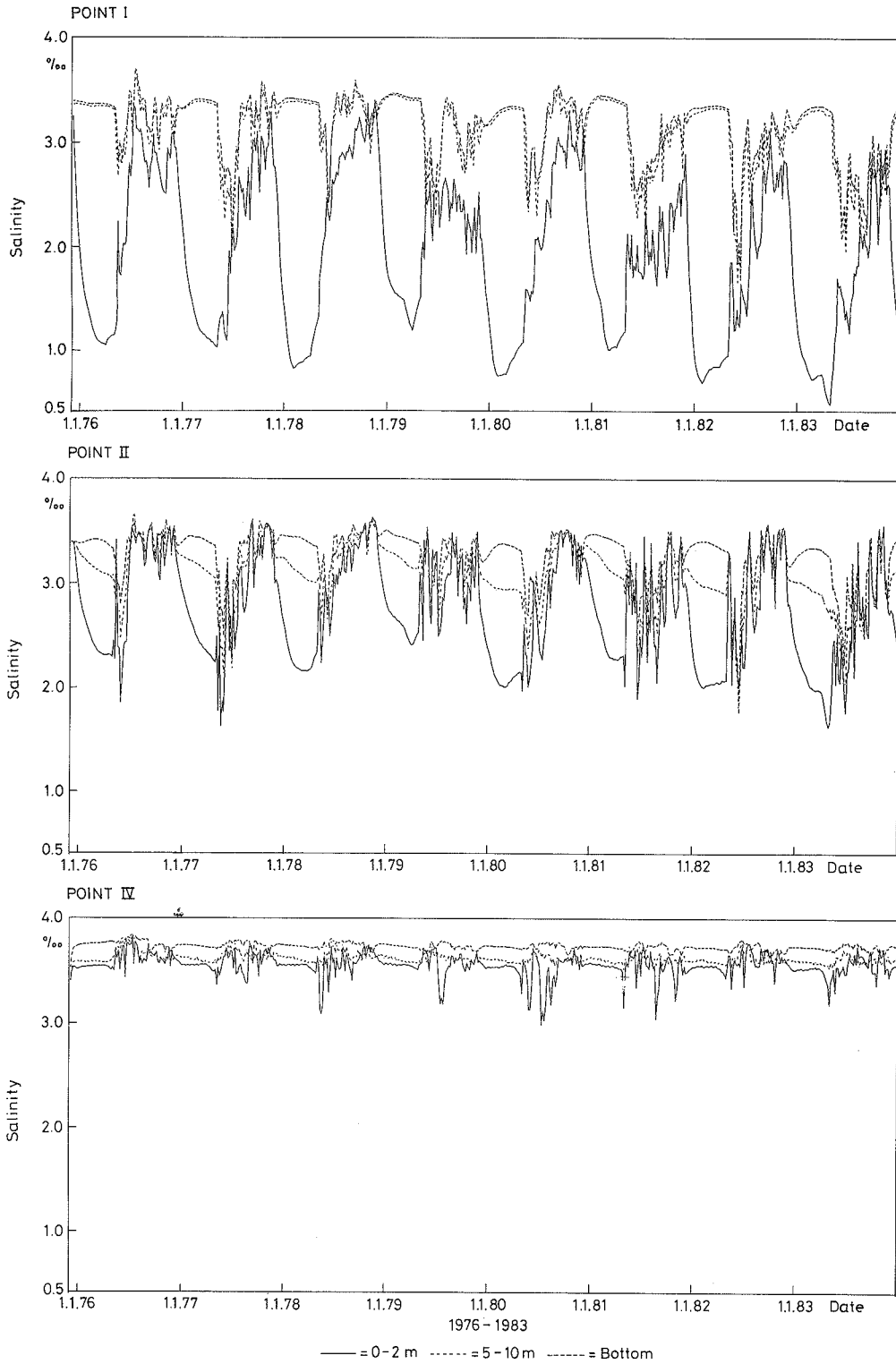


Fig. 48. Salinity time-series from the 1 m, 7.5 m and bottom depths in the points I, II and IV of Fig. 46.

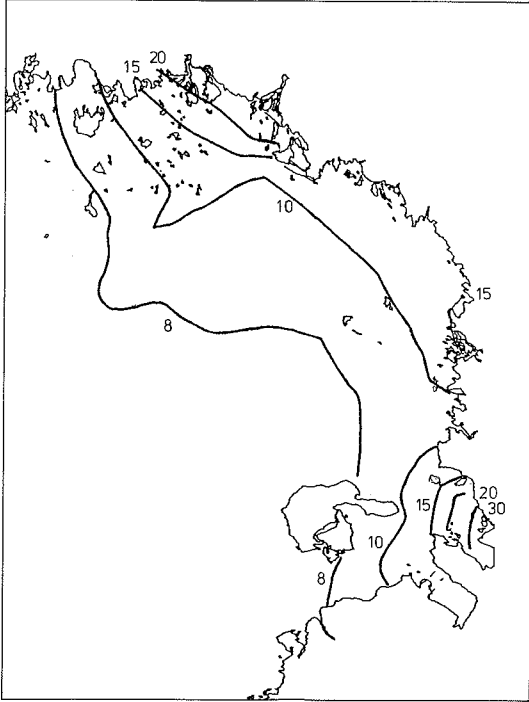


Fig. 49. Average upper layer (0—1 m) phosphorus distribution during an open water period in the north-eastern Bothnian Bay.

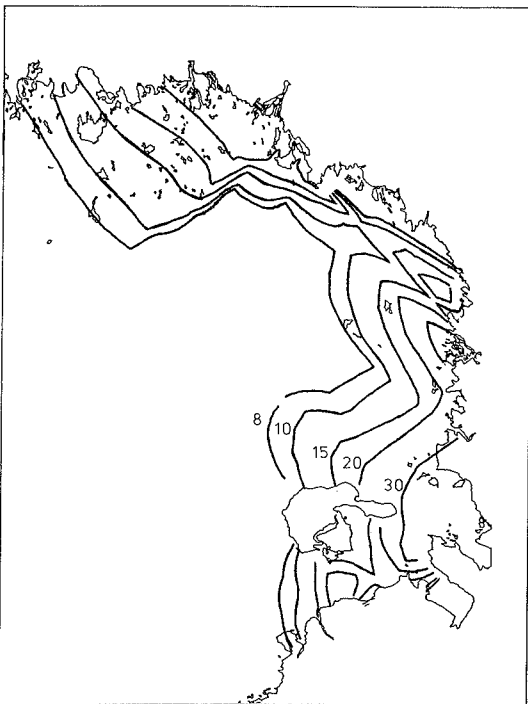


Fig. 50. Modelled spring phosphorus concentration in the upper layer in the north-eastern Bothnian Bay.

this area comes from the rivers or is mixed into the river water). In the north-easternmost corner of the calculation area the effect of some small rivers is discarded in the calculation and this gives a different result than the measurements.

The oxygen and phosphorus distribution off the town Kemi at the end of the ice covered period are shown in Fig. 51. As was mentioned before all the factors that affect the transport were not taken directly into account in the calculation. That is why a small horizontal diffusive velocity was added to the calculation near the coast. Diffusion doesn't describe the real transport mechanism very well but gives an average transport of the pollution off the bays.

Phosphorus time-series from some points off the town Kemi are shown in Figs. 52 and 53 and oxygen time-series in Figs. 54 and 55. The water quality time-series agree generally well with the measurements especially for the phosphorus. Some reasons for the deviations are:

- the spatially varying wind field is not taken into account but wind data from one point is used
- unknown input factors (e.g. not accurate loading information)
- the stratification effects are not modelled accurately, e.g. the waste and river waters can move in shallow epilimnion in certain stratification conditions, in the model there has been however used a constant thermocline depth
- the atmospheric oscillations are not taken into account in the wintertime simulation
- the calibration of the parameter values has not been fully completed (this is always true because the resources are always limited).

## 7.6 Simulation of the oilspill transport after the Eira accident

To evaluate the needs for further development of the transport and drifting model, the 3D model at its present state was used to simulate the transport of oil spilled during the accident of cargo ship *M/S Eira*.

The accident took place in the central part of the Gulf of Bothnia in September 1984 with a total of 200 metric tons of oil released to the sea. The cost for the clean up procedures amounted to 10 million marks.

The model was applied for the entire Gulf of Bothnia with local refinement at the Quark, where a horizontal resolution of 2.5 km was used. The oil was forced to remain at the topmost 10 cm layer by

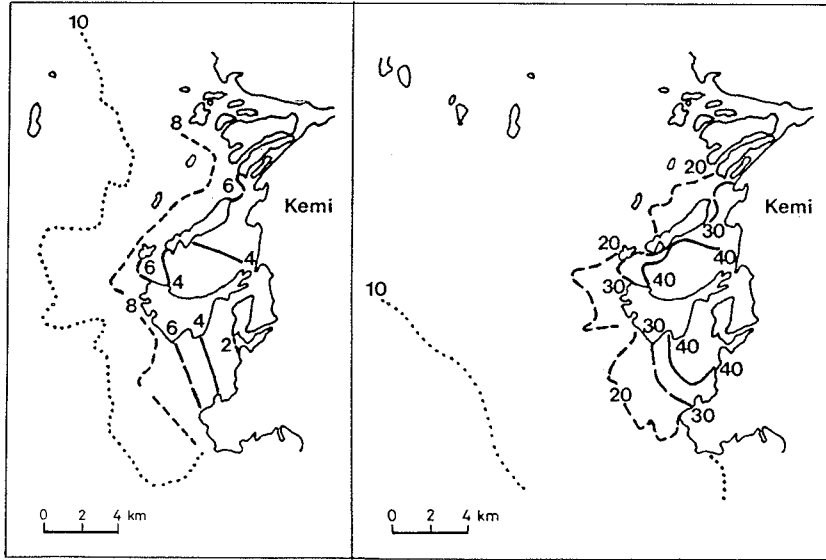


Fig. 51. Spring oxygen (left) and phosphorus (right) distribution off the town Kemi in the surface layer.

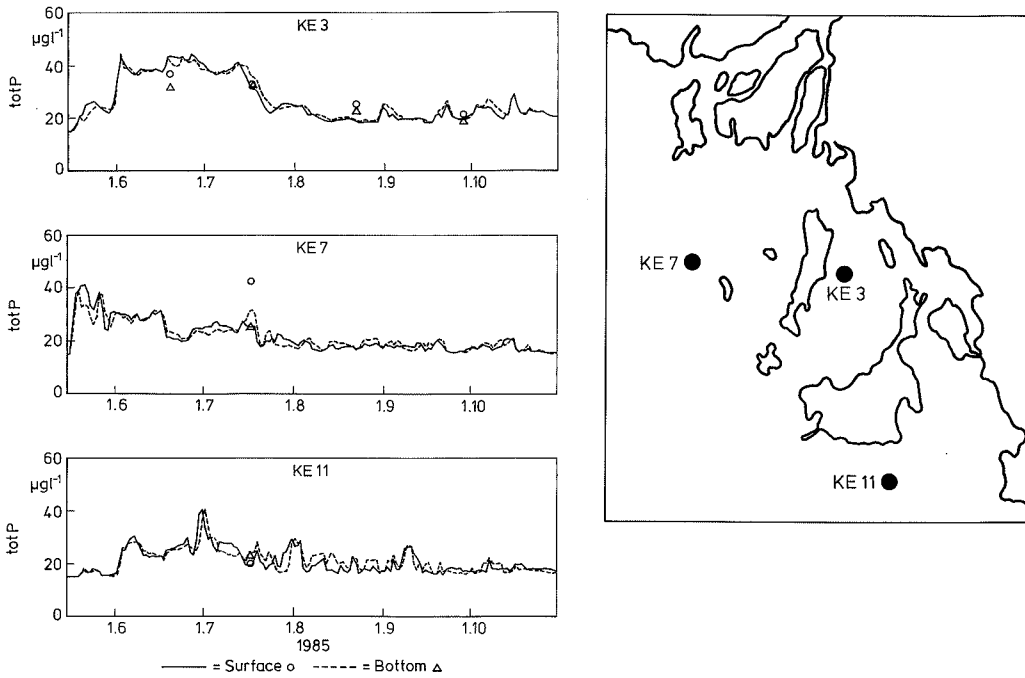


Fig. 52. Phosphorus time-series in summer 1985 off the town Kemi.

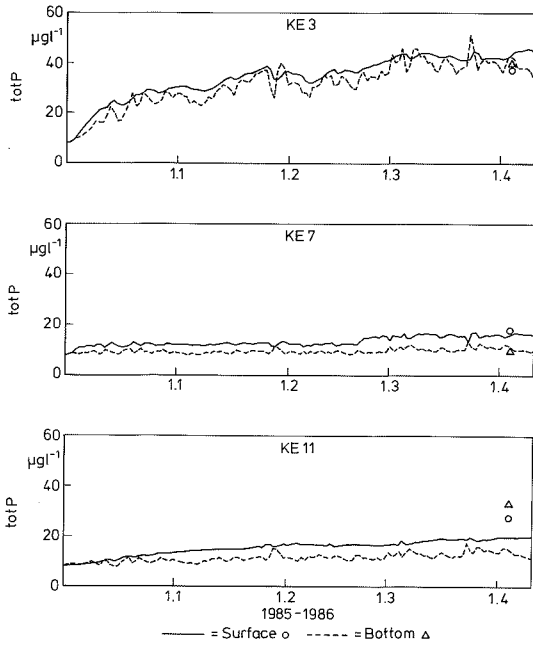


Fig. 53. Phosphorus time-series in winter 1985—1986 off the town Kemi.

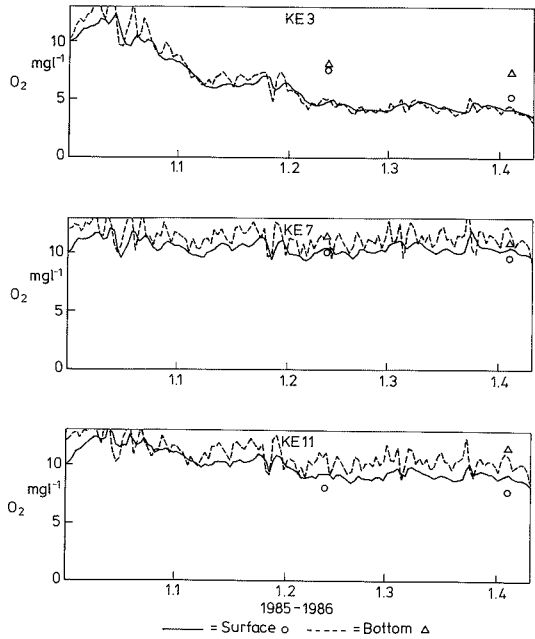


Fig. 55. Oxygen time-series in winter 1985—1986 off the town Kemi.

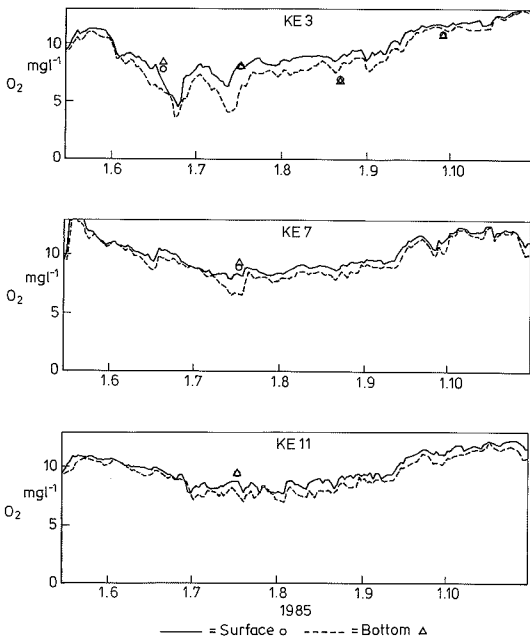


Fig. 54. Oxygen time-series in summer 1985 off the town Kemi.

removing vertical velocities from the model. Calculated flow fields for the surface layer for SW and NW winds are shown in Figure 56. The most interesting feature in these figures is probably the deviation of the surface current from the wind direction.

The amount of oil released and the duration of each spill event was estimated from the report published after the accident. These values are, however quite inaccurate. The location of the oil spill was based on aerial surveys made each day. As the times of these flights were not known, the model results were plotted as midnight values. The observed and modelled locations of the spilled oil is shown in Figure 57 for September 1 and September 2, 1984.

The modelling was performed assuming two separate spill events. At Sept. 1 oil was already approaching the Vallgrund island. During the next day, wind shifted to west. The observed transport of the oil against the wind was not correctly described by the model. This can partly be due to the insufficient description of the winds as the model used no areal variation of the windfield.

In Sept. 3 the float was found to the west of the



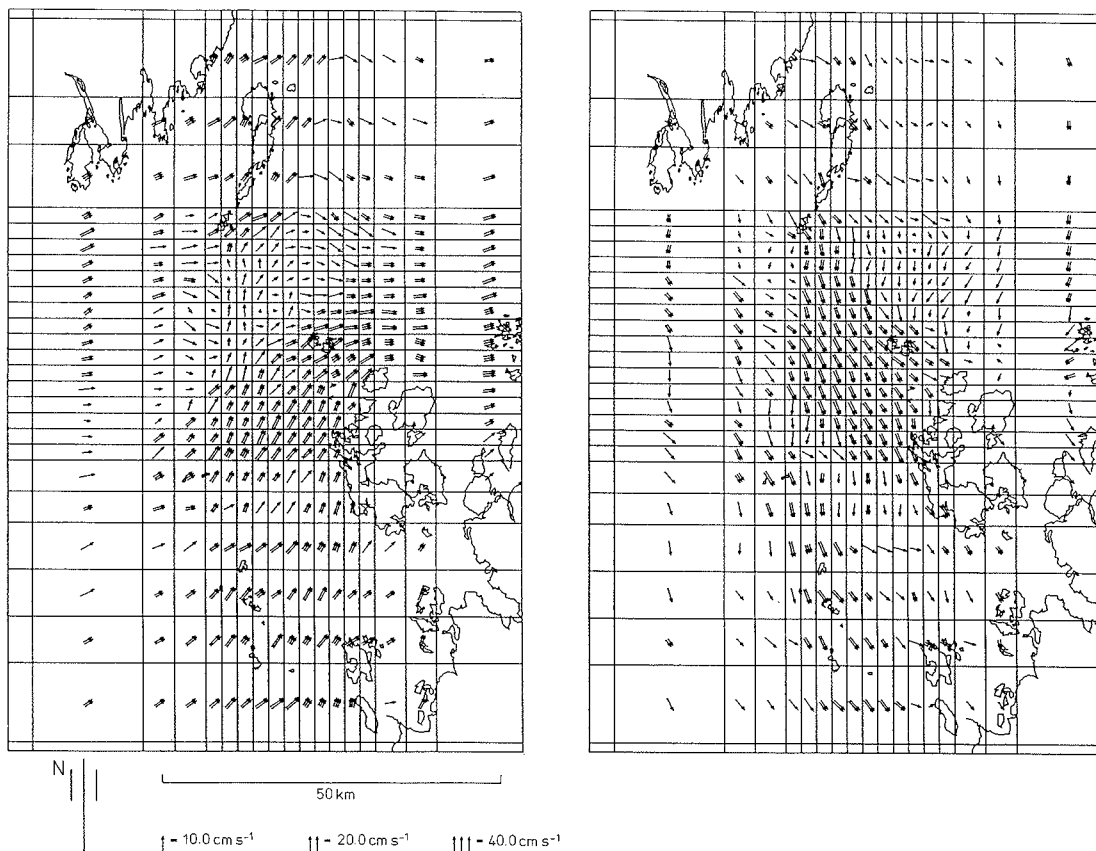


Fig. 56. The flowfield at the Quark for SW (left) and NW (right) wind of  $5 \text{ m s}^{-1}$  calculated with the 3D model.

Vallgrund island. Next day a new spill was released from the ship and the oil drifted southwards. To visualize the total area affected by oil a computer run was made with continuous release of oil. The result is show in Fig. 58. Considering the inaccuracies in the observations and the model approach the model described the transport of the oil quite well.

## 7.7 Simulation of the drifting objects

To investigate the models ability to describe the drift of solid objects subjected to water currects and wind, measurements were organized in June 1989 near the Vallgrund island. The objects — oil barrels and a boat halfway filled with water and a mannequin in a life jacket — were relased from a boat and they were positioned in half hours

interval for a period of two to six hours depending on the flow conditions.

During the second deployment in September 1989, flexible floats made of pieces of styrox and coated with plastics were also used. The floats were equipped with weights to reduce their wind resistance. Radio transmitters were attached to the floats, so that they could be located from a helicopter.

The results from the experiments were compared with model simulations. Flow fields calculated with the model were used with the addition of wind resistance on that part of the object lying above the sea surface. Both the wind resistance factor and the deviation angle from the wind speed were estimated based on the observations.

The results from calibration were satisfactory. The direction of the transport was quite well simulated. The errors in the transport distance varied from 2 to 25 from the observed.

Based on this calibration, the model was applied to a case where a fisherboat was announced

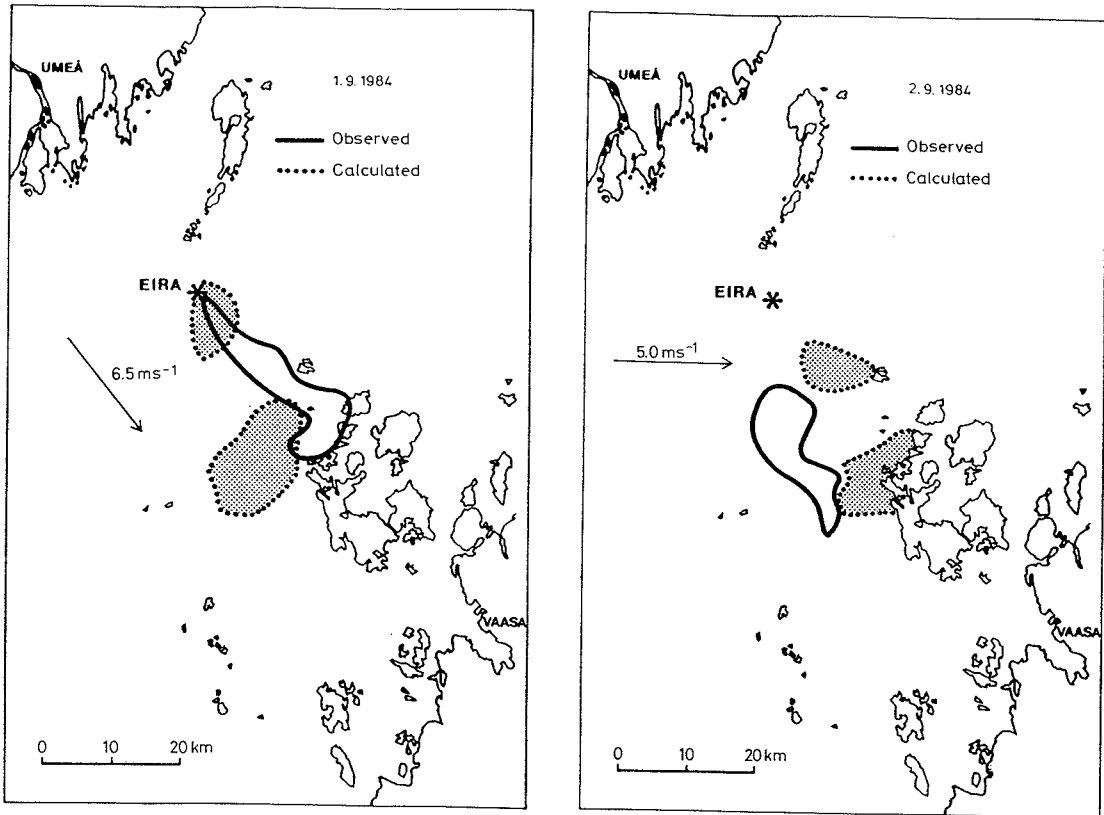


Fig. 57. Comparison of model results with observed transport of oil Sept. 1 (left) and Sept. 2 (right). Observed areas of oil spillage and model calculation (shaded).

missing. The fisherman Holm was last seen November 9., 1985 at 3 p.m. to the west of the Mikkelinsaaret islands, north from the town of Vaasa. The boat was not found in the search November 9.—11, 1985, but it was found in the following spring from the shore of Holmögadd in Swedish territorial waters with Holms dead body in it. As a cause for the failure of the search it was suspected that boat drifted northwards faster than expected.

The northernmost search sector in November extended to the Finnish boundary of territorial watershed, where the boat was assumed to have drifted by 4 p.m. according to calculations by the Finnish Meteorological Institute. According to our model calculations the boat should have crossed the boundary of territorial watershed already at 5 a.m. the same morning, and should have been 10—20 km in the Swedish side at the time of search. The boat should have drifted to the shore of the Holmö island the same evening and possibly got loose during a northerly storm that started November 11, The model predicted that the boat

should then have drifted with the storm nearby the Holmögadd island, where the dead body was found in spring of 1986. The trajectory of the boat is shown in Fig. 59.

## 7.8 Sensitivity tests for improved water quality monitoring

### 7.8.1 General requirements for effective sampling program

The sensitivity of field results to the changes of loading and weather should be taken into account when evaluating the significance of the data observed. In addition to the long-term trends caused by loading levels and to the direct effects of incidental releases, the observed data is considerably influenced by the short-term, seasonal, yearly and long-term variations of the natural factors, e.g. winds, water level changes, water temperature,

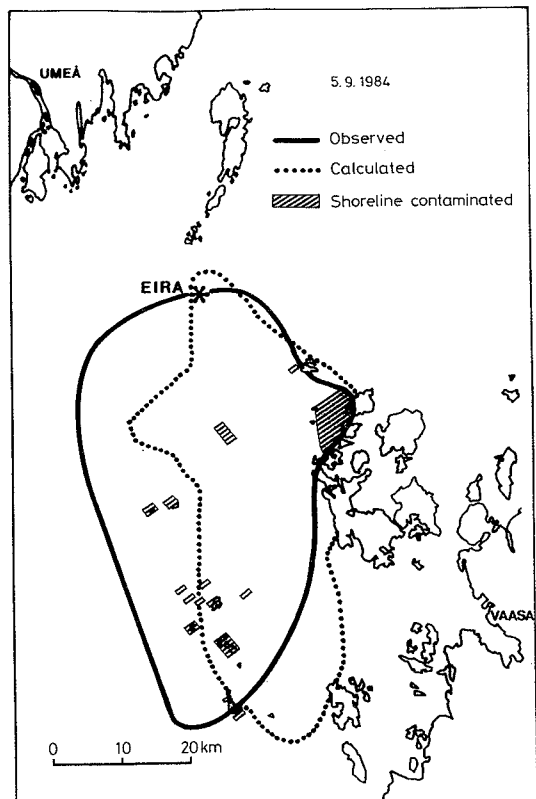


Fig. 58.  $M_v$  results calculated by using continuous release of oil compared with observed areas effected by oil compared in Sept. 5.

stratification, river flows, biogeochemical reactions and (bio)accumulation.

An ideal sampling program depends on the aims of the measurements and on that what is wanted to be found or checked. In most cases the main attention is directed to the observation of the loading effects — both incidental and trends. For elimination of the effects of the base level changes, a few points are usually included to check the background effects far away from the discharge points. No attention, however, is usually paid to eliminate the effects of natural factors like those of winds or river flows. Unfortunately these effects most often dominate with orders of magnitude over the background and loading effects.

Thus, in order to obtain observations as meaningful as possible, the data should be quite insensitive to the weather conditions, or dependence of results on the weather should be clearly analyzable. As another requirement, the effects which are of major interest should be detectable as clearly as possible. Furthermore, the results should

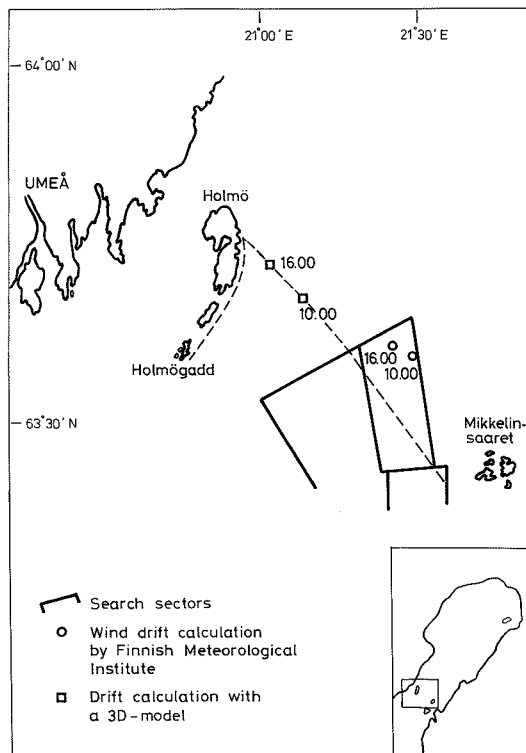


Fig. 59. Comparison of the 3D model with calculation by the Finnish Meteorological Institute. Estimated positions of the boat at Nov. 10, 10 a.m. and 4 p.m. and assumed drift of the boat towards Holmögadd, Nov. 12.

be representative for a wider area, i.e. they should be insensitive to minor inaccuracies in the location of the sampling point. From practical point of view, the sampling points should be easily accessible with minor risks under any conditions of weather, and the sampling tour should not take too much time.

### 7.8.2 Analysis of the variations of water quality

For outlining an effective sampling program, the variations of total phosphorus concentration and conductivity were analyzed in the north-eastern Bothnian Bay, in the coastal zone between Kemi and Oulu, based on twenty years measurements and on model simulations (Figs. 60—62).

In most areas the sampling frequency of measurements was far from sufficient for any judgements about the short-term variation. On the other hand the long-term variations between different years with different rains, temperatures

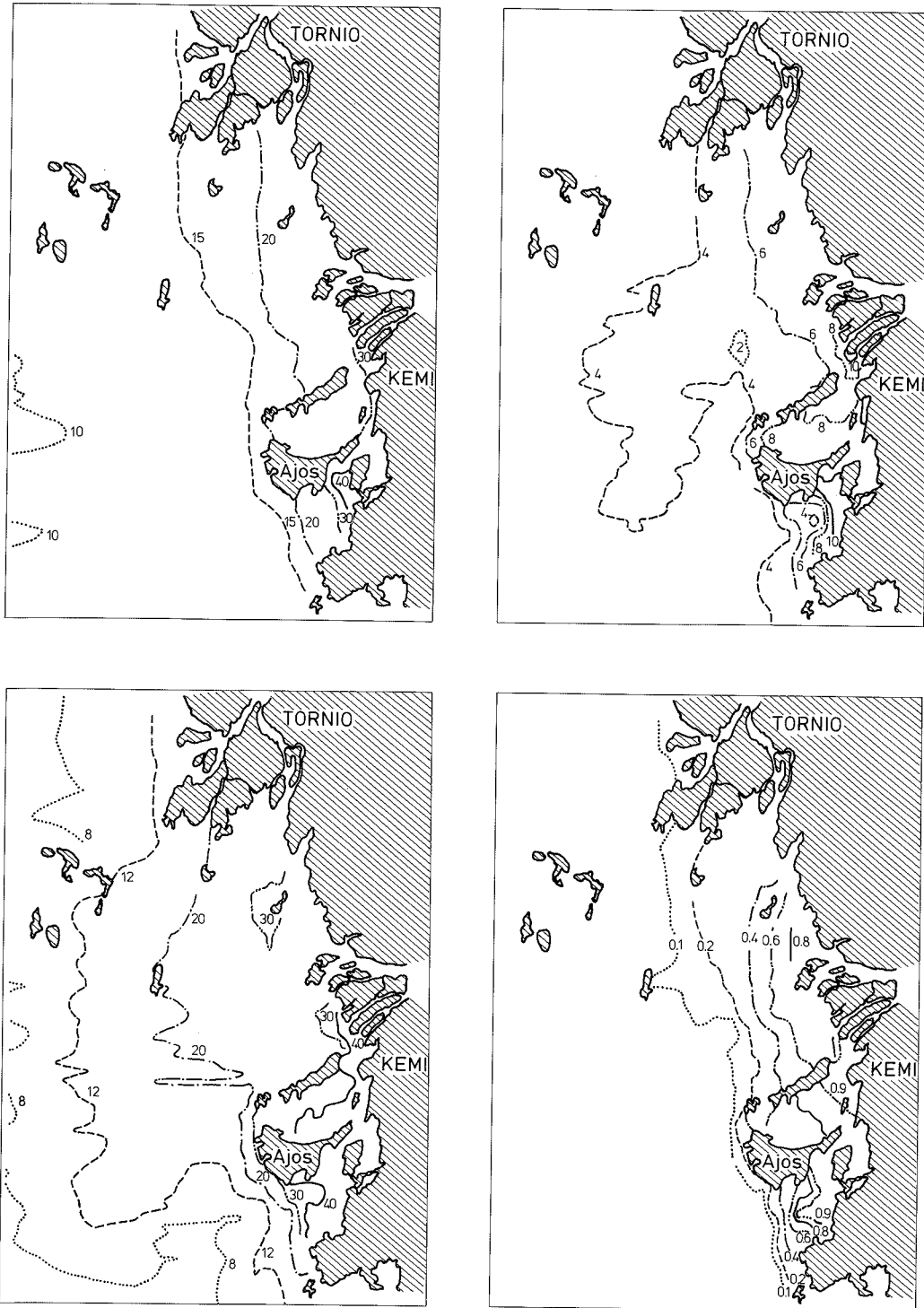


Fig. 60. Results from the phosphorus simulation of summer 1985. Average concentration (upper left), standard deviation (upper right), range of phosphorus concentration (lower left) and probability isolines for concentration exceeding  $20 \mu\text{g l}^{-1}$ .

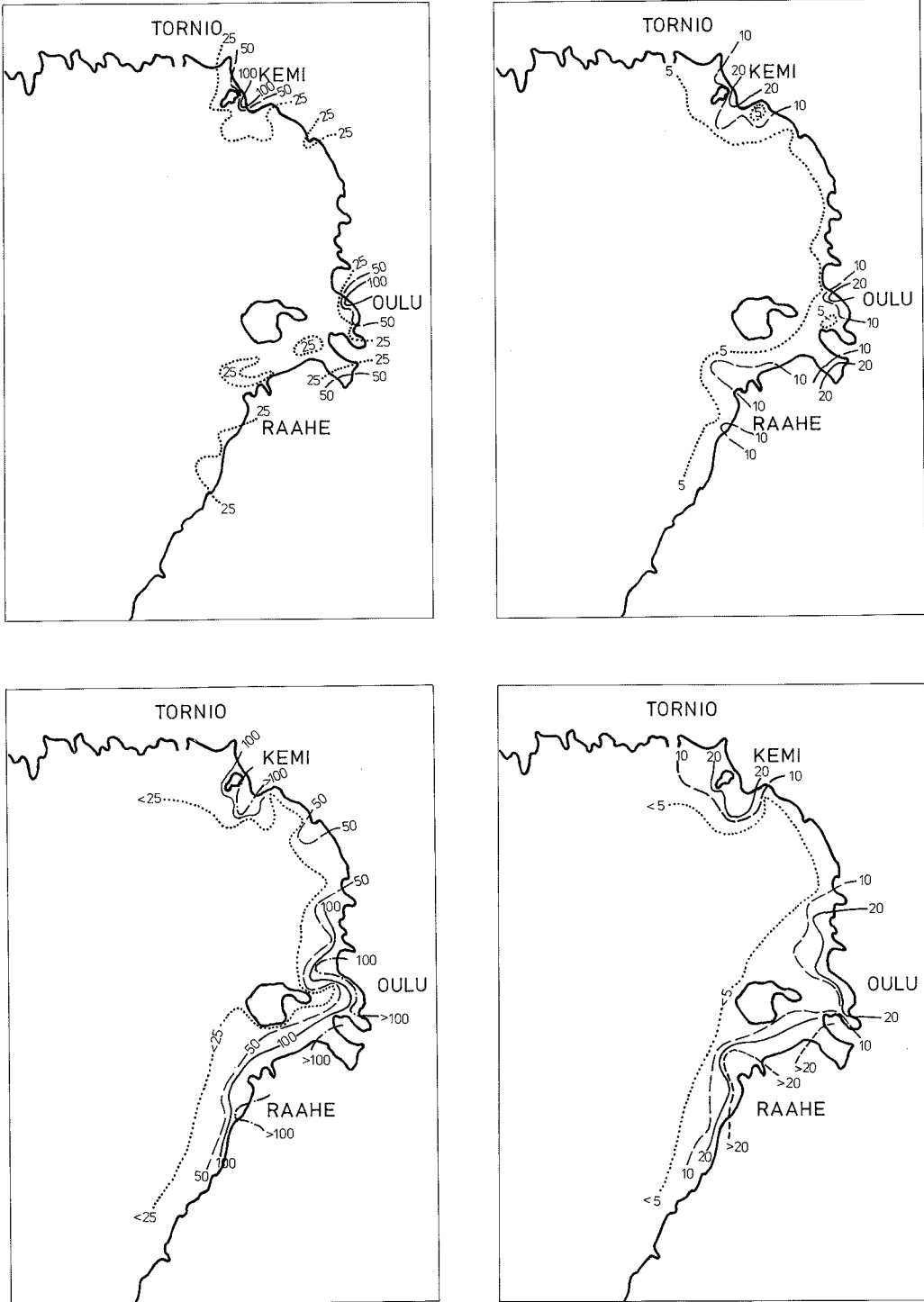


Fig. 61. Measured range (left) and standard deviation (right) of phosphorus concentration. Average values from 12 years: summer (upper figures) and entire year (lower figures).

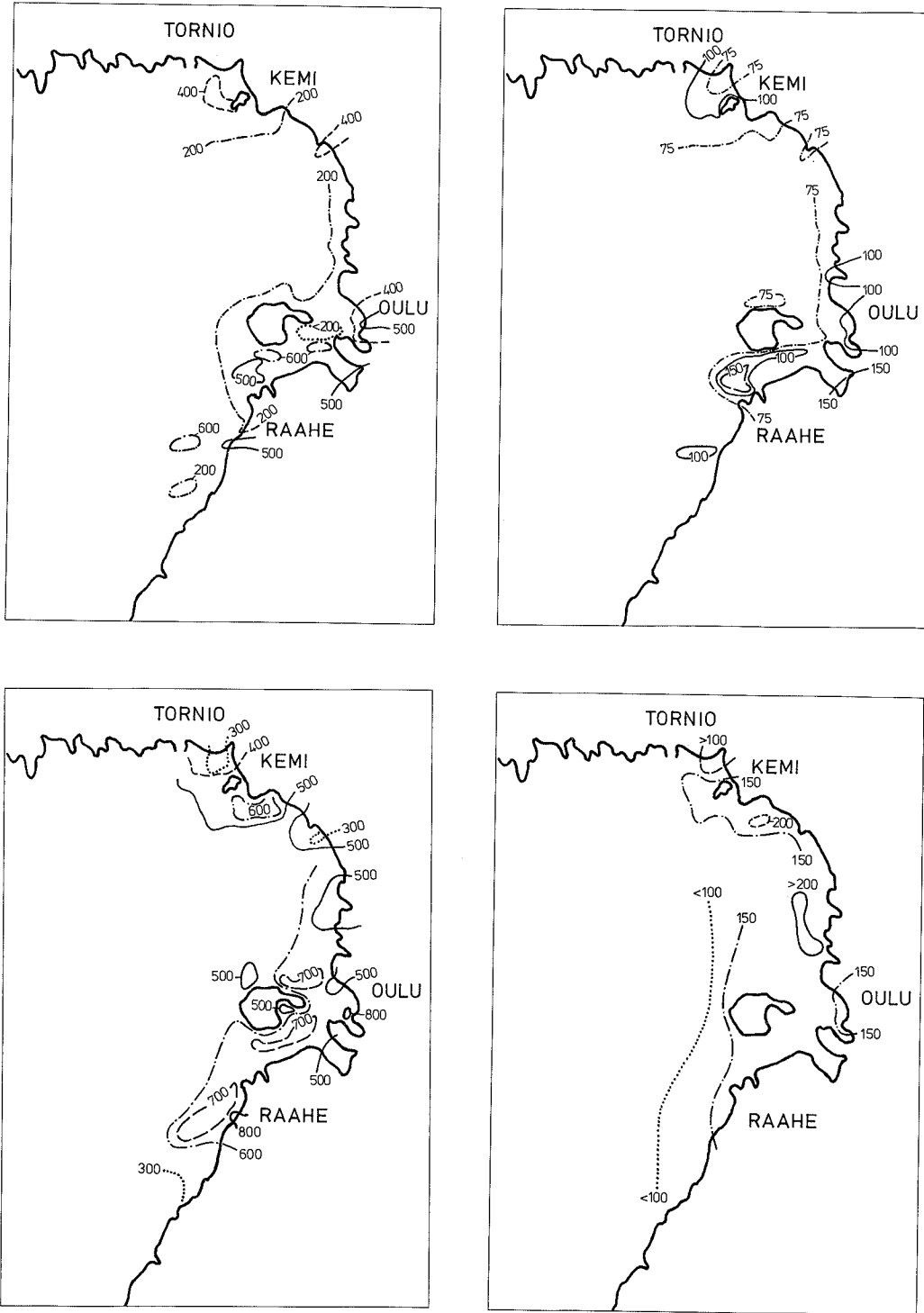


Fig. 62. Measured range (left) and standard deviation (right) of conductivity. Average values from 12 years: summer (upper figures) and entire year (lower figures).

and river discharges are included within the analysis of the observed data. The short-term variations within one year were emphasized in the simulations.

Difficulties in obtaining representative results from the measurements are mainly associated with the short-term variation, caused by winds during the open-water period. The rains, temperatures and river flows affect the dilution of concentrations and the decay of variation with distance but in most cases the water exchange caused by winds and pressure gradients is much more significant source of variation than the long-term effects of river inflows and the reaction kinetics. In a low-flow year the variation can be larger than in a wet year, and the extension of waste water effects can be wider, but the time behaviour of the variation need not to be considerably changed. The north-eastern part of the Bothnian Bay was divided to three different classes (Fig. 63) in order to assist the outlining of the development of the monitoring program.

In the model results the variation is slightly smoothed by the averages used in the simulation

(grid box averages of results, areal averages of model parameters and forcing factors, and time averages of forcing and loading).

## 8 PROCEEDING OF THE DEVELOPMENT WORK

### 8.1 Model for chemical and oil spill accidents

The development of an operative model for chemical and oil spill accidents in the Finnish coastal areas will be accomplished in 1990—1992. The project is about 45 man months per year. The project is accomplished as a cooperation between the Finnish Institute of Marine Research (FIMR), NBWE and Environmental Impact Assessment Centre of Finland (EIA).

The result of the development work will be an operative model that will help the personnel in

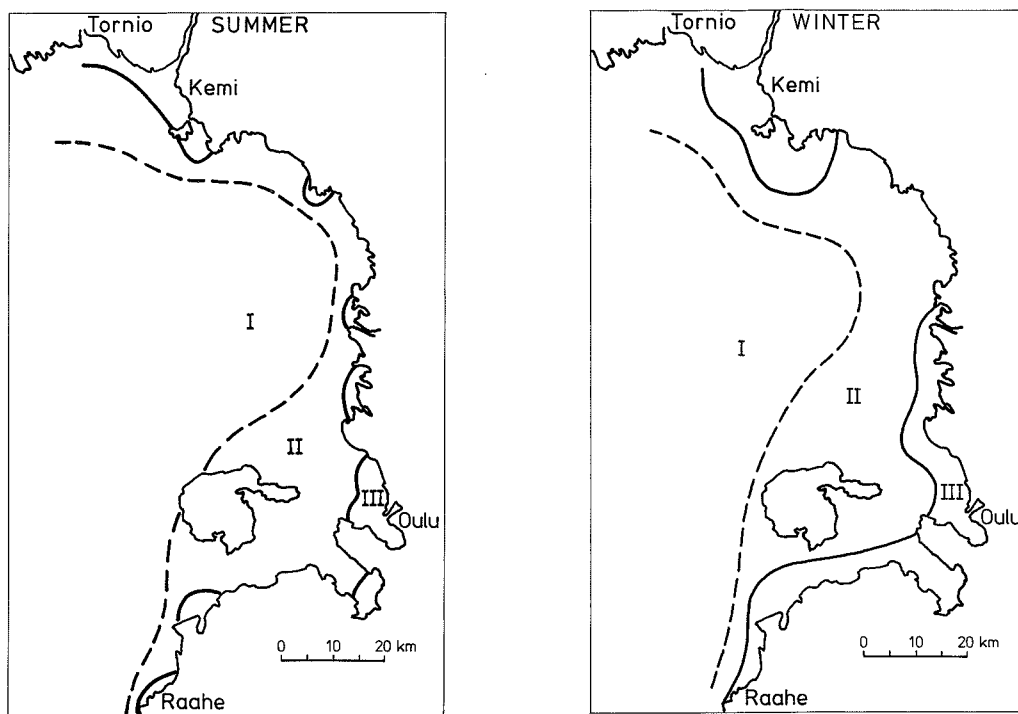


Fig. 63. Classification of the north-eastern part of the Bothnian Bay based on variation of the phosphorus concentration and conductivity.

charge of chemical and oil accident combatting to plan the combatting actions and to trace the oils or chemicals in sea. The model will also contain a part that helps to trace floating objects (objects in sea accidents). The project has strong international contacts which started during the Bothnian Bay project.

## 8.2 Water quality model

In addition to the physical factors — currents, temperature, salinity, fresh water concentration, water levels — the total phosphorus concentration was described in the present study as an example of the numerous possible components or indicators of water quality. Thus, an enormous need exists for further development of the model. Next to phosphorus the most obvious components to be modelled may be the other principal nutrient, nitrogen, and perhaps silicon and carbon, and the biologically available fractions of the nutrient concentrations (based on their origins or chemical forms).

Along with the simulation of nutrients, several other components, e.g. factors of largely physical type affecting the penetration of light and illumination in the water — like water colour, turbidity, concentration of suspended solids or particulate matter — could be modelled. The scientific, public, political and practical interest on the interrelated factors of acidity, alkalinity and pH and on several types of toxic components — e.g. heavy metals and organic chlorine compounds — has recently considerably increased which calls for their indicators to be modelled in the near future, too.

Based on the information about the available nutrients, prevailing temperature, illumination and about the inhibition by toxic components the algal growth, phytoplankton biomasses, primary production and other deformations can be modelled as well as their distribution between different biological groups or even species. The algal biomasses affect further (and reciprocally, through predation, are affected by) the zooplankton biomass, its growth and distribution between different groups and species.

The nitrogen dynamics and algal respiration, reaeration through free surface, and biological and chemical oxygen demand in water and in sediments all contribute to the oxygen concentration of water. In its modelling, the several components of biological oxygen demand, BOD, can be subdivid-

ed by their decay rates, origins and forms (whether diluted, suspended or settled). Special cases of the BOD-components are the very slowly decaying humic substances which also have influence on the water colour and on other properties of water.

All factors dissolved or suspended in the water are transported with the water currents. Thus the computation of these water quality components must be coupled with relevant simulation of their transport (and dispersion). On the other hand, the properties of bottom are not moving directly with water currents. Still they are in continuous interaction with the properties of water and can be included within the water quality model.

The bottom types and conditions are important for the spawning of fish and the zoobenthos considerably controls the fish growth. Thus the fish stocks — possibly subdivided into species and age groups — can be finally added to the water quality model, too. Also the most easily visible effects of eutrophication, viz. the growth of aquatic plants and the increased periphyton or mucus formed on the stones, water structures, fishing gears and boats, can be included to be described in the water quality model. The effects of fish on birds or men eating them and all other economic, social and health consequences of environmental impacts are closely related with the output of the water quality models and can be coupled with them.

It is not difficult to find out thousands of indicators for water quality. At the time being, simulation of transport and reactions for most of them is an impossible task, partly because measurements are deficiently available and the reaction kinetics of most of the possible indicators are not known, and partly because of the limitations of the computer memory and speed.

All factors having influence on the relevant indicators of water quality need not to be modelled, neither simultaneously nor separately. Besides the model results, the field measurements and other estimates can also be utilized as the basis of calculations. The water quality indicators to be included in the model depend mainly on the nature of the area considered, on its biology and on the type of problems to be solved. Simulation tests can be of considerable help in final selection of the model components. Typically the number of indicators for one model has ranged from 3 to 5. It can seldom exceed 20 to 25.

Main problems in the further development of the water quality models seem to include — versatile interactions between several indicators in nature which makes it difficult or impossible to distinguish from the measurements the



- specific effects of each interaction;
- information gap (tradition gap and perhaps also confidence gap) between a large majority of hydrobiologists and hydrophysicists which makes it difficult or impossible to convert the descriptive biological data of most detailed substructures to integrated numerical quantities;
- description of the competition dynamics between different species or biological groups and of the changes in species composition;
- selection of the indicators which are the most important and essential to the problems considered; and
- measurement limitations, and shortage and inaccuracy of forcing data which make it difficult or impossible to decide whether the agreement or disagreement between model and field results is real and whether it basically originates from the model structure or from the discrepancies of the input data. Of special importance are the forcing factors, e.g. loading, discharges, winds and water depths. If they are missing, inaccurate or misleading (incorrect) then the comparisons between model results and field data are of little value for evaluation of the model and for directing its further development.

### 8.3 International co-operation

#### 8.3.1 Co-operation tasks realized and projects in the near future

The seas and oceans, as well as the atmosphere, are internationally influenced and utilized. Their conservation and fighting against their pollution is a most international problem. Close international co-operation is absolutely needed in their research as well. This improves the possibilities for the local experiences, local requirements, local test data and the most reliable forcing data to be taken into account in the model development and applications.

Possibilities for international co-operation were open to be included in the present project already. The practical results of this appear as the state-of-the-art survey of the model use, as the comparison between 3D and vertically 1D descriptions for the development of stratification and as the preliminary comparisons between the Swedish and Finnish 3D models for the Gulf of Bothnia. Further comparisons and interactions had to be postponed, because of the lack of staff clearly obliged and

devoted to maintain the co-operation, and because of the urgent demand of model applications to other areas. These reduced time from visits and from maintaining the international contacts.

- A useful basis to continue the co-operation is created in the present study including its data files, skills developed, preliminary contacts and the model survey. In addition to the present study, several other activities are also scheduled or going on which both promote and urgently need international co-operation. These include especially
- the Gulf of Bothnia Year 1991 agreed between Sweden and Finland,
  - the Swedish Sea Model Project scheduled for the whole Baltic,
  - EUREKA/EUROMAR subproject OPMOD (Operational model for short-term forecasts of regional seas) started in Germany, Finland, France, Norway, Portugal, Spain and Sweden,
  - EUREKA/EUROMAR subproject VISIMAR (Visualization of simulation of marine environment) started in Finland, France, Germany and Norway and planned in a few other countries,
  - Several subprojects for measurements and data acquisition within EUREKA/EUROMAR and within the MAST (Marine science and technology), SCIENCE and STEP (Systems and techniques for environmental protection) programs of the European Community (EC).

#### 8.3.2 Coordination needs and alternatives

International co-operation will not be solved by any of these projects although all of them contribute and stress the need for co-operation. The commercial aspects coupled with model applications may further complicate the international and institutional relations. The commercial interests are emphasized especially by the EUREKA ideas, partly by the formation of separate institutes for model applications, and finally by the increased demand of environmental impact assessments which is the main cause of this development. Unsurpassable problems are not to be expected since in most cases the benefits of co-operation are directly proportional to the work done for it.

Nevertheless, international coordination and consulting, utilization and help within the model development and applications could still better eliminate the suspicions and problems and could even considerably promote the co-operation and its benefits. Besides EC and its joint research institutes, the International Institute for Applied Systems Analysis IIASA at Laxenburg, Austria, is

an obvious alternative. Being neutral, versatile, experienced, and covering the most countries involved in the modelling activities, IIASA seems to be the most appropriate place for taking the responsibility of raising the co-operation. Its development work could be financed partly by the institutes budget from member organizations, by commercial applications and partly by the national and international projects which need co-operation. The financing possibilities of other alternatives are more limited unless new organizations are planned to be created.

Independently of the place or even existence of coordination and amassing of model development, the co-operation is necessary to be continued and even intensified from the points of view of both national and research advantages. In any case, successful management of co-operation requires at least half-daily work for taking care of the contacts and information exchange permanently. For larger test applications outside the Finnish water areas (e.g. to North Sea, Mediterranean, Ladoga, Great Lakes of America etc.) some additional support may be needed for computations but otherwise the preparedness to co-operation is largely available as the result of the present project e.g. in the form of extensive data files in specified formats ready for being used as model input. This preparedness will hopefully be utilized in continuing co-operation, preferably for the development of water quality models with proper inclusion of the transport effects.

## 9 CONCLUSIONS

### 9.1 Modelling

The first task of the Bothnian Bay project was to study and model the dynamics of an enclosed sea area. The currents, spreading of the river waters and formation of the temperature distribution were the most important part of this work. Lot of effort was devoted to the problem of obtaining improved local accuracy for the areas that are of special interest. New high-resolution techniques were developed and applied to large sea areas. Water quality simulations were done to gain further information on the basic dynamics of the area and to aid the planning of the water quality monitoring program. Generally the new methodologies utilized during this project have been shown to be feasible and they will be applied in the future in other studies.

### 9.2 Water quality monitoring

The second goal of the project was to develop the water quality monitoring program in the Bothnian Bay area. Monitoring contains a huge historical data-base and consumes yearly considerable resources so that any extensive changes should be studied thoroughly. Indeed, some aspects of monitoring based on the Bothnian Bay study can be given.

The dynamics of the Bothnian Bay area are governed by the seasonal variations as follows:

- ice covered period is characterized by accumulation
- spring season is characterized by spreading
- summer is characterized by oscillations and finally
- autumn is characterized by mixing.

This should be taken into account in the planning of the monitoring program because e.g. the variance can vary considerably from season to season. In addition to the season the characteristics of the forcing factors affect the variance. The most dominant forcing factor is the wind. The the wind variability has a strong effect on the water quality in any given point. Variance also depends strongly on the distance from the major input sources. Near a discharge point or river estuary the gradients are stronger than in the open sea due to mixing.

The Bothnian Bay project has given some information about the variance distributions in the area. The results must be used carefully because there is a large discrepancy between the model and measurement variances. The reasons for the large differences between the mean variance of the measurements and model results are:

- the sampling frequency is quite different for the measurements and for the model (for the measurements of the order of 1 month, for the model of the order of 1000 seconds)
- the inputs for the model are averaged
- the concentrations calculated are averages over some predetermined time and space intervals
- the measurements span over 12 years and the model result shown are for one open water period.

The areas in the Bothnian Bay could be classified into three categories according to the variance:

- low variance (for the total phosphorus  $< 5 \mu\text{g l}^{-1}$ , corresponds to  $10 \mu\text{g l}^{-1}$  mean values) in the open sea
- medium variance ( $5\text{--}10 \mu\text{g l}^{-1}$ ) in the transition zone between the coastal and open sea areas
- high variance ( $> 10 \mu\text{g l}^{-1}$ , corresponds to

20  $\mu\text{g l}^{-1}$  mean values) near the loading sources on the coast.

The low variance zone is by far the most extensive one. The need for high frequency measurement program of course is decreased in the low variance areas.

Another criteria for the selection of the measurement points and determination of the measurement frequency might be the probabilities of the concentrations exceeding some predetermined threshold values. The threshold values could be based on biological effects. The effects are however not easily determined in natural conditions because not only the probabilities and concentrations but also the duration of a given concentration value determine the effects.

The representativeness of the measurements is of primary importance because the conclusions concerning for instance the long term water quality development can be reliable only when the random oscillations are not a dominant part of the data. Without the knowledge of the dynamics of the monitored area it is however impossible to estimate the meaning of any given measurement. One of the possibilities to facilitate the understanding of the dynamics is the use of the models.

When the measurement program is combined with a model application the measurement results are more easily understood and the causal relations resulting in any given water quality distribution can be studied and tested. A reliable model can save the monitoring effort because then measured samples are needed from fewer points. The resources that can be saved in the routine monitoring programme could be directed in specific measurement programs. The model, however can never completely replace even routine measurements because a new phenomena must usually be first measured before it can be incorporated in the model. A model needs input and verification data and no model can take into account all the factors in nature.

- the open sea monitoring program (SMHI, FIMR)
- for Finnish side the coastal water monitoring program (NBWE) and
- 25–30 separate resipient control programs (private consultants).

All these programs are reported separately. The data of open sea monitoring is in the registers of the SMHI and the FIMR and the coastal data in the register of the NBWE. For the future research work it would be beneficial if all water quality data from the Bothnian Bay were situated in one

register.

In the water quality monitoring two objectives can be separated:

- to get a reliable knowledge about the seasonal and year to year variations and average values (intensive monitoring)
- to gain knowledge about areal distribution of the water quality (mapping)

The present monitoring in the coastal waters of the Bothnian Bay is biased in the respect that both objectives mentioned above are mixed in the same sampling net. Intensive monitoring calls for frequent sampling in few points whereas mapping requires sufficient areal coverage. The common water quality monitoring and mapping strategy, where all separate programs are taken into consideration should be prepared. The outlines for the development of monitoring are presented in Fig. 64.

In winter, river waters including waste waters form a layer on the surface. The stratification of river water at surface begins immediately after the formation of the ice cover. By April the river waters cover the entire northeastern part of the Bothnian Bay. Most of the river waters discharged during the winter stay in the area off the river mouths until spring. The dispersion of these waters varies only slightly from year to year. Therefore, the monitoring in winter need not be so frequent as in summer but the sampling should have wide areal coverage. The sampling frequency in the present intensive monitoring made by the NBWE (sampling every month) is sufficient during the winter.

Model applications show that the residence time in the resipient areas is 2–3 weeks in summertime. The spread of loading substances depends on the wind conditions. Monitoring programs where sampling frequency is 1–3 times per open water period is far too sparse to give an understanding about the average distribution of water quality or the average water quality of the season. The intensive monitoring made by the NBWE includes 2–4 sampling times per month and it gives quite a good insight to the water quality in the outer parts of the resipients during the summertime.

In Fig. 63 of section 7.8 is presented the classification of the northern Bothnian Bay into the sensitivity classes. There should be intensive monitoring in each class for the most important resipients. A good basis for this is the intensive monitoring made by the NBWE. The sampling point outside Hailuoto is a suitable reference for the whole monitoring of the northeastern Bothnian Bay (sensitivity class I). The monitoring sites off

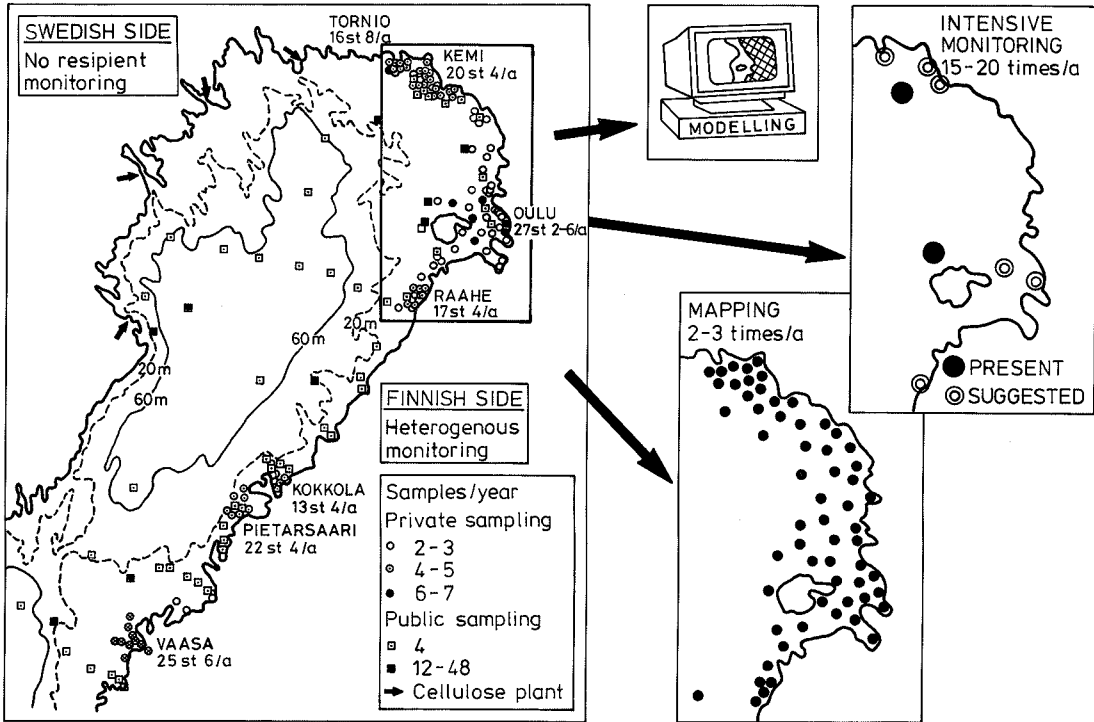


Fig. 64. The outlines for the development of present monitoring policy. Development towards a) intensive monitoring, b) mapping and c) modelling.

the towns of Kemi, Tornio, Kokkola and Vaasa (class II) would be completed with intensive stations near the loading points off Tornio, Kemi, Veitsiluoto, Oulu, Raahe, Kokkola and Pietarsaari (class III). Monitoring for the stations in loading areas should be more frequent than the intensive monitoring of the the NBWE. In these stations automatic sampling and monitoring could be utilized.

The influence of river and waste waters is most widespread in spring, when river waters discharged during winter and floodtime spread above the thermocline being formed over a large area. About 40–50 of the total area of the Bothnian Bay is influenced by river water in spring and early summer. Suitable times for mapping the water quality of northern Bothnian Bay are late winter (April) and early summer (June) and also the time, when the water is as warmest (August), in which time adverse effects have been occurred.

The mapping of the water quality calls for the sampling net, which is prepared for large sea areas instead of small resipients. The present monitoring program should be developed by cutting down the dense sampling net in resipient areas and spreading

out the sampling points more evenly throughout the Bothnian Bay.

### 9.3 Development needs

The project has shown some urgent development needs. The vertical mixing in connection with the 3D phenomena is one of them. Another critical factor is the horizontal variability of the wind fields and the right representation of the winds in the model. The data-bases and measurement programs that are the basis of the modelling work should be developed in order to meet the new data demands. The information retrieval procedures should be developed in order to facilitate the easy accessibility of the data. (The problems with data could be alleviated by the introduction of the new information systems in the NBWE (National Board of Waters and the Environment).) One special area of interest is the wintertime flow. It has not been easily studied so far because of the lack of the measurement instrumentation for slow velocities.

## 9.4 Proceeding of the Bothnian Bay project

Numerous projects that are connected to the Bothnian Bay project have been started. We have discussed the model for chemical and oil spill accidents, water quality models, development of multigrid methods and international cooperation. A direct sequel of the Bothnian Bay project will be the development of an operational model system for some chosen locales in the Bothnian Bay region. The "operationality" means the following characteristics of the system:

- there is a continuous readiness to apply the model
- the forcing factor and measurement data can be easily updated or is updated automatically
- the model framework can incorporate many different models and updates of the models
- the models can be used by nonspecialists.

The model system should help the planning and monitoring of the application region. It should also facilitate the water quality research projects in the Bothnian Bay region. The long term water quality trends should be explained by the model. The model framework should aid the oil and chemical accident combatting and sea rescue.

## 10 SUMMARY

### 10.1 General

The dynamics of the Bothnian Bay, the northernmost sub-basin of the Gulf of Bothnia in the Baltic Sea was studied mainly by means of numerical models. The model results were supplemented, supported and confirmed by flow velocity measurements, drifting experiments, and by data of water temperature, salinity and water quality components sampled for more than twenty years.

Main aims of the work included

- comprehensive interpretation of the heterogeneous field data,
- recommendations for more effective field sampling,
- improved basis for water quality management and planning,
- improved readiness for future applications, and
- special attention to help adequate response to sea accidents.

### 10.2 Research area

The Bothnian Bay is a brakish water basin with mean salinity of about 0.3 ‰. The area is ice-covered for 4–5 months a year, between November and May. During that time the salinity and water quality are quite unequally distributed with sharp horizontal and vertical gradients across the coastal zone and across the halocline at 1–5 metres depth. During the open-water period (regularly through June to October) the gradients are far less prominent.

In south the area is connected to the other parts of the Baltic Sea through a narrow sound, the Quark, 60 km wide with mean depth of 15 metres. The fresh water discharge from rivers to the Bothnian Bay amounts to about  $3200 \text{ m}^3 \text{ s}^{-1}$  ( $100 \text{ km}^3 \text{ a}^{-1}$ ) as an average, and the sea water inflow through the Quark approximately to  $9500\text{--}13000 \text{ m}^3 \text{ s}^{-1}$  ( $300\text{--}400 \text{ km}^3 \text{ a}^{-1}$ ). The waste water discharges of pulp and paper mills, chemical industry, metal industry and municipal sources from Sweden and Finland affect the water quality in the area but are less important to the regional hydrodynamics.

The surface area of the Bothnian Bay amounts to  $36\,800 \text{ km}^2$  and the water volume to  $1490 \text{ km}^3$ . Thus the mean depth of the area is 40.5 metres while the maximum depth is 140 metres. With the average discharges the residence time is approximately three years.

### 10.3 Research background

The study was preceded by a literature review and by an inquiry concerning the experiences of model applications in more than 100 research institutes, companies and universities. Later on, most of the most important model centres were visited, too.

All of the different approaches — viz. literature, inquiry, visits and conference contacts — resulted in quite unique impressions and conclusions of the nature, essence and state-of-the-art of the model use and development. The model experience (in number of applications) most closely correlated with the work (in person-work-years, pwys) done for the models. Similar expertise (more than 60 model applications with 25 pwys) to that of NBWE and EIA (formerly VTT's Reactor Laboratory) was found especially in the Netherlands, Denmark, USA and France.

The idea of a "best model" even for a well

defined problem or application turned out to be quite questionable, as the experience of the user and his familiarity with the model most strongly affect the successful completion of the work. Properly used, most of the methods reported lead to realistic results. Most of the different approaches, on the other hand, supplement each other.

Finite difference and explicit methods dominated the numerical schemes, although implicit methods seemed to be increasingly common in newer models. Finite element-, boundary integral- and pseudo spectral methods still were peculiarities which hardly ever were used in solving practical problems.

## 10.4 Data acquisition

For the models, the Bothnian Bay was digitized at an accuracy of 0.2 to 0.5 mm (100—1500 meters) from marine charts printed at scales from 1:300 000 to 1:50 000. The southern part of the Gulf of Bothnia was digitized at much coarser resolution. The depth information thus gained was approximately from 100 000 points.

To effectively handle such amount of data a grid generation program was devised. With the program, numerous grids for local and regional applications were generated. Manual corrections for the grids were needed in general on shorelines and narrow straits, especially when the digitized map had changed. Also depths in areas with insufficient depth information had to be subjectively estimated.

Weather and wind observations were obtained from the Finnish Meteorological Institute, ice- and water level observations from the Finnish Institute of Marine Research. The loadings of Finnish industry and communities were collected to an input file for the models. River discharges and concentrations were obtained from NBWE. From the Swedish side there still remained some defects to river discharges and industrial loadings.

Water quality data was much more sparse than expected. Out of the 15 000 analyzes reported, less than 2000 could be made available representing some 200 observation sites in the Finnish coastal area.

The lack of available water quality data supported the fact that even in research one should be able to get rid of the collection-economy. Measurements merely for the sake of collecting information to data bases without specific need and foreseeable interpretation is a waste of

resources, which should be avoided. Directing the resources thus freed to interpretation of the measurements and study of the new problems would be much more beneficial to the understanding of the present and forecoming environmental changes, their consequences and remedies.

Current measurements were carried out especially in the regions of Kalajoki and Kemi. They were used to fill in the gaps left from earlier measurements in regions of Kemi, Kuivaniemi, Oulu, Kokkola, Pietarsaari and the Quark. The dependency of flow velocity components on winds, river discharges and local water level changes was studied for each measurement station. Using 12 hour or daily averages these factors usually explained 40 — 90 of the flow variation during the typical measurement period of 30—45 days.

Current measurements can thus reliably be generalized to concern any wind, discharge or water level change as long as the thermal stratification resembles that of the measurement period. Generally applicable and lasting results have hence been achieved with modest resources when enough attention is paid to the interpretation of the results.

## 10.5 Development of the models

The computation of the density effects with the 3D model was improved by implementing the heat exchange between water and air to the model. Calculation of the incoming solar radiation, based on inclination of the sun and on local cloudiness data was found out to be more accurate than the use of direct observations made usually far away from the modelled area. Especially the rapid warming of the waters in shallow shorelines and its spreading to the open sea and deeper layers were clearly and demonstratively visible.

Description of transport suffered in the model mainly from vertical numerical diffusion. This defect was notably reduced when the layers were allowed to follow the movements of the water masses — like water level changes are calculated. At the same time an option was added for direct calculation of the layer velocities instead of indirect calculation initially included in the model. This restricted the stability criteria of model time step but on the other hand better utilized the advantages of vector processors resulting in more effective, physically sound code on a super-computer.

A turbulence model (k-ε) was added to the

model to compute thermal stratification and vertical mixing. Technically, the solution worked fine but some doubts remained about its validity. Especially doubtful was the sensitive and seemingly random dependency of the boundary condition for the turbulent kinetic energy dissipation rate on the surface layer thickness.

The use of stepwise changing steady state flowfields in transport calculations — well suited for local applications — turned out to give quite misleading results in large sea areas. The approach can no longer be used on scales of some 100 km, unless as a temporary expedient forced by limitations of computer efficiency. In local applications (of the order of 50 km or less) the approach is still quite feasible. Until recently it has been necessary to separate the current- and transport calculations to get practical results as it has been impossible to compute currents for many years or even for months with computers of modest performance.

During the project currents calculated by the Finnish 3Dwf and the English Phoenix were compared. Phoenix was applied by SMHI (Swedish Meteorological and Hydrological Institute). The results were similar although the different structures of the models' grid systems made accurate comparisons difficult. Two temperature models were also compared, viz. the 3Dwt and Probe developed by Urban Svensson. After extensive development of the vertical exchange coefficient Probe gave better results in one open sea point than the 3D model. Because Probe is 1D it can't however describe the temperature differences in different parts of the basin or the heat exchange between the open sea and the coastal areas.

A 2D multigrid model was developed during the project to calculate flowfields and water levels with high resolution to large areas. Less than 30 minutes was required to compute flowfields (with Micro-VAX II) for the entire Bothnian Bay with horizontal resolution of some 500 meters (512×512 grid points).

The methods for visualizing the model results were considerably improved and standardized. In addition to flexible and informative visualization of the 3D model results a program was designed to simulate and animate the transport and diffusion of materials released to sea.

## 10.6 Model use

The models developed during the project were mainly used to study the dynamics of the Bothnian

Bay. As a standard approach, problems with the boundary conditions at wide open boundaries were avoided by extending the calculation domain as much as possible further from the point of interest with less detailed resolution. In this way the boundaries of the calculation domain reached the real coast or in any case were so far away that they could be assumed closed.

The effects of different loading alternatives on the water quality off the town of Kemi were studied as a local application. The transport of oil during the M/S Eira accident and the drift of fisherman Holm in his boat were well described by the models. The models had earlier been used with success to compute the drift of sea guards in Liminganlahti, near Oulu.

The variations of water quality components were studied based on measurements and model results. A proposal was made to rationalize the water quality monitoring program by separating the intensive monitoring of a few points (to clarify the temporal changes) from the less frequent areal mapping.

## 10.7 Proceeding of the work

Contacts for co-operation were realized with significant centres of modelling work especially in Sweden, the Netherlands, Canada and USA. Co-operation is further developed by mutual projects with these institutes as well as with institutes from Denmark, Soviet Union, France and Spain.

European co-operation is going on especially within EUROMAR-projects OPMOD and VISIMAR. Under preparation is also Nordic co-operation to develop models for chemical accidents in sea areas. In Finland the work started as a separate project in 1990.

The Bothnian Bay project has further improved the national co-operation. Along with the increase in international contacts this strengthens the future of Finnish model research. The 3D models of Bothnian Bay and Kemi region are installed at the disposal of the Water and Environment District of Lapland to be used e.g. in the further preparation of the water quality monitoring program.

The planning of proper sites for fish farming and evaluation of their effects is a direct continuation of the project. The administrative changes to the monitoring programs will take time — meanwhile the proposals are getting more exact and the needs are becoming more and more clear. With the

financing from the Academy of Finland work is carried out to develop the description of biological processes.

## ACKNOWLEDGEMENTS

In the year 1987 the Water and Environment District of Lapland made an initiative on a study of the effects of the currents on the water quality of the Bothnian Bay. The initial agreement on the study was signed by the National Board of Waters and the Environment (NBWE), Technical Research Centre of Finland (VTT), Finnish Marine Research Institute (FIMR), University of Oulu and the Water and Environment District of Lapland (WEDL).

The work was directed by a leading group consisting of the following persons: Prof. Seppo Mustonen (NBWE), Dr. Lea Kauppi (NBWE), Dr. Kari Kinnunen (WEDL), Prof. Pentti Mälkki (FIMR), Prof. Pekka Hiismäki (VTT/REA) and Prof. Erkki Koskela (Univ. of Oulu). The project was financed by the Academy of Finland, VTT, NBWE and the University of Oulu.

The processing of the data has been mainly done by Mr. Kari Lehtinen (the Water and Environment District of Central Finland) and Mr. Pawel Simbierowicz (VTT). Mr. Simbierowicz was also in charge of the development and programming of the multigrid model and the mesh generation program. Mr. Lehtinen applied the Probe model system for the calculation of the turbulence and temperature and was involved in the temperature model comparisons. Dr. Lars Gidhagen from Swedish Meteorological and Hydrological Institute and Indic Ltd. applied the Phoenix 3D model to the Bothnian Bay. Tech. Lic. Markku Virtanen (VTT and Environmental Impact Assessment Center of Finland, EIA) organized and analyzed the inquiry of the model use in abroad. He also went through the whole manuscript and contributed invaluable to many chapters and wrote the summaries. Dr. Juha Sarkkula (Hydrological Office, NBWE) was in charge of the flow measurement program and in the derivation of the statistical dependencies from them. Mr. Heimo Vepsä (the Water and Environment District of Oulu, WEDO) was involved in the development of the oil and drifting model and in the application of the 3D models to the Kemi region. He has also

been an active part in the preparation of this manuscript. Mr. Jorma Koponen (Academy of Finland, VTT and EIA) has been in charge of the development and application of the 3D models. Most of the figures were drawn by Ms. Helena Heikkinen and Ms. Anita Kaarakainen in WEDO.

The work group wishes to express their gratitude to Dr. Erkki Alasaarela (WEDO), project manager who has been the driving force behind the scenes. His knowledge of the physics and ecology of the study area has been most valuable. He has also been the initiator of the two new projects (monitoring and ecological food webs) that will be a direct continuation of the Bothnian Bay project.

Helsinki, March 1992

## YHTEENVETO

### Puitteet ja tavoitteet

Pohjanlahden pohjoisosan, Perämeren, virtausoloja ja niiden vaikutuksia tutkittiin vuosina 1987–90 pääosin matemaattisilla malleilla. Laskennan tuloksia varmennettiin, tuettiin ja täydennettiin virtausnopeusmittauksilla, ajelehtimiskokeilla sekä tiedoilla veden lämpötiloista, suolaisuudesta, pitoisuuksista ja muista ominaisuuksista, joita alueelta oli kerätty parinkymmenen vuoden ajalta.

Työn päätavoitteita olivat

- runsaaksi luullun, hajanaisen mittausaineiston yhtenäinen tulkinta,
- perusteiden vahvistaminen näytteenoton tehostamiseksi,
- vesiensuojelun, -hoidon ja -käytön ja niiden suunnittelun perusteiden lujittaminen,
- valmiuksien parantaminen uusiin sovelluksiin erityisesti rannikkoalueille, ja
- merialueiden onnettomuustilanteiden torjuntaja pelastustoimia auttavien laskentavalmiuksien alustava testaaminen ja pohjustaminen.

### Tutkimusalue

Suomen ja Ruotsin välisen merialueen pohjoisosa, Perämeri, ulottuu lähes 350 km:n pituisena ja yli 100 km:n levyisenä Vaasan ja Uumajan edustalta pohjoiseen Kemiin, Tornioon ja Haaparantaan.



Alueen pinta-ala on 36 800 km<sup>2</sup>, vesitilavuus 1490 km<sup>3</sup>, keskisyvyys 40,5 m ja suurin syvyys 140 m. Pohjanlahden eteläosaan, Selkämereen, Perämerta yhdistää matala Merenkurkku, jonka leveys on kaikkimillaan 60 km ja keskisyvyys 15 m.

Merenkurkun kautta virtaa Perämerelle Selkämeren suolaista vettä keskimäärin 300—400 km<sup>3</sup> a<sup>-1</sup> (9500—13000 m<sup>3</sup> s<sup>-1</sup>). Jokivesien keskivirtaama Perämerelle on 100 km<sup>3</sup> a<sup>-1</sup> (3200 m<sup>3</sup> s<sup>-1</sup>), jolloin alueen viipymäksi tulee noin kolme vuotta. Perämeri on jäässä vuosittain 4—5 kk marraskuun ja toukokuun välisenä aikana. Tällöin sekä suolaisuus että veden laatu ovat yleensä jyrkästi kerrostuneita ja eriytyneitä siten, että jokivesien vahvin vaikutus leviää suistoista avomeren suuntaan 1—5 metrin kerroksena heti jään alla. Avoveden aikana pitoisuudet sekoittuvat selvästi tasaisemmin sekä vaakattua syvyysuunnassa. Perämeren suolapitoisuus on keskimäärin 0,3 ‰.

Jätevesikuormitusta purkautuu alueelle Suomen ja Ruotsin metsäteollisuudesta, kemian teollisuudesta, metalliteollisuudesta ja asutuskeskuksista. Merialueen virtauksiin ei purkujärjestelyillä juuri ole vaikutusta. Veden laatuun jätevesipäästöt vaikuttavat yhdessä jokivesien, hajakuormituksen, luonnonhuuhtouman, kaukokulkeutumisen ja pohjasta vapautuvan sisäisen kuormituksen kanssa.

## Taustaselvitykset

Tutkimus aloitettiin kirjallisuushaulla ja kyselyllä, joilla selvitettiin mallien käyttöä ja ajankohtaista kehitystä eri maissa. Kysely postitettiin parillesadalle tutkimuslaitokselle, yhtiölle ja yliopistolle erityisesti Länsi-Eurooppaan. Vastauksia saatiin 105 mallista noin 60 laitokselta. Tärkeimpiin tutkimuskeskuksiin tutustuttiin työn aikana lisäksi vierailukäynnin. Eri lähestymistavat — kirjallisuus, kysely, konferenssiyhteydet ja seikkaperäiset tutustumiskäynnit — antoivat kaikki keskenään varsin yhtenäisen kuvan mallityön luonteesta, sisällöstä ja vaatimuksista sekä toteutuneesta kehityksestä eri maissa ja alueilla. Laskentaperusteet ja -menetelmät olivat vakiintuneet eri tahoilla keskenään varsin samalle tasolle. Mitään mullistavia uudistuksia ei ollut tekeillä eikä suunnitteillaakaan. Yleisimpänä työvaiheena eri laitoksissa oli mallien sovittaminen henkilökohtaisille tietokoneille. Mallien kehitys oli määräytynyt nimenomaan käytännön tarpeista, tarkasteltavina olleiden sovellusten ohjaamina. Tältä pohjalta ohjelmien painotuserot ilmenivät lähinnä ratkaisujen yksityiskohdissa. Mallien kehitys, soveltamistaidot ja käyttökokemus kasvoivat kaikkialla rinta rinnan lähes tasatahtia tehdyn työmäärän kanssa. Oleellista oli lisäksi monitahoinen eri

tieteenalojen välinen yhteistyö, jota ilman laajimmatkkaan laitokset eivät olleet töistään suoriutuneet. Suomen vesi- ja ympäristöhallinnon ja VTT:n reaktorilaboratorion, nykyisin YVA:n, veroista laskentakokemusta (yli 60 sovellusta 25 henkilötyövuodella) löytyi ennen kaikkea Delft Hydraulicista Hollannista, DHI:stä Tanskasta, LHF:stä Ranskasta sekä HydroQual -yhtiöstä New Jersey'n osavaltioista USA:sta.

Ajatus "parhaan" mallin valitsemisesta edes tarkasti rajattuun tarkoitukseen tai sovellukseenkään jäi mielettömyydeksi, koska viime kädessä käyttäjän kokemus ja työvälineen tutuus hyvin paljolti vaikuttavat työn onnistumiseen. Oleellisinta työssä ei ole laskenta eikä malli, vaan mallin soveltaminen ja tulosten tulkinta, ts. se mitä tulokset vesistössä merkitsevät. Oikein käytettyinä useimmilla menetelmillä päästään hyviin lopputuloksiin. Toisaalta eri lähestymistavat omalta osaltaan täydentävät toisiaan. Ratkaisutavoista differenssimenetelmä ja eksplisiittiset ratkaisut hallitsivat sovelluksia, joskin uusimmissa malleissa implisiittiratkaisujen osuus näytti selvästi lisääntyneen. Elementtimenetelmä, reunaintegraalimenetelmät ja taajuustason käänteisratkaisut olivat edelleen erikoisuuksia, joita ei juuri käytännön tehtäviin ollut sovellettu.

## Tietojen koonti

Perämeren ja sen saarten rantaviivat ja syvyyskäyrät digitoitiin 0,2—0,5 mm:n (100—1500 metrin) tarkkuudella karttalehdiltä 1:300 000—1:50 000. Erillisten pisteiden syvyystietoja talletettiin siinä määrin kuin niitä kyseisille merikorteille oli merkitty. Selkämerelle käytettiin huomattavasti harvempaa erotustarkkuutta. Syvyystietoja kertyi kaikkiaan lähes 600 000 pisteestä. Laajojen pistejoukkojen sujuvaksi käsittelemiseksi laadittiin optimaalisen tehokas hilanluontiohjelma. Sillä luotiin useita hilaverkkoja paikallisiin ja alueellisiin sovelluksiin. Jälkikorjauksia ohjelman tuloksiin tarvittiin erityisesti kapeissa salmissa ja yleensä rantaviivoilla, etenkin digitoitipohjan vaihduttua karttalehdeltä toiselle ja alueilla, joilta merikorteissa ei ollut riittäviä syvyystietoja.

Vuosien 1975—88 tuuli- ja sää tiedot ostettiin Ilmatieteen laitokselta. Meren jää- ja vedenkorkeustietoja saatiin Merentutkimuslaitokselta. Suomen teollisuuden ja asutuksen kuormitustiedot koottiin yhteen laskennan syöttötiedoiksi. Jokien virtaamat ja pitoisuudet saatiin vastaavasti Vesi- ja ympäristöhallituksesta. Ruotsin osalta jokitiedostoihin jäi vielä puutteita ja teollisuuden kuormitustietoihin vajavuuksia.

Veden laadusta tietoon saadut mittaustulokset

osoittautuivat paljon ennakotietoja niukemmiksi. Tehdyksi kirjatuista yli 15 000 havainnosta saatiin käyttöön vajaa 2000 tietoa paristasadasta pisteestä Suomen rannikolta. Vesipiirien näytteenoton ja kuormittajien velvoitetarkkailun tulokset olivat varsin hyvin saatavilla, VYH:n vedenlaaturekisterin vähän jäykemmin ja heikommin, mutta avomeren intensiiviasemista ei kertynyt juuri mitään tietoja käytettäviksi.

Saatavissa olleiden vedenlaatutietojan puutteellisuus vahvisti käsitystä, että tutkimuksessakin olisi aika päästä eroon keräilytaloudesta. Mittaukset tietojen keräämiseksi pelkästään varastoon, ilman tiedossa olevaa tarvetta ja tulosten tulkintaa, ovat voimavarojen haaskausta, jota tulisi tuntuvasti supistaa. Vapautuvien voimavarojen suuntaaminen edes osittain tulosten tulkintaan ja uusien ongelmien selvittelyyn auttaisi paljon paremmin yksilöimään sekä tapahtuneiden että tulossa olevien ympäristömuutosten kehitystä ja syitä ja suunnittelemaan tehokkaampia torjuntatoimia.

Merialueen virtauksia mitattiin erityisesti Kälajoen ja Kemin edustoilta. Mittauksilla täydennettiin aiemmin Kemin, Kuivaniemen, Oulun, Kokkolan, Pietarsaaren ja Merenkurkun alueilta tehtyjä havaintoja. Kaikista virtausmittauksista analysoitiin virtausnopeuskomponenttien riippuvuudet tuulista, lähialueen jokivirtaamista ja paikallisista vedenkorkeusvaihteluista. Vuorokauden tai puolen vuorokauden keskiarvoina tarkasteltuina nämä tekijät selittivät yleensä 40—90 % virtausten vaihteluista 30—45 vrk:n havaintojaksoilla. Tältä pohjalta mittaustulokset ovat varsin luotettavasti yleistettävissä vastaamaan mitä tahansa eteen tulevaa tuulta jokivirtaamaa ja vedenkorkeusmuutosta niin aikoina, jolloin kerrostuneisuus on mittausten tulkintajakson mukaista. Tulosten ymmärtämiseen tähdänneellä tulkinnalla on virtausmittauksista saatu huomattava hyöty alueen virtausdynamiikan ymmärtämiseen.

## Laskentamenetelmien kehitys

Kolmiulotteista virtausmallia kehitettiin liittämällä sen tiheysvaikutusten laskentaan lämmön vaihto ilmakehän kanssa. Auringon korkeuskulma paikallisten pilvisyystietojen varjostamana antoi mittausten kanssa paremmin yhteensopineita tuloksia kuin kaukaisten säteilyhavaintojen käyttö syöttötietoina. Erityisesti veden keväinen lämpeneminen rannoilta ja vaikutuksen eteneminen paljolti kulkeutumalla avomerelle ja syvempiin vesikerroksiin tulivat laskennassa selvästi ja havainnollisesti esiin.

Kulkeutumisvaikutuksia pyörästi mallissa erityisesti syvyysuuntainen numeerinen sekoittuminen.

Sitä saatiin tuntuvasti vähennetyksi lisäämällä malliin mahdollisuus, jolla kerrosten väliset rajapinnat saattoivat osittain seurata vesimassojen liikkeitä, samaan tapaan kuin veden pinnan vaihteluitakin lasketaan. Kerrosten välisten nopeuserojen laskennasta siirryttiin samalla kerrosnopeuksien suoraan laskentaan. Tämä tiukensi aika-askelen stabiiliusrajoituksia, mutta pystyi paremmin käyttämään hyväksi vektoriprosessorin etuja, jolloin ratkaisu nopeutui supertietokoneella.

Kerrostuneisuuden laskennan ja syvyysuuntaisen sekoittumisen säätelämiseksi malliin liitettiin mukaan pyörteiden liike-energiaa ja niiden siirtymisnopeutta kuvaava  $k-\epsilon$ -malli, josta sekoittumiskertoimet edelleen määritettiin. Teknisesti ratkaisu toimi hyvin, mutta sen luonnonmukaisuudesta ei saatu varmuutta. Erityisesti jäi epäilyttämään energiansiirtonopeuden reunaehdon jyrkkä ja näennäisen mielivaltainen riippuvuus kerrospaksuudesta veden pinnalla.

Paikallisiin sovelluksiin varsin hyvin sopinut portaattain vaihtuneiden vakiintuneiden virtaustilanteiden käyttö kulkeutumisen laskentaperusteena johti laajalla merialueella melkoisiin vääristymiin. Sitä ei ole syytä käyttää enää 100 km:n luokkaa olevilla etäisyyksillä, elleivät tietokoneiden hitaus tai ajoaikarajoitukset tätä ehdottomasti vaadi. Paikallisiin, alle 50 km:n sovelluksiin portaattain vaihtuvat virtaukset ovat edelleen käyttökelpoisia. Viime vuosiin asti virtaus- ja kulkeutumislaskennan erottaminen toisistaan on ollut välttämätöntä käytännön tulosten saamiseksi, koska virtausten laskenta useiksi vuosiksi tai edes kuukauksiksi ei tietokoneiden hitauden takia ole ollut mahdollista.

Projektin kuluessa vertailtiin virtauksia, jotka oli laskettu suomalaisella 3Dwf:llä ja englantilaisella Phoenixilla. Jälkimmäistä sovelsi SMHI (Sveriges Meteorologiska och Hydrologiska Institut). Tulokset olivat samankaltaisia, joskin mallien hilarekenteen erilaisuus vaikeutti vertailua. Lämpötilamalleista vertailtiin suomalaista 3Dwt:tä ja Urban Svenssonin kehittämää Probea. Probe antoi vertikaalisen sekoittumiskertoimen kuvauksen kehittämisen jälkeen paremman kerrostuneisuusrakenteen yksittäisessä avomeripisteessä kuin 3D-malli. Koska Probe on yksidimensioinen malli, se ei pysty kuitenkaan kuvaamaan altaan eri osien erilaista lämpötilakehitystä eikä lämmön siirtymistä avomeren ja rannikon läheisten alueiden välillä.

Kaksiulotteisena mallina kehitettiin optimaalisen tehokas moniverkkoratkaisu pinnaankorkeuksien ja virtausnopeuksien laskemiseksi hyvin tiheällä erotustarkkuudella laajoillekin alueille. Koko Perämeren virtaukset saatiin sillä ratkaistuksi runsaan puolen kilometrin tarkkuudella ( $512 \times 512$  pisteen hilaverkolla) alle puolessa tunnissa (Mikro VAX

II:lla).

Muilta osin erityisesti tulosten visuaalinen havainnollistaminen kuvaruudulla edistyi ja vakiintui työn aikana merkittävästi. Kolmiulotteisen mallin tulosten monipuolisten ja havainnollisten tarkastelumahdollisuuksien lisäksi laadittiin esineiden ja päästöjen kulkeutumisen ja päästöjen sekoittumisen laskemiseksi tietokoneohjelma, jonka lähtökohdan, päästömäärät, tuulet ja sääolot sekä tarkastelualueen käyttäjä voi valita joustavasti ja seurata sen jälkeen tilanteen kehittymistä kuvaruudulta.

### Mallien käyttö

Kehitettyjä malleja käytettiin erityisesti Perämeren alueellisen dynamiikan tarkasteluun sekä reuna-arvojen laskemiseen paikallisille sovelluksille. Irrallisten reuna-arvojen syötön sijasta käytännöksi vakiintui mahdollisimman laajan alueen ottaminen samalla kertaa tarkasteltavaksi reunoiltaan hyvin karkealla, ydinalueisiin verrattuna jopa satakertaisella hilavälillä. Tällöin alueen reunat saatiin niin loitolle, että ne voitiin olettaa suljetuiksi silloinkin, kun ne eivät suoranaisesti ulottuneet rannoille.

Paikallisena sovelluksena laskettiin Kemin edustan jätevesien päästöjärjestelyjen vaikutuksia merialueelle. M/S Eiran öljyonnettomuuden vaikutusalueet ja kalastaja Holmin katoaminen etsintälentojen ulottumattomiin Merenkurkussa saatiin laskennassa varsin hyvin selitetyiksi. Jo aiemmin oli malleilla laskettu osuvasti merivartijaveneen ajelutimisreitti Liminganlahdella. Pitoisuuksien ja vaikutusosuuksien vaihtelua merialueella tarkasteltiin sekä mittaus- että laskentatuloksista. Tältä pohjalta muotoiltiin selkeä esitys tarkkailuohjelmien selvittämiseksi ja keventämiseksi erottamalla harvoin tapahtuva alueellinen kartoitus ja muutamien pisteiden taajaan toistuva aikavaihtelujen seuranta toisistaan.

### Työn jatkuminen

Työn tuloksena avautui yhteistyösuhteita erityisesti Ruotsiin SMHI:hin, Hollantiin Delft Hydrauliciin, Kanadaan Sisävesien tutkimuskeskukseen sekä USA:han Princetonin yliopistoon ja HydroQualiin, jotka kaikki ovat varsin merkittäviä tutkimuslaitoksia. Yhteistyön nostaminen käytännön tasolle etenee edelleen, kuten myös yhteydet Tanskaan, Neuvostoliittoon, Ranskaan ja Espanjaan.

Euroopan sisäinen yhteistyö jatkuu varsinkin EUREKA:n kahdessa EUROMAR-työssä, OP-MOD- ja VISIMAR-projekteissa. Valmisteltuna on lisäksi pohjoismaisen yhteistyön tiivistäminen

kemikaalio-onnettomuuksien torjuntaa auttavien laskentavalmiuksien nopeaksi parantamiseksi. Suomessa tähän tähtäävä työ käynnistyi erillisenä hankkeena vuonna 1990.

Perämeri-projekti on entisestään tiivistänyt kansallista yhteistyötä. Kansainvälisten yhteyksien luittumisen rinnalla tämä edelleen vahvistaa Suomen mallitutkimuksen asemaa. Kolmiulotteiset Perämeren ja Kemin edustan sovellukset siirretään Lapin vesi- ja ympäristöpiiriin käyttöön mm. tarkkailun tehostamiseksi. Perämeren, Kemin edustan, Oulun edustan ja Merenkurkun sovellukset ovat työn aikana jo paljolti olleet Oulun vesi- ja ympäristöpiiriin käytettävänä.

Kalankasvatuksen mahdollisten sijoituspaikkojen vaikutusalueiden laskenta etenee työn välittömänä käytännön jatkona. Tarkkailuohjelmien hallinnollinen muuttaminen vaatii aikansa, mutta muutosehdotukset täsmentyvät ja niiden perusteet vahvistuvat jatkuvasti. Suomen Akatemian rahoituksella työtä jatketaan biologisten prosessien erityisesti ravinne-, levä-, bakteeri- ja eläinplankton-dynamiikan tarkemmaksi kuvaamiseksi.

### REFERENCES

- Alasaarela, E. 1976. Methods for investigating the spread of river and waste waters in brackish water area. *Aqua Fennica*, 6, pp. 59—70.
- Alasaarela, E. 1980. Phytoplankton and Environmental Conditions in the Northern Part of the Bothnian Bay. *Acta Universitas Ouluensis*, Series A, No: 7, 144 p.
- Alasaarela, E. and Koponen, J. 1989. The waste water transport in the northern Bothnian Bay (in finnish). *Vesitalous*, No. 5.
- Alasaarela, E., Koponen, J., Lehtinen, K. and Vepsä, H. 1989. The spreading and effects of pulp and paper industry waste waters off the town Kemi (in finnish). Technical report, Water and Environment District of Oulu. 31 p.
- Anderson, E.A. 1954. Energy budget studies, Water-loss investigations. Technical report, USGS Professional Paper 269. Lake Hefner studies.
- Arakawa, A. 1972. Design of the UCLA general circulation model. Numerical Simulation of Weather and Climate 7, Dept. of Meteorology, Univ. of California, Los Angeles. 116 p.
- Bengtsson, L. 1973. Mathematical models of wind-induced circulation in a lake. Symposium on Hydrology of Lakes, Helsinki, July 1973. IAHS-AISH Publication No. 109, pp. 313—320.

- Bolz, S.H. 1949. The dependency of infrared counter-radiation on cloud mass (in german). *Z.f. Meteorologie*, 3: 5—6.
- Boris, J.P. and Book, D.L. 1973. Flux-corrected transport. I. Shasta, a fluid transport algorithm that works. *J. Comput. Phys.*, 11:38—69.
- Boris, J.P. and Book, D.L. 1975. Flux-corrected transport. II. Generalizations of the method. *J. Comput. Phys.*, 18:248—283.
- Brady, D.K., Graves W.L. and Geyer, J.C. 1969. Surface heat exchange at power plant cooling lakes. *Publ.* 69—901, Edison Electric Institute, New York.
- Brusaert, W. 1975. On a derivable formula for long wave radiation from clear skies. *Water Resources Research*, 11(5):742.
- Dake, J.M.K. and Harleman, D.R.F. 1969. Thermal stratification in lakes: analytical and laboratory studies. *Water Resources Research*, 5(2): p. 484.
- de Vahl Davis, G. and Mallison, G.D. 1972. False Diffusion in Numerical Fluid Mechanics. Rept. 1972/FMT/1, Univ. of New South Wales, School of Mech. and Ind. Eng.
- Dongarra, J.J. 1988. Performance of Various Computers Using Standard Linear Equations Software in a Fortran Environment. Technical Memorandum 23, Argonne National Laboratory, 9700 South Cass Avenue, Argonne, Illinois.
- Fisher, H.B. (ed.) 1981. Transport Models for Inland and Coastal Waters, Proceedings of a Symposium on Predictive Ability. Academic Press. ISBN 0—12—258152—0, 542 p.
- Fletcher, C.A.J. 1988a. Computational Techniques for Fluid Dynamics. Volume I. Springer Verlag, Berlin-New York, ISBN 3—540—18151—2, 409 p.
- Fletcher, C.A.J. 1988b. Computational Techniques for Fluid Dynamics. Volume II. Springer Verlag, Berlin-New York, ISBN 3—540—18759—2, 484 p.
- Forsius, J. 1985. Flow measurements off the town Kemi in winter 1985 (in finnish). Technical Report, National Board of Waters and the Environment, Hydrological Office. 12 p.
- Hackbush 1985. Multi-Grid Methods and Applications. Springer Series in Computational Mathematics; Vol. 4. Springer Verlag, Berlin-New York, edition. ISBN 3—540—12761—5, 377 p.
- Hansen, W. 1956. Theorie zur Errechnung des Wasserstandes und der Strömungen in Randmeeren nebst Anwendungen. *Tellus* 8, pp. 287—300.
- Heaps, N.S. 1971. On the numerical solution of the three-dimensional hydrodynamical equations for tides and storm surges. *Memoires Societe Royale des Sciences de Liege*, 6é serie, tome I, pp. 143—180.
- Hela, I and Voipio, A 1960. Tracer dyes as a means of studying turbulent diffusion in the sea. *Finnish Academy of Sciences, Serie A. VI. Physica*, 9 p.
- Huttula, T. and Sarkkula, J. 1980. Currents in the sea area off the Kemi town in autumn 1979 (in finnish). Technical Report, Hydrological Office.
- Huttula, T. and Sarkkula, J. 1981. Currents in coastal area off the Tornio town during open water period (in finnish). Technical Report, Hydrological Office.
- Huttula, T., Koponen, J., Lehtinen, Sarkkula, J. and Filatov, N. 1989. Systems Analysis Applications to Water Research. Publications of the Water and Environment Research Institute No. 3. National Board of Waters and the Environment, Finland, Helsinki. 61 p.
- Häkkinen, S. 1979. On the hydraulic-numerical flow model of the Baltic Sea (in finnish). Biannual Meeting of the Finnish Geophysical Society, Oulu.
- Idso, S.R. and Jackson, R.D. 1969. Thermal radiation from atmosphere. *J. of Geophysical Research*, 74.
- Jerome, J.W. 1983. Approximation of Nonlinear Evolution Systems. Volume 164 of Mathematics in Science and Engineering. Academic Press, New York. ISBN 0—12—384680—3, 280 p.
- Józsa, J., Sarkkula, J. and Tamsalu, R. 1990. Calibration of modelled shallow lake flow using wind field modification. Technical Report, VITUKI, National Board of Waters and the Environment and Estonian Academy of Sciences, 6 p.
- Juutilainen, J. 1980. Effects of Reareation on the Waste Water Loading (in finnish). Master's thesis, Helsinki University of Technology, Department of Technical Physics.
- Karttunen, H., Lounamaa, K. and Serimaa, O. 1990. Cray X-MP users manual (in finnish). CSC publications 4, VTKK/CSC, Helsinki. ISSN 0785—711X, 364 p.
- Kennedy, R.E. 1944. Computation of daily insolation energy. *Bull. of the American Meteorological Society*, 30.
- Kinnunen, K. 1978. Tracing Water Movements by means of Escherichia Coli Bacteriophages. Publications of the Water Resources Research Institute No. 25, National Board of Waters, Helsinki.
- Kinnunen, K., Niemi, J. and Eloranta, J. 1978. Adaptation of the EPAECO-model to a lake in Central Finland. Modelling the Water Quality of the Hydrological Cycle. IAHS-AISH Publication No. 125, pp. 115—127.
- Kinnunen, K., Nyholm, B., Niemi, J., Frisk, T., Kylä-Harakka, T. and Kauranne, T. 1982. Water Quality Modelling of Finnish Water Bodies. Publications of the Water Research Institute No. 26, National Board of Waters, Helsinki, 99 p.
- Klein, W.H. 1948. Calculation of solar radiation and the solar heat load on man. *J. of Meteorology*, 5(4).
- Koponen, J. 1984. A Three Dimensional Current and Water Quality Model (in finnish). Master's thesis, Helsinki University of Technology, 98 p.
- Koponen, J. 1991. Application of complex environmental numerical models. Doctor of technology thesis, Helsinki University of Technology. To be published.
- Kuoppamäki, R. and Kuusi, J. 1973. Experiences of lake current measurements obtained in connection with waste water flow studies. Symposium on Hydrology of Lakes, Helsinki, July 1973. IAHS-AISH Publication No. 109. pp 3—7.
- Kuoppamäki, R., Virtanen, M., Jokinen, O., Rämö, E., Kämäräinen, V. and Mälkki, P. 1977. Estimating the Applicability of Mathematical Models Describing the Dispersal of Waste and Cooling Waters (in finnish). SITRA, The Finnish National Fund for Research and Development, YVY Research 28, 209 p.
- Lappalainen, K.M. 1975. Phosphorus loading capacity of lakes and a mathematical model for water progress. Tenth Nordic Symposium on Water Research, Nordforsk 1974, pp. 425—441.
- Lappalainen, K.M. 1977. Mathematical means for helping analysis of the results of water research (in finnish).

- Seminar on Physical and Chemical Analysis Methods, Vekary ry., pp. 107—121.
- Lehtinen, K. 1984. Mathematical modelling of temperature in a water body (in finnish). Publ. of National Board of Waters, National Board of Waters in Finland, Helsinki. 21 p.
- Marciano, J.J. and Harbeck, G.E. 1954. Mass-transfer studies. Technical Report, USGS Professional Paper 2657, Lake Hefner studies.
- Myrberg, K. 1990. Testing a two-level flow model with stationary winds and simple basins. International Council for Exploration of the Sea, ICES C.M.1990/C:20, 10 p.
- Mälkki, P. and Tamsalu, R. 1985. Physical features of the Baltic Sea. Technical Report 252, Finnish Marine Research.
- Niemelä, S. and Kinnunen, K. 1968. An experiment with *Escherichia coli* T bacteriophage as a tracer in river flow studies. *Geophysica* 10, pp. 121—124.
- Patankar S.V. 1980. Numerical Heat Transfer and Fluid Flow. Series in Computational Methods in Mechanics and Thermal Sciences. Hemisphere Publishing Corporation, McGraw-Hill Book Company. ISBN 0—07—048740—5, 197 p.
- Raithby, G.D. 1976. Skew upstream differencing schemes for problems involving fluid flow. *Computer Methods in Applied Mechanics and Engineering*, 9(2): 153—164.
- Rautalahti-Miettinen, E., Sarkkula, J. and Virtanen, M. 1981. The effects of a pulp mill on an ice-covered lake system. *Aqua Fennica* 11, pp. 36—42.
- Roache, P.J. 1982. *Computational Fluid Dynamics*. Hermosa Publishers, Albuquerque, N.M. ISBN 0—913478—05—9, 446 p.
- Rämö, E. 1976. Three-dimensional mathematical models in studies of lake currents. *Aqua Fennica* 6, pp. 26—33.
- Sarkkula, J. 1989. Measuring and Modelling Flow and Water Quality in Finland. VITUKI Monographies No. 49, Water Resources Research Centre VITUKI, Budapest. 41 p.
- Sarkkula, J. and Virtanen, M. 1978. Modelling of water exchange in an estuary. *Nordic Hydrology*, 9, pp. 43—56.
- Sarkkula, J. and Virtanen, M. 1983. Application of mathematical flow field models in Finland. IHP Report No. 56, Sweden, pp. 93—111.
- Simons, T.J. 1973. Development of the Three-Dimensional Numerical Models of the Great Lakes. Inland Waters Directorate, Scientific series No. 12., Canada Centre for Inland Waters, Burlington, Ontario. 26 p.
- Simons, T.J. 1980. Circulation models for lakes and inland seas. *Can. Bull. Fisheries and Aquatic Sci.*, No. 203, 145 p.
- Simons, T.J. and Kielman, J. 1984. Hydrodynamics of Lakes, chapter 'Some aspects of baroclinic circulation models', p. 235—285. Volume 286 of CISM Courses and Lectures, Springer Verlag, Wien-New York.
- Svensson, U. 1978. A mathematical model of the seasonal thermocline. Technical Report 1002, University of Lund, Dept. of Water Resources Eng., Sweden. pp. 111—150.
- Swinbank, W.C. 1963. Long-wave radiation from clear skies. *Quarterly J. of Royal Meteorological Society*, 89.
- Temam, R. 1977. Navier-Stokes Equations, Theory and Numerical Analysis. Volume 2 of Studies in mathematics and its applications. North-Holland Publishing Co., Amsterdam-New York-Oxford, edition. ISBN 0—7204—2840—8, 500 p.
- Tetons, O. 1930. About some meteorological concepts (in german). *Z. Geophysik*, 6.
- Tjomsland, T. 1978. Simulation of Currents in Mjösa Lake by means of a Three-Dimensional Mathematical Model (in norwegian). Norwegian Institute of Water Research NIVA, Oslo.
- Uusitalo, S. 1960. The numerical calculation of wind effect on sea level elevations. *Tellus*, 12, pp. 427—435.
- Versteegh, J. 1990. The Numerical Simulation of Three-dimensional Flow through or around Hydraulic Structures. PhD thesis, Technische Universiteit Delft.
- Virtanen, M. 1977. Description of Flow and Mixing in Water Bodies with a 2-dimensional Mathematical Model (in finnish). Technical licenciate thesis, Helsinki University of Technology. 128 p.
- Virtanen, M. 1984. Tracer and model studies of a river and an estuary. *Isotope Hydrology 1983*, Internal Atomic Energy Agency IAEA, Vienna, Austria, pp. 695—708.
- Virtanen, M., Koponen, J., Dahlbo, K. and Sarkkula, J. 1986. Three-dimensional water-quality — transport model compared with field measurements. *Ecological modelling*, 31, pp. 185—199.
- Virtanen, M. and Käki, A. 1990. Tracer studies for transport and mixing in surface waters. Internal Atomic Energy Agency, Advisory Group Expert Meeting on the Use of Artificial Tracers in Hydrology, 19—22 March, 1990, Vienna, Austria, 12 p.